# Introduction to Analytical Methods for Internal Combustion Engine Cam Mechanisms

A typical finger follower cam mechanism for a high performance engine

J. J. Williams

# Introduction to Analytical Methods for Internal Combustion Engine Cam Mechanisms

Springer

J. J. Williams
Oxendon Software
Market Harborough
UK

ISBN 978-1-4471-4563-9 ISBN 978-1-4471-4564-6 (eBook)
DOI 10.1007/978-1-4471-4564-6
Springer London Heidelberg New York Dordrecht

Library of Congress Control Number: 2012946758



Printed on acid-free paper

Springer is part of Springer Science+Business Media (www.springer.com)

*To Wendy*

# Foreword

It is now over 40 years since the Cosworth DFV made its race winning debut in a Formula 1 event and surprisingly since then there has been a remarkable lack of good technical information relating to race engine design. It was, therefore, with great pleasure I received the first draft of this book that covers Jeff Williams's significant contribution to design and manufacture of race engine cam mechanisms.

During my career I have been very fortunate to have worked at Cosworth, Ferrari and Ilmor. I saw first-hand how the challenge of race engine design was approached at each of these successful companies.

The design-led approach at Cosworth was an inspiration. The clear thinking and directness of the late Keith Duckworth was unforgettable.

The development-led approach at Ferrari was in complete contrast. However, not until witnessing horse power increases that in a season were multiples of anything achieved at Cosworth did the value of a well-organised development activity become clear.

At Ilmor the leadership of the late Paul Morgan demonstrated very successfully an approach that was focused on gathering the input from all departments rather than biasing the activity towards any one of them. Few projects embodied this good working relationship between departments better than that of the F1 cylinder head design to incorporate a curved finger follower. All departments worked well together, design, simulation, metallurgy, rig test and manufacturing.

All strove to solve the not insignificant problems encountered on the way to the introduction of a very successful arrangement with measurable performance benefits. Such projects clearly require all departments to play their part, yet significant performance steps always seem to be preceded by one or more extraordinary contributions and for this project I can recall two. Finding a surface coating that allowed the steel finger follower to survive was one such contribution and the cam design software written by Jeff Williams the other.

The software, used by the designers, allowed them to quickly evaluate different arrangements viewing outputs such as pivot loads, entrainment velocity, pressure angles, cam profiles, etc., and allowed modification to inputs such as valve

accelerations, finger follower geometry, spring loads, etc. The huge number of equations and manipulations required for the presentation of this information as a useable design and manufacturing aid, is in itself a significant achievement. However, achieving it within the very tight time frame imposed by the engine run date, along with the incorporation of features peculiar to each designer's preference was in my view key to the project's success and a clear indication that good information is crucial and particularly welcome when it arrives. So to now have this and a wealth of other good information in this one excellent publication will, I am sure, see its widespread use as a teaching aid as well as a great reference for the experienced engine design or development engineer.

Stuart Grove
Chief Engine Designer F1 (1994–2005)
Ilmor Engineering Ltd

# Preface

Not long after I graduated, I was involved in looking into a problem with one of the early nuclear power stations. What surprised me was that those who had designed it, together with those responsible for overseeing the commissioning, seemed to have very little relevant knowledge. Some years later I found that due to government policies, university teaching had ceased to provide attractive employment, and I would need to move back into industry. I remembered my experience with the power station, and sought a subject about which little seemed to be known to those involved. I found that automotive cam design and analysis seemed to be such a subject. I therefore studied the literature and then the current practice and managed to gain employment back in industry.

The literature did not address many of the problems which needed to be solved. It was helpful in presenting solutions to some problems, but many aspects were not covered. It was eventually decided that it would be worthwhile to try and produce new solutions from first principles. These were frequently based on diagrams which others had already produced in part or whole. Therefore the notation may, in places, have been copied from existing diagrams. Once a mechanism has been correctly represented by a diagram, and the relevant parameters have been identified, the analysis should follow fairly easily. Obtaining the correct diagram and establishing which quantities will be prescribed by the designer, and which need to be determined is an iterative process, which may not be apparent in the following chapters.

There are two schools of thought as to how design decisions should be made using digital computers. There are those who believe that the more complex the computer model is the better and having written a suitable program, they are more inclined to have implicit belief in the results. Unfortunately this has led to many engineering failures. The mathematical model will be no better than the accuracy of the boundary conditions, loads and material properties which are specified and frequently assumed to be linear. The results, which are obtained from computations involving complex computer models, are less likely to be questioned by the designer, because the software has been expensive to purchase or develop. Engineering judgement is needed and very often, nonlinear behaviour of components,

material or boundary conditions, or failure to create the mathematical model correctly can lead to misleading results, which may be assumed to be correct by inexperienced designers.

An alternative approach is to create a model which is simple and relies on a linear model and boundary conditions, which if they are approximate, or time and wear dependent are understood to be so and allowed for empirically by the designer. The nonlinear behaviour of pneumatic valve springs and some steel springs with unevenly wound coils can however be included with simple but approximate models. This method allows a design decision to be made relatively quickly and if a more complex model is subsequently needed, this can be used together with rig testing and prototype development. I am a believer in this approach which also requires judgment experience and thought from the designer, but I have been very fortunate in having worked with experienced, talented and knowledgeable designers.

The lack of knowledge of the relevant tribology and the best materials and surface coatings together with financial constraints has resulted in many failures in cams and followers. The latter can fail due to excessive wear on surfaces which involve interaction between cam and follower, and the heel of finger followers and the valve stem. The same problem can occur with rockers which can also lead to wear of the end of the valve stem.

The most commonly used heel is cylindrical as it is easy to machine. This leads to movement of the line of contact across the end of the valve stem together with a relative rotation by the follower heel. The movement across the valve stem causes a bending moment in the valve stem, and it is unlikely the combined motion will generate much of an oil film. The use of a suitable involute heel can ensure that a centrally positioned line of contact will remain central, which obviates the bending moment in the valve stem due to axial loads, but there is still relative motion between the two components due to follower rotation, and again there is little prospect of a substantial oil film being entrained. A good surface coating and finish, and a material which permits a hard substrate, are essential to ensure these poorly lubricated contact areas do not fail, due to avoidable wear.

The premature failure of some finger followers and the associated cams was explained by A. Dyson in a seminal paper, published in 1980. He showed that for some cam shapes and finger follower curvatures insufficient oil was entrained between the contacting surfaces and that this could be avoided by decreasing the follower radius. This has the effect of increasing the contact stress and to avoid surface pitting superior, but more expensive materials are required which have a higher yield stress. At this time this form of failure was prevalent in cars manufactured in large numbers by two multinational motor companies, and resulted in a large after-market in third party replacement camshafts and followers.

During the Second World War some cams and followers made for the Rolls Royce Merlin engine suffered from the same problem. This was not so much a problem in war time as many engines were destroyed due to enemy action. However these engines are still used in the Spitfire, Hurricane and Lancaster of the Battle of Britain flight, and in Spitfires, Hurricanes and P51 Mustangs used for

recreational flying, where this problem is often apparent. It would now be very easy to design new cams and followers with good oil entrainment. Other cam mechanisms can suffer from the same problem, but failures due to poor entrainment are less common than with finger followers. In this book the method for computing the entrainment velocity is given for all the cam mechanisms considered.

Algorithms are now available for computing the oil film thickness between cam and follower, but these require considerable knowledge of the many properties of the oil and these are frequently highly nonlinearly dependent on the temperature and pressure of the oil at and in the immediate vicinity of the line of contact. In the writer's opinion, for an initial design, ensuring good entrainment velocity should normally suffice.

The advent of the digital computer and related software and in particular the widespread use of personal computers which are relatively cheap and powerful now permits every designer to have his own machine. This has transformed methods of analysis, but there is always the problem that designers, who lack sufficient experience and knowledge will still produce poor designs which they consider acceptable because a computer has been used. This is in many ways similar and as equally dangerous as the belief that if something has been published in a book or a technical paper it is necessarily correct.

The completed analysis can be initially checked by writing a computer program and looking at the results. Most designers will have their own preferences and ideas on how they want the design data input, especially the units, which may not be those used for the calculations. For example, valve mass may be input in g, but the calculations will be easier if masses are in kg. There will also be preferences as to what is output both graphically and numerically and how the user interface is arranged. If the designer finds the program easy to use, fatigue and mistakes should be reduced. The final design of the user interface and establishing what the designer requires is often also an iterative process.

The engine designer has to consider many parts of the engine before finalising his design. A few years ago there was a V10 racing engine with a wide V-angle to achieve a lower centre of gravity. Unfortunately this engine suffered from vibration problems and the V-angle was eventually reduced by about 35 %. Although the valve timing was not known exactly, a good guess could be made, and as the V-angle was known, a calculation similar to those described in Chap. 9 showed that there would be significant interaction between the camshaft torques, which was likely to induce torsional vibration. If designing a V engine the valve timing and the V-angle should be considered and the total camshaft torque checked, before designing the cylinder block.

There is no point in designing something, if it cannot be manufactured, or if it is unlikely to work reliably. Interaction with those involved in manufacturing, assembling and developing the engines can be very worthwhile, not only for the designer, but also for the analyst. Those on the shop floor may have problems whose solution result in improved design, performance or reliability. Their experience in their particular part of the whole production process is frequently considerable, and suggestions and criticism are often very valuable.

This text is intended as an introduction to a large subject, and where possible the mathematics used is elementary and should be familiar to most Engineers. Cubic Spline Interpolation and the Fast Fourier Transform do not need to be completely understood for the reader to use them, as the relevant algorithms are well documented. Some parts of the text, in particular, Chap. 3, is not easy to read, and although the contents of Chap. 10 is well documented elsewhere, this work has been included as some of the subject matter may be hard to access, as the best book on this subject is out of print.

I have been very fortunate in having had many colleagues, who have been talented, knowledgeable and helpful, and to whom I give sincere thanks for the help, advice and information they have given me. Amongst these were: H. Alten, K. P. Baglin, T. Brightwell, A. J. Cook, M. Dhaens, the late A. Dyson, S. B. Grove, M. J. Illien, G. Langham, the late P. J. Morgan, the late C. J. Morrison, H. Tsuda, and I. Watson.

However all errors and omissions in this book are mine.

Great Oxendon, November 2011 J. J. Williams

# Contents

# Chapter 1
# Introduction

**Abstract** The necessary concepts are introduced starting with the valve lift curve, and its design using the valve acceleration curve. There is a need to obtain a smooth curve by considering the jerk, which is the first derivative of the acceleration. The three commonest cam mechanisms which are used to actuate poppet valves are illustrated and their respective merits discussed. Some of the relevant parameters are then briefly described. The elementary mathematics of curvature is introduced, followed by an introduction to cam torque. The concept of oil entrainment is described and examples are given of good and poor entrainment velocity curves. The forces due to the valve spring and valve assembly inertia are considered and used to determine the contact stress for a flat translating follower. A simple example of rigid body kinetics is analysed using a simplified model of a curved finger or swinging follower. The derivation is then given of the equation for the maximum speed to maintain cam–follower contact for a translating flat follower, and an example given of good use of the energy stored in the valve spring. Finally a list is given of suggested units for data input, the computation, and the output.

## 1.1 Cam Mechanisms

Cam mechanisms are widely used in various forms of machinery, including internal combustion engines to actuate poppet valves. It is this particular application which is of interest here, but some of the mechanisms considered may well be suited to other machinery such as that used for printing and packaging.

Various methods of controlling the gas flow through an internal combustion engine have been used or investigated. However the use of cams to provide positive cam acceleration usually in conjunction with a spring to provide the force for negative acceleration has remained the most widespread method. Desmodromic cam mechanisms, which employ a second cam to provide the force for negative

J. J. Williams, *Introduction to Analytical Methods for Internal Combustion Engine Cam Mechanisms*, DOI: 10.1007/978-1-4471-4564-6_1, © Springer-Verlag London 2013

acceleration instead of a spring have been and are still used for some applications. Among the other methods which have been used are rotary valves and sleeve valves. Pneumatic and inductive devices have also been tried but have not achieved widespread application.

At present it appears that the cam mechanisms currently used for automotive and similar applications will continue to be used for some time into the future. Well designed cams to provide reliable control of the gas flow can now be designed and manufactured using present knowledge, materials, surface finishes, design, and manufacturing methods. Providing over-zealous cost considerations do not prevent the design and manufacture of a reliable product, there is now little reason why failures in service due to poor lubrication or valve spring failure should occur.

No oil film thickness calculations will be described, and mechanisms for variable valve timing and lift will not be considered, nor will the simulation of elastic effects in order to establish possible unstable behaviour at high speeds, when inertia loading can cause significant elastic deformation of relatively rigid components.

Analytical methods for the synthesis of valve lift curves and the analysis of the more widely used valve actuation mechanisms are considered in later chapters. The remainder of this chapter introduces some of the relevant concepts. Some of the necessary concepts for design, manufacture, and successful operation of the more widely used automotive cam mechanisms are described in subsequent chapters.

### *1.1.1 Early Cam Design Methods*

In the early twentieth century there were many forms of mechanism used to operate poppet valves. On some very low speed engines there was no inlet cam, as the very weak valve spring allowed atmospheric pressure to open the valve during the intake stroke. The majority of classes of mechanism included in this book were used in some form or other, but not all were found to work well and many designs were discarded, only to be reconsidered for use years later.

The valve lift curve needs to provide the prescribed valve lift and dwell or period the valve is open. The valve motion needs to be as smooth as possible to ensure stable behaviour of the mechanism at higher speeds where inertia loads will be higher and may result in significant elastic deformations of the components.

Incredible as it may now seem, some cam shapes were designed using straight lines and circular arcs to create the cam shape, with a protractor used to establish the dwell. However some of these designs were used with some success, although on high performance engines valve spring failure was not uncommon. Later designs used graphical methods of construction, which still limited the accuracy of the finished cam. Before the advent of the digital computer, computation to produce more precise cam shape data, and other relevant design parameters was very time consuming, which limited the optimisation process.

Unfortunately some lessons have to be periodically re-learnt and decades later some very successful racing engines were still suffering valve spring failures due to poor design of the valve lift curve, even though this was obtained by mathematical computation, and advances in metallurgy and surface treatments resulted in valve spring materials that had improved considerably.

### *1.1.2 Modern Cam Design Methods*

The advent and widespread use of personal computers together with the development of programming software with a graphical user interface has transformed the cam design process. This has meant that more complex methods of synthesising the valve motion can be used to improve the stability of valve motion, and mechanisms which were previously used with only semi-empirical design analysis could be more rigorously analysed.

Cam manufacture was frequently by grinding while copying a larger version of the same shape using a size reducing mechanism. This method was not very accurate and careless or incompetent grinding would sometimes lead to burning of the cam nose and consequential softening of the material which would lead to early failure.

The invention of the CNC cam grinding machine has resulted in more accurate cam shape manufacture providing the data supplied by the designer is sufficiently accurate and precise. Precision will not provide the desired result if the data is not also accurate. Similarly accuracy will not provide the desired result if the data is not also sufficiently precise. Computing the cam shape, and then possibly transforming the cam shape data into a form which can be used by the CNC grinding machine requires algorithms which do not result in significant arithmetical errors. To compute the cam shape given only the follower curvature and the valve lift curve requires the computation of a valve velocity curve. This is computed using numerical differentiation, which involves the subtraction of numbers of almost equal size with a consequent need for good numerical accuracy and precision of the data supplied if comparatively large errors are not to result when computing the cam shape. If the CNC cam grinding machine will accept the cam shape data as a series of polar or Cartesian coordinates this requirement may not be so stringent.

Although modern computing hardware and software permit computation to a relatively good precision this is not necessarily a guarantee of good accuracy. By minimising the number of computations required and ensuring that any interpolation is as accurate as possible, and any iterative processes result in only very small errors, it is usually possible to obtain satisfactory data for cam manufacture and operation.

## 1.2 The Cam Lift Curve

The first matter for consideration by the designer is the cam lift curve. The usual way to design a cam lift curve is to start with the acceleration diagram. In the method described the curve consists of a series of piecewise continuous sections, whose parameters can be specified by the designer. The primary design curve is acceleration, and the velocity and displacement curves are obtained by integration. The problem then consists of two simultaneous equations in two unknowns. The velocity must be zero on the nose and the maximum lift can be specified by the designer. The method used here considers half the acceleration curve and the unknowns are the maximum and minimum values of the acceleration from base circle to nose.

The acceleration needs to vary smoothly if the valve motion is to be well controlled, and if a metal valve spring is used, there is a need to limit valve spring vibration or surge.

There are many methods for formulating the acceleration curve and the one below is partially by way of illustration, but it can be used for successful cam design. In this work the cam lift curve is designed in two halves. The closing side is also designed from the base circle to the nose, and the result is then mirrored. This design method requires that the acceleration is such that its derivative on the nose is zero. The magnitude of the acceleration and the lift on the nose must also be the same for the opening and closing sections.

A typical acceleration curve is shown in Fig. 1.1a. Note that the slope of the acceleration curve is zero on the nose of the cam in this case. This is not necessary but the slope should change smoothly, in other words the second derivative of the acceleration curve should be piecewise continuous. Integration of this acceleration curve results in the velocity curve, as shown in Fig. 1.1b, which shows that the velocity is zero on the nose. Integration of the valve velocity curve gives the valve lift curve shown in Fig. 1.1c.

When designing the lift curve the designer should endeavour to obtain a smooth curve and this is best achieved by examining the curves of the first and second derivatives of the acceleration curve. The first derivative of acceleration is called the jerk. The second derivative of acceleration is sometimes called the quirk, but there would seem to be no generally accepted term for this.

The jerk is generally accepted as being related to valve spring surge and there is limited experimental evidence to indicate that a smoother quirk also helps reduce spring surge, especially for push-rod mechanisms which are usually more flexible and more prone to unstable behaviour. The jerk and quirk associated with the acceleration diagram are shown in Fig. 1.1d, e.

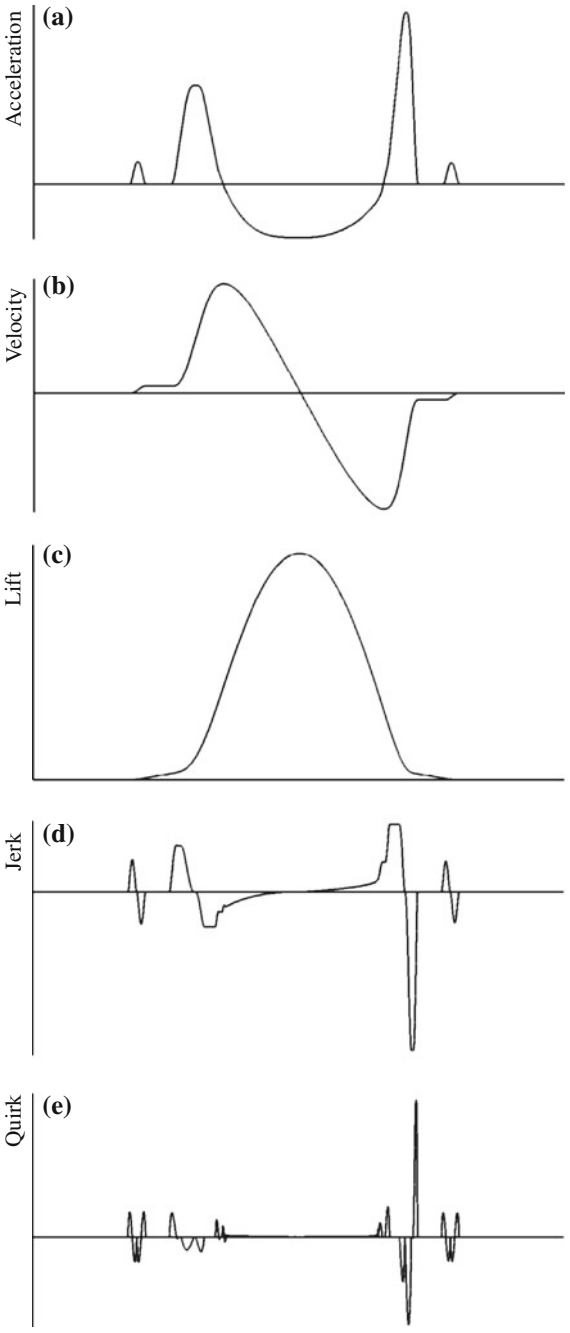


**Fig. 1.1** **a** Valve acceleration. This is the primary cam design curve. **b** Valve velocity. This is obtained by integrating the acceleration. **c** Valve lift curve. This is obtained by integrating the velocity. **d** Valve jerk curve. This is obtained by differentiating the acceleration. **e** Valve quirk curve. This is obtained by differentiating the jerk


**Fig. 1.2** A simple ramp. This is a poor design

### *1.2.1 The Opening Ramp*

When the engine is cold there will be an initial tappet clearance which will close as the engine achieves running temperature. Wear can also increase this tappet clearance. It is therefore necessary to provide an initial ramp to gently take up the tappet clearance before the lift curve begins. At the start of the ramp the acceleration should begin smoothly.

If the designer were to start the initial ramp with constantly increasing lift, for example, then the acceleration at the start would be a Dirac spike as shown in Fig. 1.2. Mathematically the Dirac Delta Function is a spike of infinite height and infinitesimally small width, which when integrated has an area equal to the change in velocity. This would imply that there would be a flat of very small width. In practice this is not realisable as the digital information supplied to the grinding machine is at finite intervals and the laws of motion do not permit a sufficiently fast response by the grinding machine. The result is a small section which has a large radius of curvature, which in turn still gives a short period of high acceleration and the associated higher derivatives of the acceleration will also be large. This will still look like a short flat on the finished cam, which may cause concern when the cam is subsequently inspected, and will cause high contact loads for a short period.

The preferred method for this initial section of the ramp is a smooth increase in acceleration from zero to a maximum value followed by a smooth decrease to zero or a lower positive value. The remainder of the ramp will be a region of lower acceleration, which in the analysis given below is either constant or zero, as shown in Fig. 1.3. Other forms for this section can be adopted. At the end of the ramp the lift is specified by the designer, and is dependent upon the tappet clearance and experience.

### *1.2.2 The Closing Ramp*

The closing ramp shape is basically a mirror image of the opening ramp, and a similar procedure to that outlined above is required. However in some high performance engines the forces associated with the deceleration of the valve as it returns to its seat can significantly shorten the length of the valve stem, especially if the diameter of the stem is small, and the mass of the head of the valve is large. There is therefore a possibility that the valve may hit the seat with a relatively high velocity which may lead to damage to the valve seat or to fracture of the valve

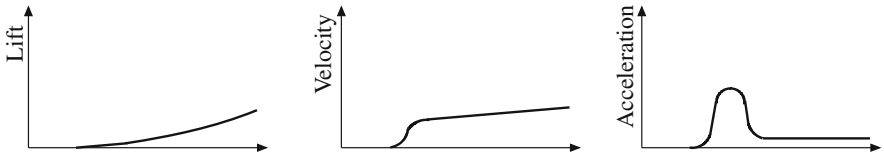


**Fig. 1.3** A good ramp design. There are no sudden changes in acceleration

stem. In order to avoid this, the designer needs to increase the closing ramp height, and this requires an estimate of the stiffness of the valve mechanism. This stiffness can perhaps best be measured using a valve and camshaft assembled in the cylinder head, but without the valve spring. A progressively increasing and then decreasing load should then be applied, while the valve is held open by the cam. The load can be measured by a load cell and the displacement by a dial gauge. The resulting load—displacement curve will probably be non-linear and exhibit significant hysteresis. Some judgement is then needed in deciding an appropriate value for an approximate linear stiffness. Although this may seem rather imprecise, it is unlikely that a more precise procedure would be justified. By examining the approximate elastic displacement and the associated velocity curve as the valve approaches its seat the designer can obtain a better estimate of the required closing ramp height. The cam design method advocated here is otherwise for a rigid system apart from spring stiffness. More detailed modelling to simulate the elastic dynamic response of the mechanism and spring surge is not considered here.

### *1.2.3 Cam Lift and Dwell*

The values of lift and dwell are dependent on the engine size and application. Better gas flow can be achieved by designing asymmetric cam lift curves.

## 1.3 Forces and Cam Tribology

The designer needs to know any relevant forces acting on components of the cam mechanism, together with contact stresses between some components and the oil entrainment velocity. The detailed calculation of these quantities will depend on the type of cam mechanism.

The spring controlled part of the curve needs to be designed for efficient use of the energy stored in the spring. While ignoring any spring surge effects, a curve of cam angle against the limiting speed for positive contact force during the spring controlled part of the curve will show how well this part of the acceleration curve has been designed. Some allowance needs to be made in the case of metallic springs for spring surge and settlement, and for friction and rotation of the ends of the springs, as all these effects reduce the force tending to close the valve.

A metallic spring will not reliably produce the force–deflection curve obtained from a quasi-static test. Over a period of time if the engine is left with a valve open the spring will tend to settle and some of the initial fitted compressive force will be lost. When a valve opens at high engine speed the ends of the spring may rotate relative to the spring platform and retainer. This results in a lower effective spring rate and lower natural frequencies than those for a spring with fixed ends. The tribology of the rubbing surfaces at the ends of the valve springs is complex and very difficult to model accurately. The frictional behaviour is highly non-linear, and will vary with wear. Simulation of these effects is therefore of limited value.

## 1.4 Implementation

The advent of personal computers and the wide availability of software for programming in a variety of languages have together transformed the cam design process. It is now possible to produce interactive programs which have graphical user interfaces. These permit the designer to rapidly ascertain the effect of the relevant design parameters on the resulting cam design. The cam design process is a complex constrained optimisation which requires experience and judgement to obtain good results. To obtain a well designed program the program writer needs an understanding of the influence of the design parameters, the design process and the manufacturing processes required. The cam designer needs knowledge of the strengths of available materials, and suitable surface treatments, to ensure the final design can be manufactured economically and that it will perform reliably.

## 1.5 Cam Mechanisms for Automotive Applications

There is a considerable range of mechanisms, which have been employed over the years, but not all of them will have been analysed, as before the widespread use of digital computers, much design relied of intuition and experience. The following cam follower mechanisms are those most widely currently employed.

### *1.5.1 The Flat Translating Follower or Inverted Bucket*

This is the most common cam mechanism, it is one of the simplest analytically, and also amongst the cheapest to manufacture. A typical design is shown in Fig. 1.4. There are however some disadvantages with this design. In order to adjust the valve clearance a range of variable thickness shims or biscuits is required. It is usually easy to avoid problems due to poor oil entrainment, but high contact stresses on the nose of the cam, especially at low engine speeds can lead to scuffing failure when running-in.

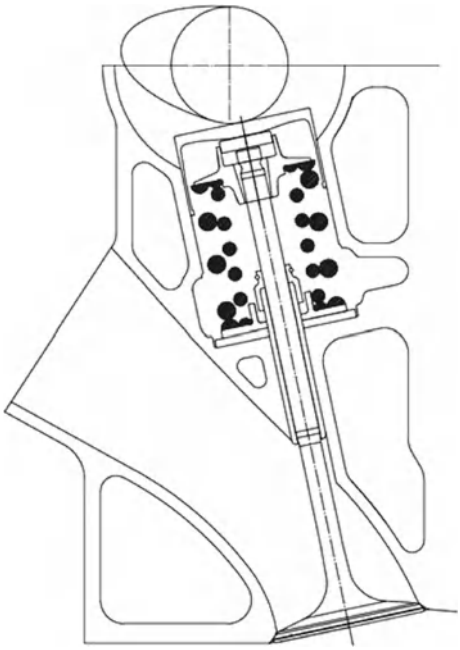

**Fig. 1.4** A flat translating cam follower. *Note* The double interference valve springs. *Courtesey* Graham Langham

One disadvantage compared to other designs is that there is a limit to the maximum valve speed, as this is directly related to the required tappet diameter. To some extent this problem can be reduced by extending the region of low acceleration in the region of maximum velocity, or having a period of zero acceleration, which results in a corresponding period of constant maximum velocity. The centre of the tappet is often offset slightly from the cam centre line to induce tappet rotation, which reduces wear.

### *1.5.2 The Curved Translating Follower*

This mechanism can have a circular cylindrical contact surface which is free to rotate about its axis, which is parallel to the cam axis, or a contact surface which is part of a cylinder, as shown in Fig. 1.5. Either of these can have an axis of translation which is in line with the axis of cam rotation or is offset.

A rotating follower is likely to have to be of small diameter to avoid excessive mass, and this can give rise to large pressure angles and resultant transverse forces, which may be reduced on one side by offsetting the follower. The small diameter will tend to result in higher contact stresses. It has the advantage that there should be lower frictional losses and lubrication should not be a problem.

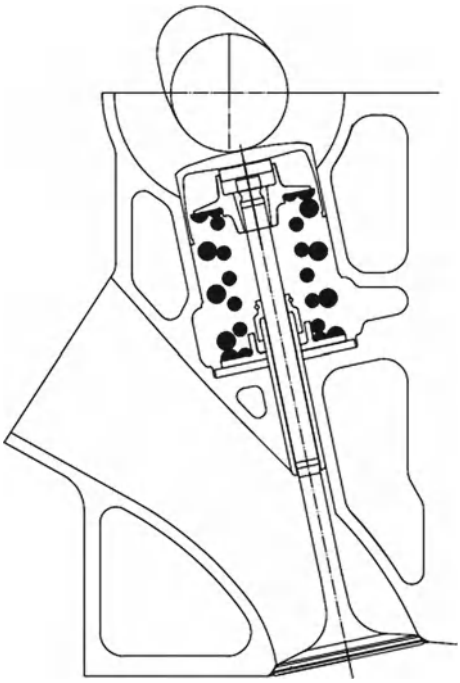

**Fig. 1.5** A curved translating cam follower. The cam is slightly concave on one flank. *Courtesey* Graham Langham

A follower whose contact surface is part or whole of a cylinder has to be constrained to remain aligned to the direction of cam rotation to maintain line contact. Again there may be problems with high transverse forces if the follower radius is too small, but the problem with maximum valve speed is reduced, and a more compact follower can be made. This may permit the designer to have four valves per cylinder with higher valve lift than would be possible with a flat tappet, if the space between the cylinder bores is limited with a consequent limitation on tappet bore size.

### *1.5.3 The Curved Finger Follower*

This mechanism shown in Fig. 1.6 offers some advantages over other mechanisms but is more expensive to manufacture and requires more complex calculations. The advantages are that the effective mass of the follower can be less than that of a translating follower, and the maximum cam velocity does not usually present a problem in terms of a maximum pressure angle. This is therefore the preferred mechanism for high performance engines, but has been widely adopted for other internal combustion engines. The mechanism can be made more compact as the cam lift can be less than the valve lift and rubbing speeds can be reduced when

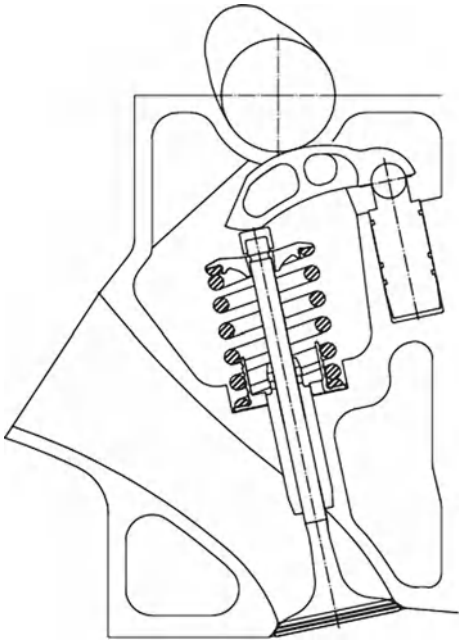

**Fig. 1.6** A curved finger follower. *Note* The single valve spring and concave flank. *Courtesey* Graham Langham

high valve lifts are required, but contact forces will be increased. This mechanism can present tribological problems if care is not taken to ensure good oil entrainment between cam and follower. The solution to this problem may require a smaller follower radius with consequent higher contact stresses. This may then necessitate the use of higher quality steels for both cam and follower.

The pressure angle for the cam shown in Fig. 1.8b is shown in Fig. 1.7. The maximum and minimum values of pressure angle can be used by the designer to ensure that the follower pad is sufficiently large. An allowance should be made to accommodate cams with larger valve lift and higher valve velocity which can then be used without need for new followers.

Some CNC cam grinding machines will not accept X $\sim$ Y or R $\sim$ $\theta$ coordinates, and the cam shape data has to be transformed into corresponding data for a radially translating curved follower. The asymmetry of the mechanism results in two differing sets of data for opposite directions of cam rotation. A similar transformation may also be required for an offset translating curved follower.

## 1.6 The Effect of Follower Radius on Cam Shape

Another advantage of a flat follower is that all cams will be convex, as shown in Figs. 1.4 and 1.8a. This means that a large grinding wheel can be used for manufacture. The wheel wears more slowly and does not have to be dressed so often.

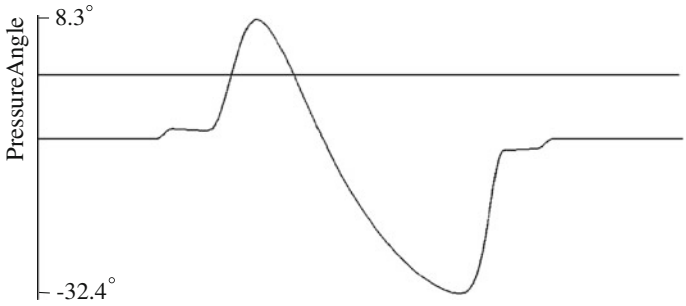


**Fig. 1.7** Pressure angle for a finger follower cam. Note it is not zero on the base circle

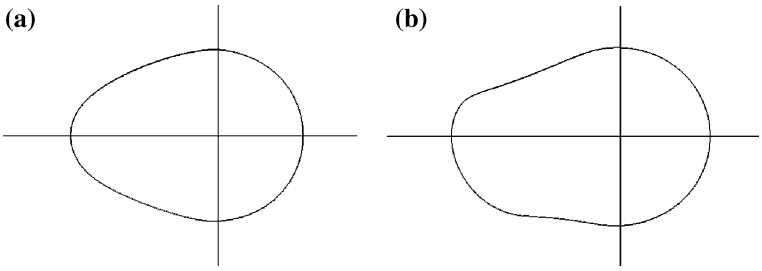


**Fig. 1.8** **a** A convex cam **b** A concave cam

Curved followers such as those shown in Figs. 1.5 and 1.6 can have one or both flanks concave. This is especially the case with small radii in conjunction with high rates of valve acceleration which can result in concave cam flanks with small minimum radii of curvature. To avoid undercutting these will require very small radius grinding wheels for accurate manufacture and such small wheels tend to wear relatively quickly. The small radii can also result in high contact stresses, which may result in surface pitting due to higher contact stresses causing fatigue failure, or scuffing during the initial running in period.

## 1.7 Quantities Required by the Cam Designer

When designing the valve lift curve the designer should ensure that the jerk and the quirk are minimised within the constraints imposed by performance requirements. In order to assess the suitability of a design for a given application, the designer needs to consider the minimum radii of the cam, the consequent contact stresses, at low speed, when spring forces tend to predominate, and at high speed where the inertia forces are large. During the spring controlled part of the lift curve the maximum speed without loss of contact between cam and follower should be as high as possible to optimise the energy stored in the spring.

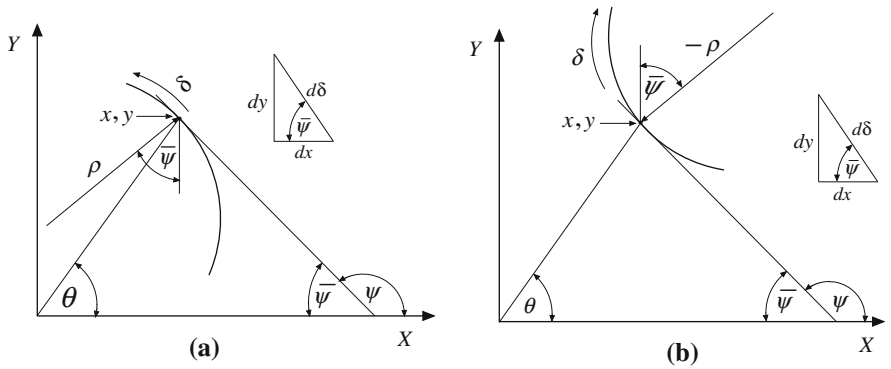


**Fig. 1.9** **a** A convex surface. **b** A concave surface

For curved finger followers the oil entrainment velocity should always be considered to ensure adequate lubrication. The pivot forces should also be reviewed. For relatively flexible mechanisms such as those involving push-rods, the flexibility and consequent oscillatory response needs to be investigated using a simulation program and rig tests, where the behaviour of the mechanism can be viewed using a stroboscope.

## 1.8 Elementary Concepts for Curvature

### *1.8.1 Notation*

| | |
|---|---|
| $x, y$ | Coordinates of contact point |
| $\delta$ | Distance around cam |
| $\theta$ | Angle of cam rotation |
| $\rho$ | Radius of curvature |
| $\overline{\psi}$ | Angle of tangent at point of contact |

### *1.8.2 Curvature*

With notation of Fig. 1.9a, and using Leibnitz's notation for derivatives:

For a convex surface, at $x, y$ as $y$, $\theta$, and $\delta$ increase, $x$ and $\overline{\psi}$ decrease.

Considering an infinitesimal length of the curve $d\delta$ we can write:

$$\cos\overline{\psi} = -\frac{dx}{d\delta} \tag{1.1}$$

and

$$\sin\overline{\psi} = \frac{dy}{d\delta} \tag{1.2}$$

and

$$\rho = -\frac{d\delta}{d\overline{\psi}} \tag{1.3}$$

Hence from Eqs. (1.1) and (1.3):

$$\rho\cos\overline{\psi} = \frac{dx}{d\overline{\psi}} \tag{1.4}$$

and from Eqs. (1.2) and (1.3):

$$\rho\sin\overline{\psi} = -\frac{dy}{d\overline{\psi}} \tag{1.5}$$

With notation of Fig. 1.9b:
For a concave surface, at $x, y$ as $y$, $\overline{\psi}$, $\theta$, and $\delta$ increase, $x$ decreases.
Considering an infinitesimal length of the curve $d\delta$ we can again write:

$$\cos\overline{\psi} = -\frac{dx}{d\delta} \tag{1.1}$$

and

$$\sin\overline{\psi} = \frac{dy}{d\delta} \tag{1.2}$$

As $\rho$ is now negative:

$$-\rho = \frac{d\delta}{d\overline{\psi}} \tag{1.6}$$

Hence from Eqs. (1.1) and (1.6):

$$\rho\cos\overline{\psi} = \frac{dx}{d\overline{\psi}} \tag{1.7}$$

and from Eqs. (1.2) and (1.6):

$$\rho\sin\overline{\psi} = -\frac{dy}{d\overline{\psi}} \tag{1.8}$$

Equations (1.7) and (1.8) are the same as Eqs. (1.4) and (1.5). Therefore the same curvature equations apply for convex and concave surfaces.

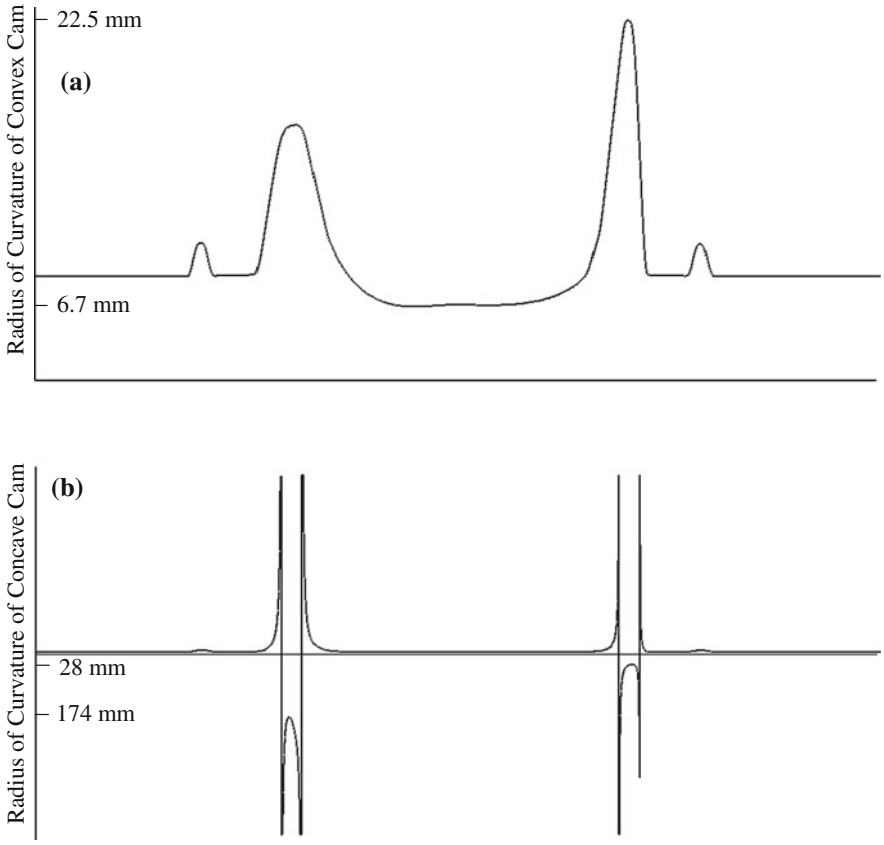


**Fig. 1.10** **a** Radius of curvature of a convex cam **b** Radius of curvature of a concave cam

The convex cam shape shown in Fig. 1.8a is for a flat follower cam whose acceleration diagram is shown in Fig. 1.1a. The radius of curvature is shown in Fig. 1.10a. The largest radius of curvature is 22.5 mm on the closing flank and the smallest radius of curvature of 6.7 mm occurs just before the nose. The larger radii of curvature are associated with periods of higher positive acceleration.

Figure 1.10b shows the curvature of the concave cam shape shown in Fig. 1.8b which has the same acceleration diagram as the previous cam, but for a curved finger follower. For a concave cam at a point of contra-flexure, the radius of curvature tends to infinity. This can occasionally cause floating point overflow when computing curvatures, but use of double precision arithmetic helps to avoid this problem. In Fig. 1.10b the maximum and minimum values of radius have been limited to 500 mm. The two minimum radii of curvature are −174 and −28 mm.

As mentioned previously, it is much easier and cheaper to grind a convex cam as the grinding wheel diameter can be large and consequently wears more slowly and requires dressing less often. In the particular case of this concave cam flank,

the grinding wheel radius would need to be significantly less than 28 mm to prevent under cutting and such a small wheel would need frequent dressing. It is therefore preferable for the designer to avoid such small negative radii.

## 1.9 Cam Torque

The cam torques shown in Fig. 1.11a, b are both for the flat follower cam shown in Fig. 1.5a. Whereas the positive and negative torques shown in Fig. 1.11a are roughly equal in magnitude, in Fig. 1.11b the greater inertia force due to higher valve accelerations at higher engine speeds has resulted in larger torques, which combined with a higher maximum acceleration on the closing side has resulted in a negative torque of even greater magnitude than the opening torque. The work done is proportional to the area under the torque curve and ignoring any frictional effects the two areas are equal and the net work done over one revolution is zero. In practice there are large frictional effects, which lead to significant power dissipation at higher engine speeds.

For most automotive applications including some racing engines the effects of inertia loads at high engine speeds are not sufficiently large to cause any problems. However for high speed engines such as those used in Formula One and Indy Cars, cam torques can be produced at higher speeds due to inertia forces, which for certain combinations of V-angle and cam timing add together to produce large oscillatory torques. These can produce forced torsional vibrations of the valve train and may then cause significant changes in valve motion relative to the crankshaft and may result in valve-piston contact, and consequent engine failure.

Since the advent of the Fast Fourier Transform these torques can easily be analysed in terms of engine orders and the largest orders, for a V8 for example, are usually, 4, 8, and 12. A Sarazin and Chilton [1, 2] reactive damper can be used to damp the more dominant orders, although design for the 12th and higher orders is increasingly difficult.

## 1.10 The Concept of Entrainment Velocity

To introduce the concept of entrainment velocity it is helpful to initially consider the two contra-rotating contiguous disks as shown in Fig. 1.12. (Some machines used for tribological research are of this nature.) The velocities of the point of contact are given by

$$V_{c1} = R_1 \omega_1 \tag{1.9}$$

and

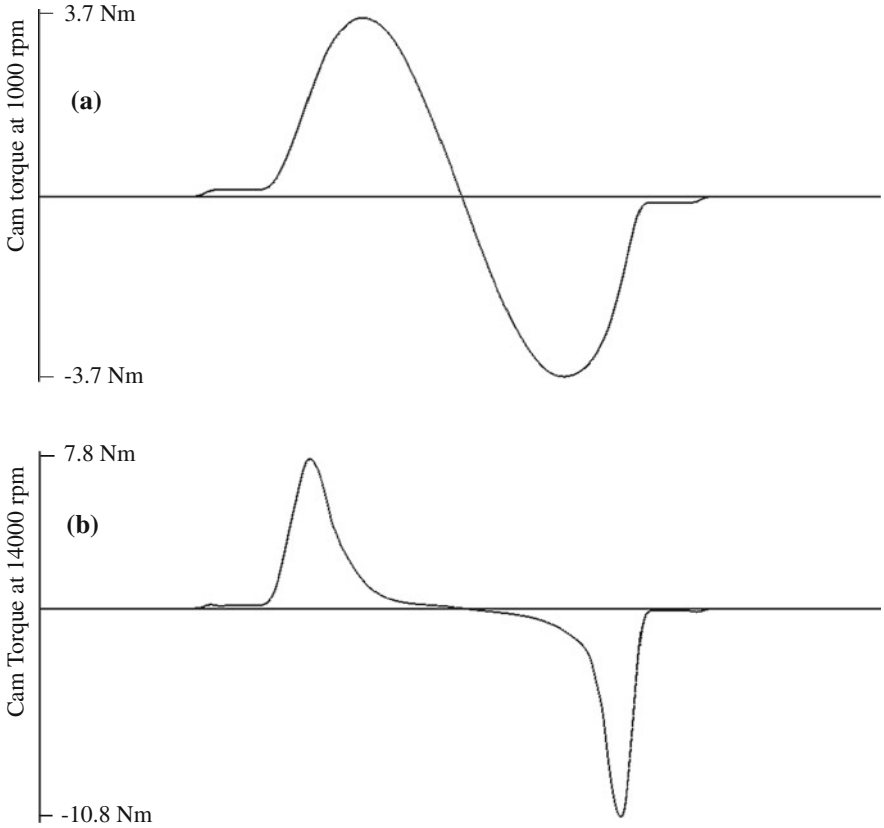


**Fig. 1.11** **a** Cam torque at 1,000 rpm **b** Cam torque at 14,000 rpm

$$V_{c2} = R_2\omega_2 \tag{1.10}$$

where $R_1$ and $R_2$ are the radii of the disks, while $\omega_1$ and $\omega_2$ are the angular velocities in radians/s. If the conjunction is submerged in oil, then the oil will be entrained by viscous effects and will aid the formation of an oil film. The sliding velocity between the two surfaces is:

$$V_{slide} = V_{c1} - V_{c2} \tag{1.11}$$

The entrainment velocity is:

$$V_{ent} = V_{c1} + V_{c2} \tag{1.12}$$

or

$$V_{ent} = \frac{V_{c1} + V_{c2}}{2} \tag{1.13}$$

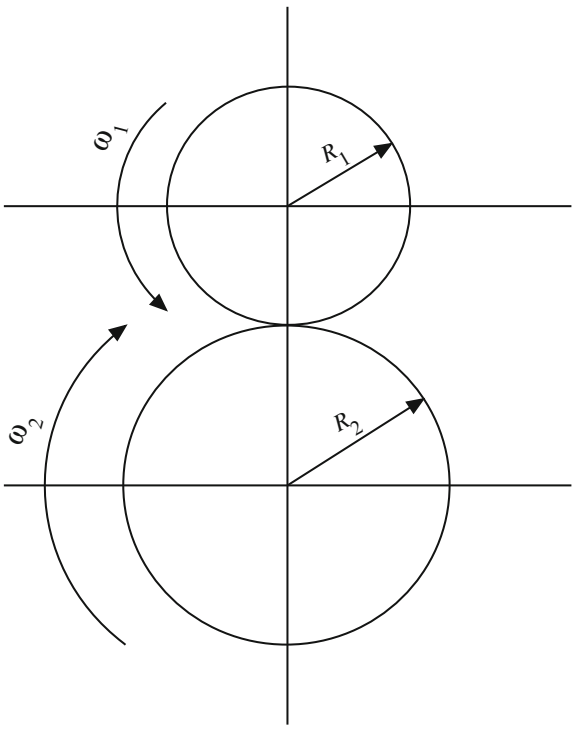


**Fig. 1.12** Fluid entrainment between two cylinders

Both these definitions are to be found in the literature. The first will be used here. When supplying entrainment velocity data to anyone else it is important to specify which definition has been adopted.

If the direction of rotation of one of the disks is reversed then there is the possibility that

$$V_{ent} = V_{c1} + V_{c2} = 0 \tag{1.14}$$

In this situation no oil will be entrained and any force acting between the disks will squeeze the oil film until the film thickness is a similar magnitude to the surface roughness, and it is then likely that scuffing will occur.

### *1.10.1 Oil Entrainment for a Flat Translating Follower*

For a flat follower it is possible, in the case of some geometries, that the entrainment velocity becomes very small or is instantaneously zero. Any appreciable period with poor oil entrainment can lead to premature wear of cam and follower. In Fig. 1.13a there are two areas where the entrainment velocity is small or zero. This is for a flat follower cam with a base circle radius of 12.5 mm. This would, however, be an acceptable design.

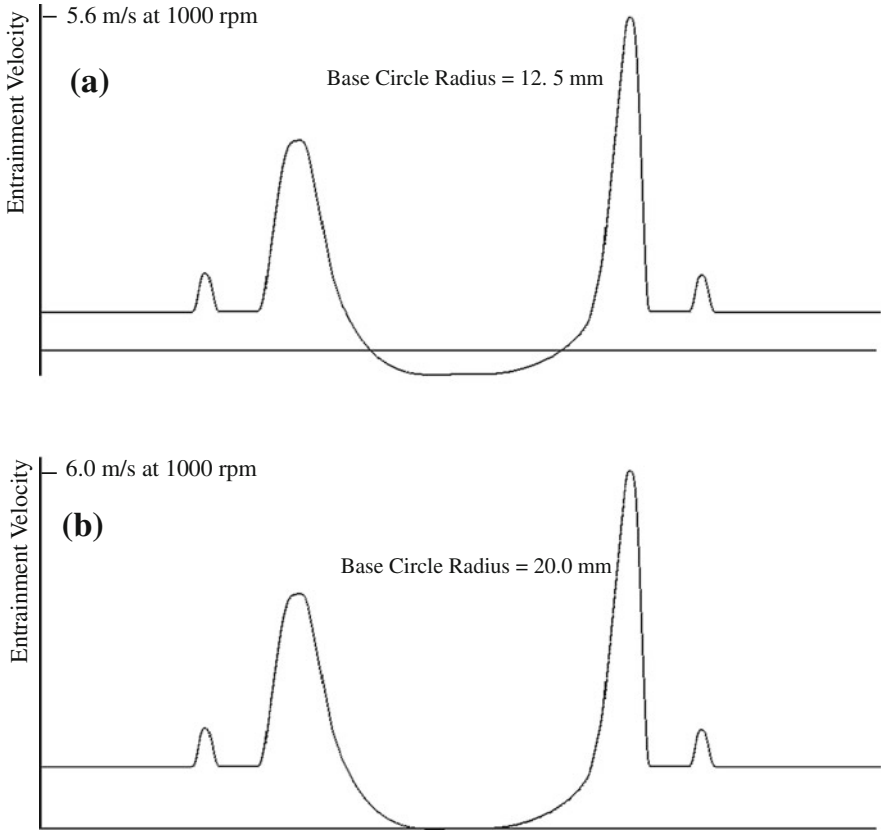


**Fig. 1.13** **a** Good oil entrainment **b** Poor oil entrainment

In Fig. 1.13b the base circle radius has been increased to 20.0 mm and there is a long period on the nose of the cam where the entrainment velocity was very small or zero. This design would be prone to scuffing on the nose of the cam and damage to the follower in the contact area. This example is somewhat contrived as a base circle radius of 12.5 mm is a far better choice, and a value of 20.0 mm would not normally be chosen by the designer for a cam with this cam lift and dwell.

### *1.10.2 Oil Entrainment for a Curved Finger Follower*

For some other cam mechanisms, in particular the curved finger follower, the periodic reversals of the follower velocity allow the possibility of periods when the entrainment velocity becomes very small or is instantaneously zero. Dyson [3] showed that any appreciable period with poor oil entrainment can lead to premature wear of cam and follower.

The best solution to this problem is usually to decrease the follower radius. This will lead to higher contact stresses, which may require better quality substrate material of higher yield stress, (to prevent surface pitting), for both cam and follower, with consequent higher cost. The alternative is to increase the follower radius, which results in a period of negative entrainment velocity, and also gives two short periods of very low entrainment velocity.

## 1.11 Forces for Translating Followers

### *1.11.1 Notation*

| | |
|---|---|
| $A$ | Effective area of piston in pneumatic spring |
| $F_C$ | Contact force between cam and follower |
| $F_I$ | Inertia force |
| $F_V$ | Force acting along valve axis |
| $F_S$ | Spring force |
| $k$ | Spring rate |
| $M_E$ | Effective mass of valve, spring and retainer etc. |
| $n$ | Polytropic process exponent |
| $P_0$ | Gas pressure with valve closed |
| $P$ | Gas pressure at lift, $s$ |
| $s$ | Valve lift |
| $s_0$ | Spring compression with valve closed |
| $\ddot{s}$ | Valve acceleration |
| $V_0$ | Cylinder volume with valve closed |
| $V$ | Cylinder volume with valve at lift $s$ |
| $\beta$ | Pressure angle |

### *1.11.2 Contact Force*

For a metallic spring the spring force is:

$$F_S = k(s_0 + s) \tag{1.15}$$

and for a pneumatic spring:

$$V = V_0 - A.s \tag{1.16}$$

Assuming polytropic processes for compression and expansion:

$$P = P_0\left(\frac{V_0}{V}\right)^n \tag{1.17}$$

Hence the spring force is:

$$F_S = P.A \tag{1.18}$$

The inertia force is:

$$F_I = M_E\ddot{s} \tag{1.19}$$

The total valve force is therefore:

$$F_V = F_S + F_I \tag{1.20}$$

For simplicity assume that the radial valve angle is zero, i.e. the valve axis is in the same plane as the motion of the follower. The pressure angle, $\beta$, can now be defined as the angle between the valve axis and the direction of motion of the follower. (In the case of a flat follower the pressure angle, $\beta = 0$.) The contact force is therefore:

$$F_C = \frac{F_V}{\cos\beta} \tag{1.21}$$

## 1.12 Contact Stresses

### *1.12.1 Notation*

| | |
|---|---|
| $E_C$ | Young's modulus for cam material |
| $E_F$ | Young's modulus for follower material |
| $E^*$ | Contact modulus |
| $F_C$ | Contact force between cam and follower |
| $P^*$ | Force per unit width of line contact |
| $w$ | Width of line contact between cam and follower |
| $\beta$ | Pressure angle |
| $v_C$ | Poisson's ratio for cam material |
| $v_F$ | Poisson's ratio for follower material |
| $\rho_C$ | Radius of curvature of cam at line of contact |
| $\rho_F$ | Radius of curvature of follower |
| $\rho^*$ | Effective radius of curvature |
| $\sigma_{Hz}$ | Hertzian contact stress |

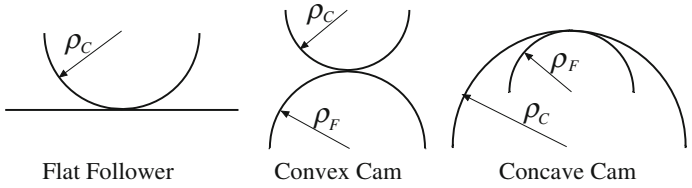


**Fig. 1.14** Contact surfaces

### *1.12.2 Contact Modulus*

The force per unit width of contact is:

$$P^* = \frac{F_C}{w} \tag{1.22}$$

and the contact modulus, $E^*$, is given by

$$\frac{1}{E^*} = \frac{1 - v_C^2}{E_C} + \frac{1 - v_F^2}{E_F} \tag{1.23}$$

### *1.12.3 Effective Radius of Curvature*

The effective radius of curvature, $\rho^*$, is given by

$$\frac{1}{\rho*} = \frac{1}{\rho_1} + \frac{1}{\rho_2} \tag{1.24}$$

With notation of Fig. 1.14:
For a flat follower, $\rho_F \to \infty$, hence:

$$\rho^* = \rho_C \tag{1.25}$$

For a curved follower and a convex cam:

$$\rho^* = \frac{\rho_C \rho_F}{\rho_C + \rho_F} \tag{1.26}$$

For a curved follower and a convex or a concave cam:

$$\rho^* = \left| \frac{\rho_C \rho_F}{\rho_C + \rho_F} \right| \tag{1.27}$$

The contact stress is given by:

$$\sigma_{Hz} = \left[\frac{P^* E^*}{\pi \rho^*}\right]^{\frac{1}{2}} \tag{1.28}$$

As an example, consider the contact stress for a cam with a flat follower. At low engine speeds the inertia forces are small and the maximum contact force is mainly due to the valve spring which is a maximum on the nose. The radius of curvature tends to be a minimum at or near the nose. The contact stress is therefore highest near the nose at low speeds as shown in Fig. 1.15a which is at an engine speed of 1,000 rpm. For this reason it is sometimes advisable to initially run-in an engine at a higher engine speed, say 2,000 rpm to avoid scuffing.

At higher engine speeds the inertia forces become more dominant and the periods of maximum contact force are associated with maximum acceleration. Figure 1.15b shows the contact stress for the same flat follower cam mechanism at 14,000 rpm.

## 1.13 Kinetics of Plane Motion of a Rigid Body

### *1.13.1 Notation*

| | |
|---|---|
| $F_C$ | Cam force |
| $F_V$ | Valve force |
| $I_{CG}$ | Polar moment of inertia about centre of mass, G |
| $I_P$ | Polar moment of inertia about pivot |
| $L_C$ | Distance from follower pivot, P, to line of action of cam force |
| $L_V$ | Distance from follower pivot, P, to line of action of valve force |
| $M_F$ | Mass of cam follower |
| $P_X$ | Pivot reaction force in x-direction |
| $P_Y$ | Pivot reaction force in y-direction |
| $R_G$ | Distance from follower pivot, P, to centre of mass of follower, G |
| $\alpha$ | Angle of line PG to x-axis |
| $\beta$ | Angle of line of action of cam force to x-axis |
| $\theta$ | Angular displacement of follower |
| $\dot{\theta}$ | Angular velocity of follower |
| $\ddot{\theta}$ | Angular acceleration of follower |

To obtain the cam force and the reactions at the pivot for a finger follower consider the kinetics of a rigid body rotating in a plane X,Y about a point, P. Figure 1.16 shows a simplified diagram of a finger follower. The line of action of the valve force is in the y-direction. The inertia forces, due to the acceleration of the follower can be considered to act at the centre of mass, G. In this section Newton's notation is used for derivatives with respect to time.

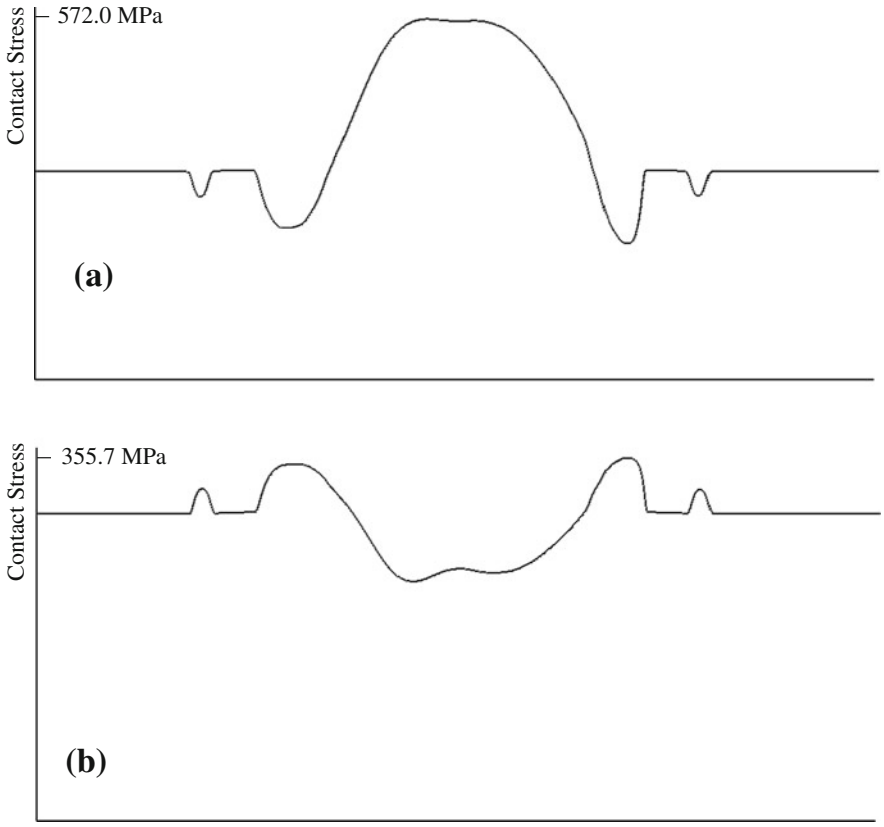


**Fig. 1.15** **a** Contact stress at 1,000 rpm **b** Contact stress at 14,000 rpm

Recall d'Alembert's principle and Newton's laws of motion. Resolving the forces in the x and y directions and summing the moments of the forces acting about the pivot, P gives three equations in three unknown quantities, the forces acting at the pivot and the contact force between cam and follower

Taking moments about the pivot:

$$L_C F_C = L_V F_V + M_F R_G^2 \ddot{\theta} + I_{CG} \ddot{\theta} = L_V F_V + I_P \ddot{\theta} \tag{1.29}$$

The Cam Force is given by

$$F_C = \frac{L_V F_V + I_P \ddot{\theta}}{L_C} \tag{1.30}$$

Forces in x-direction:

$$P_X = F_C \cos\beta + M_F R_G \left( \ddot{\theta} \sin\alpha - \dot{\theta}^2 \cos\alpha \right) \tag{1.31}$$

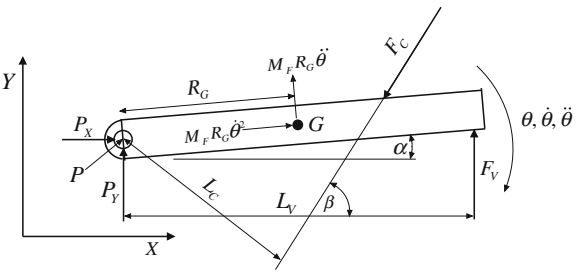


**Fig. 1.16** Rigid body rotating about pivot

Forces in y-direction:

$$P_Y = F_C \sin\beta - M_F R_G\left(\ddot{\theta}\cos\alpha + \dot{\theta}^2 \sin\alpha\right) - F_V \tag{1.32}$$

## 1.14 Maximum Speed to Maintain Cam Contact for Translating Flat Follower

### *1.14.1 Notation*

| | |
|---|---|
| $F_C$ | Cam force |
| $F_S$ | Spring force |
| $k$ | Spring stiffness |
| $M_E$ | Mass of follower, valve, shim, cotters, top spring retainer and effective spring mass |
| $N$ | Rotational speed of engine in rpm |
| $s_0$ | Spring compression valve closed |
| $s$ | Valve lift |
| $\ddot{s}$ | Valve acceleration in m/radian$^2$ |

The units are SI except where stated.

### *1.14.2 Calculation of Engine Speed for Zero Cam Force*

Recall that the spring force $F_s$ is given by

$$F_S = k(s_0 + s) \tag{1.15}$$

The valve acceleration is usually computed in mm/s$^2$ and the valve velocity in mm/s. When the data is transferred to the program for designing the cam mechanism it is preferable to change the valve acceleration to m/radian$^2$ and the valve

velocity is converted into m/radian. This ensures that curvatures, for example, are computed in m.

For a flat follower the cam force is given by

$$F_C = M_E \ddot{s} + F_S \tag{1.33}$$

In Eq. (1.33), if the acceleration is in m/radian$^2$, it will be necessary to convert this to m/s$^2$ and then if the mass is in kg then the inertia force will be in N. Engine speeds are usually considered in rpm, and therefore for this calculation the conversion from m/radian$^2$ to m/s$^2$ needs to incorporate the engine speed in rpm.

At an engine speed of $N$ rpm, the camshaft speed is $\frac{N}{2}\frac{360}{60} = 3N$ degrees/s

$$= 3N\frac{\pi}{180} = \frac{\pi N}{60} \text{ radians/s.}$$

Hence:

$$F_C = \ddot{s}\left(\frac{\pi N}{60}\right)^2 M_E + F_S \tag{1.34}$$

If the contact force between cam and follower, $F_C = 0$ then:

$$F_S = -\ddot{s}\left(\frac{\pi N}{60}\right)^2 M_E \tag{1.35}$$

Hence the maximum speed to maintain contact is:

$$N = \frac{60}{\pi}\sqrt{\frac{-F_S}{\ddot{s}M_E}} \tag{1.36}$$

*Note* This speed should only be computed when the valve acceleration is negative, as the number whose square root is required must be positive.

It is important for the designer to try and obtain the maximum use from the energy stored in the spring. The curve of speed versus cam angle during the deceleration period should therefore be as flat as possible. An example of an acceptable curve is shown in Fig. 1.17.

### *1.14.3 Spring Stiffness*

In the present analysis the spring stiffness has been assumed to be linear. Valve springs are often wound with a variable pitch to give a non-linear relation between spring compression and natural frequency to reduce spring surge. A static compression test will result in a non-linear relationship between load and deflection. This can be included in the analysis and the program. The linear equation:

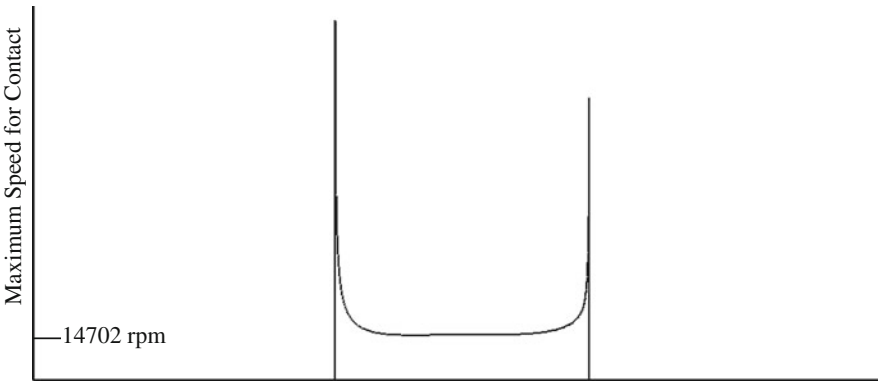


**Fig. 1.17** Maximum speed for cam and follower contact in rpm

$$F_S = k(s_0 + s) \tag{1.15}$$

Can be replaced by a non-linear equation:

$$F_S = k_1(s_0 + s) + k_2(s_0 + s)^n \tag{1.37}$$

where $n \neq 1$.

This may only provide an approximation to the measured curve which may also exhibit some slight hysteresis. Any further attempt to compute a more accurate value for the spring force is not worthwhile as when subject to the rapid changes in length when the engine is running at high speed the ends of the spring tend to rotate rather than stay fixed. This not only leads to wear on the ends of the spring but wear on the valve spring platform. This rotating motion is very difficult to measure accurately and tends to be very non-linear. There is little to be gained in attempting to model the motion as it will vary with wear and engine temperature. The effect of this rotation is to reduce the effective spring stiffness compared to that measured during a quasi-static test, when the ends of the spring do not usually rotate. Additional loss in applied spring load can result from settlement over time. These effects will result in lowering the speed at which contact will be maintained between cam and follower.

The effect of torsional oscillation of the camshaft is considered in Appendix 6. If the oscillations are sufficiently large the cam timing can be altered sufficiently to cause contact between valve and piston, and small oscillations which will tend to reduce the maximum speed at which contact can be maintained will only have a small effect, but this will be much less serious than consequent errors in valve timing which can cause valve piston contact.

## 1.15 Desmodromic Cam Mechanisms

Desmodromic cam mechanisms employ a second cam to provide the force for negative acceleration instead of a spring. This second cam is frequently and erroneously described as the closing cam. In practice both cams share control of the opening and closing processes. One particular type is still used in Ducati Motorcycle Engines. This employs two finger follower cams. Another mechanism was used in the Mercedes-Benz competition engines which raced in the mid 1950s, [4]. This mechanism had a positive acceleration cam with a curved translating follower, and the negative acceleration cam had a finger follower. The 1950s OSCA MT4 competition sports car had one version of the engine with desmodromic valve gear similar in some respects to that used by Ducati. This has recently been raced in classic car competitions.

The advantage with this type of cam mechanism is that spring surge and settlement are no longer problems, and at low speeds the contact forces tend to be lower. At higher speeds with a conventional cam mechanism, the spring force tends to offset the inertia force but this does not occur with desmodromic mechanisms, and the contact forces continue to rise with the square of the speed. In the engine speed range in which Formula One engines operate, the friction may exceed that for a mechanism with a pneumatic spring.

These desmodromic mechanisms need to be very carefully manufactured and assembled to prevent jamming of the mechanism. As a consequence, if significant component wear occurs there can be a need for frequent maintenance, although with better surface coatings and modern lubricants, this may become unnecessary. At present, this class of cam mechanism is not widely used, but there have been several patent applications in the last decade, and these mechanisms may become more widely used. These mechanisms will not be considered further in this book, but designers of this class of mechanism should be aware of the contents of Sect. 8.5.

## 1.16 A Note on Units

### *1.16.1 Units for Data Input*

Data is best input in the units which the designer usually uses for the relevant quantity, although some preferred units may vary with the designer.

Mass in kg, this is usually acceptable even though the valve mass will be in g.
Time in s
Valve lifts in mm
Spring rate in N/mm
Valve mechanism stiffness in kN/mm
Engine speeds in rpm.

Length in mm. Some designers, but not all, still prefer thousandths of an inch for valve clearances, and many engine builders still use a set of Imperial feeler gauges.
Area in $mm^2$
Volume in $mm^3$
Angle in degrees
Mass moment of inertia in $kgmm^2$
Gas pressure in MPa
Contact stress in MPa
Elastic modulus in GPa

### *1.16.2 Units for Calculations*

For forces, stresses and velocities:

Mass in kg
Lengths in m
Time in s
Angles in radians
Forces in N
Engine speeds in radians/s
Valve velocity in m/s
Valve acceleration in $m/s^2$
Stresses in Pa
Entrainment velocity in m/s

For curvatures and follower dimensions:

Valve velocity in m/radian
Valve acceleration in $m/radian^2$

For maximum contact speed:

Velocities in m/radian
Accelerations in $m/radian^2$

These are then multiplied by a function of engine speed in rpm to produce m/s and $m/s^2$ respectively.

*Note* The equations derived in Chaps. 2 and 3 are usually computed with the cam angles specified in degrees and the dimensions in mm. The lift is then given in mm, the valve velocity in mm per degree, and the valve acceleration in mm per $degree^2$.

To convert mm per degree to mm per radian multiply by $180/\pi$, and to convert mm per $degree^2$ to mm per $radian^2$, multiply by $(180/\pi)^2$.

### *1.16.3 Units for Data Output*

Time in s
Valve acceleration in km/s$^2$
Maximum engine speed for cam contact in rpm
Entrainment velocity in m/s
Radius of curvature in mm
Pressure angle in degrees
Contact stress in MPa
Forces in kN

## References

1. Sarazin GF (1937) US Patent 2079226, May 1937
2. Chilton R (1939) US Patent 2184734, Dec 1939
3. Dyson A (1980) Kinematics and wear patterns of cam and finger follower automotive valve gear. Tribology Int. June 13(3):121–132
4. Ludvigsen, K (1995) Mercedes Benz Quicksilver Century. Transport Bookman Publications, Photograph, p 353 and drawing p 373. ISBN:0 85184 051 5

# Chapter 2
# Elementary Cam Lift Curve Synthesis

**Abstract** This chapter describes the derivation and piece-wise integration of the first half of an analytically simple valve acceleration curve. Two simultaneous algebraic equations are obtained. The first equates an expression for the velocity on the nose of the cam to zero, and the second the sum of the increments of valve lift to the maximum specified lift. The two unknowns are the maximum positive acceleration, which is on the flank of the cam and the maximum negative acceleration, which is on the nose of the cam. The two equations can then be solved for these two unknown quantities. This example has been chosen for analytical simplicity, to demonstrate the method, but such an acceleration curve would not result is a good cam design with smooth valve acceleration, and should not be used in practice. A superior and useable, but analytically more complex acceleration curve is considered in the next chapter.

## 2.1 Introduction

Some of the concepts of cam lift curve synthesis were described in Chap. 1. Over the years many methods of obtaining the acceleration diagram have been used and the method described below and refined in Chap. 3 is only one of these. The example given here has been chosen for its analytical simplicity, but this type of acceleration curve should not be used in practice, as it is not a good one.

It has been said that misconceptions tend to harden into axioms, and the simple example given below is based on a method which was surprisingly still being used by at least one company for cam design in the early 1980s. The use of some cams designed with especially rapid changes in acceleration, or jerk, resulted in considerable valve spring surge and consequent spring failures, which then resulted in destruction of much of the engine. However, despite the difficulties in synthesising

J. J. Williams, *Introduction to Analytical Methods for Internal Combustion Engine Cam Mechanisms*, DOI: 10.1007/978-1-4471-4564-6_2, © Springer-Verlag London 2013

acceptably smooth cam lift curves before the advent of digital computers, they were produced and used, but this was very time consuming.

The use of cams exhibiting significant jerk with push rod mechanisms or other mechanisms subject to relatively flexible behaviour can result in a loss of cam–follower contact, which will impair reliability and power output. This sort of cam will also be far more likely to induce valve spring surge in otherwise stiffer mechanisms which apart from valve spring failure will again result in a loss of cam–follower contact at a lower engine speed. Unstable behaviour of the cam mechanism may lead to valve clash, damage to the piston, valve and valve seat, or loss of power due to poor gas flow, or a combination of these undesirable effects.

## 2.2 An Elementary Cam Lift Curve

The cam lift curve is obtained by designing an acceleration curve and then integrating to obtain a velocity curve and then a lift curve. It is convenient to divide the curve into two parts, the opening half and a closing half. These two parts meet on the nose, and at this point the curves need to be smoothly continuous. In fact we shall require them to be continuously differentiable.

For this initial example it is helpful to consider a curve with few components and consisting of analytically simple sections, with discontinuous rates of change of acceleration. A more realistic example is considered later, but this has more sections and is more complicated and the amount of algebra involved tends to mask the basic method.

When the engine is assembled it is necessary to specify a tappet clearance, $s_0$, to allow for thermal expansion of the valve stem when the engine is at working temperature. If there were no initial clearance then the valve would not be closed, when the tappet was touching the cam's base circle. It is necessary to take up this initial clearance as smoothly as possible, and one solution might be to have a ramp of length, $T_0$, linearly increasing lift to a height of $s_0$ at $T_0$.

Derivatives with respect to time are denoted in this chapter using Newton's dot notation. The slope of this ramp, $\dot{s}_0$, would then be, given by: $\dot{s}_0 = s_0/T_0$. Unfortunately, this results in an instantaneous change in the velocity, $\dot{s}_0$, which would require an infinite acceleration for an infinitesimally small time, as described in Sect. 1.2.1. This, so-called Delta function, would not be realised in practice but such a ramp design is best avoided, as the jerk needs to be as small as possible. For this initial example let the ramp have a constant acceleration, $A_0$, as shown in Fig. 2.1. The notional tappet clearance, $s_0$, is specified by the designer.

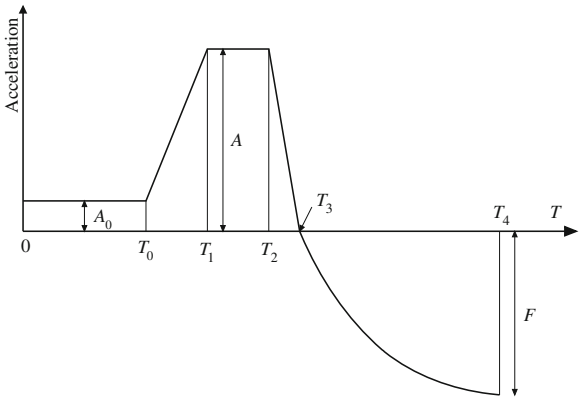


**Fig. 2.1** An elementary acceleration diagram

### 2.2.1 Notation

| | |
|---|---|
| $A$ | Maximum acceleration |
| $\bar{A}$ | Parameter defined in text |
| $\hat{A}$ | Parameter defined in text |
| $A_0$ | Initial ramp height |
| $\hat{A}_0$ | Parameter defined in text |
| $F$ | Maximum deceleration |
| $\hat{F}$ | Parameter defined in text |
| $L$ | Maximum lift |
| $s$ | Lift |
| $s_0$ | Lift at end of ramp, tappet clearance |
| $t$ | Time |
| $T$ | Time interval |

### 2.2.2 An Elementary Acceleration Curve

After the initial ramp the next three sections are linear and the final section consists of a quarter sine wave. Although this would not be an acceptable design in practice, it will permit a minimum of mathematics and will therefore be easier to follow the method. By splitting the acceleration curve into sections and integrating twice we can obtain two equations in two unknowns, $A$ and $F$. At $T_4$ the velocity is zero and the valve lift, $L$, is specified by the designer. The slope of the acceleration curve at $T_4$ is $\dddot{s}_4 = 0$.

The acceleration curve shown in Fig. 2.1 has discontinuities in slope at $0$, $T_0, T_1, T_2$ and $T_3$, which cause large instantaneous changes in the rate of change

of acceleration or jerk. This will lead to surging and premature failure of metallic coil valve-springs, and a tendency for instabilities in the motion of cam mechanisms with low elastic stiffness such as those involving push-rods. At very high camshaft speeds, even stiff mechanisms with pneumatic valve springs can have a tendency to behave in an unstable manner, if there are significantly large values of jerk. There is also insufficient flexibility to permit the designer to optimise his design, and the use of a section which is a quarter sine-wave will not allow the energy stored in the spring to be used efficiently to maintain contact between follower and cam; this limits the maximum engine speed that can safely be used before contact is lost between cam and tappet.

By considering each section in turn the equation for the acceleration is integrated twice and the constants of integration determined from the initial boundary conditions for each section.

***Constant Acceleration Ramp.*** $0 \leq t \leq T_0$, $0 \leq T \leq T_0$

With notation of Fig. 2.1:

Integrating Eq. (2.1) twice w.r.t. $t$:

$$\ddot{s} = A_0 \tag{2.1}$$

$$\dot{s} = A_0 t \tag{2.2}$$

$$s = \frac{A_0 t^2}{2} \tag{2.3}$$

At $t = T_0$:

$$\ddot{s} = \ddot{s}_0 = A_0 \tag{2.4}$$

$$\dot{s}_0 = A_0 T_0 \tag{2.5}$$

$$s = s_0 = \frac{A_0 T_0^2}{2} \tag{2.6}$$

Hence:

$$A_0 = \frac{2s_0}{T_0^2} \tag{2.7}$$

As $s_0$ and $T_0$ are specified by the designer, $A_0$ can be determined.

***Linearly Increasing Acceleration.*** $T_0 \leq t \leq T_1$, $T_0 \leq T \leq T_1$

$$\ddot{s} = A_0 + \frac{(A - A_0)t}{T_1} \tag{2.8}$$

Integrating Eq. (2.8) twice w.r.t. $t$:

$$\dot{s} = \dot{s}_0 + A_0 t + \frac{(A - A_0)t^2}{2T_1} \tag{2.9}$$

$$s = s_0 + \dot{s}_0 t + \frac{A_0 t^2}{2} + \frac{(A - A_0)t^3}{6T_1} \tag{2.10}$$

At $t = T_1$:

$$\ddot{s} = \ddot{s}_1 = A \tag{2.11}$$

$$\dot{s} = \dot{s}_1 = \dot{s}_0 + \frac{A_0 T_1}{2} + \frac{A T_1}{2} \tag{2.12}$$

$$s = s_1 = s_0 + \dot{s}_0 T_1 + \frac{A_0 T_1^2}{3} + \frac{A T_1^2}{6} \tag{2.13}$$

***Constant Acceleration.*** $T_1 \leq t \leq T_2$, $T_1 \leq T \leq T_2$

$$\ddot{s} = A \tag{2.14}$$

Integrating Eq. (2.14) twice w.r.t. $t$:

$$\dot{s} = s_1 + At \tag{2.15}$$

$$s = s_1 + \dot{s}_1 t + \frac{At^2}{2} \tag{2.16}$$

At $t = T_2$:

$$\ddot{s} = \ddot{s}_2 = A \tag{2.17}$$

$$\dot{s} = \dot{s}_2 = \dot{s}_1 + AT_2 \tag{2.18}$$

$$s = s_2 = s_1 + \dot{s}_1 T_2 + \frac{AT_2^2}{2} \tag{2.19}$$

***Linearly Decreasing Acceleration.*** $T_2 \leq t \leq T_3$, $T_2 \leq T \leq T_3$

$$\ddot{s} = A\left(1 - \frac{t}{T_3}\right) \tag{2.20}$$

Integrating Eq. (2.19) twice w.r.t. $t$:

$$\dot{s} = \dot{s}_2 + A\left(t - \frac{t^2}{2T_3}\right) \tag{2.21}$$

$$s = s_2 + \dot{s}t + A\left(\frac{t^2}{2} - \frac{t^3}{6}\right) \tag{2.22}$$

At $t = T_3$:

$$\ddot{s}_3 = 0 \tag{2.23}$$

$$\dot{s}_3 = \dot{s}_2 + \frac{AT_3}{2} \tag{2.24}$$

$$s_3 = s_2 + \dot{s}_2 T_3 + \frac{AT_3^2}{3} \tag{2.25}$$

***Sinusoidal Deceleration.*** $T_3 \leq t \leq T_4,\ T_3 \leq T \leq T_4$

$$\ddot{s} = -F \sin\left(\frac{\pi t}{2T_4}\right) \tag{2.26}$$

Integrating Eq. (2.25) twice w.r.t.$t$:

$$\dot{s} = \dot{s}_3 - F\left(\frac{2T_4}{\pi}\right)\left[1 - \cos\left(\frac{\pi t}{2T_4}\right)\right] \tag{2.27}$$

$$s = s_3 + \dot{s}_3 t - F\left(\frac{2T_4}{\pi}\right)^2\left[\frac{\pi t}{2T_4} - \sin\left(\frac{\pi t}{2T_4}\right)\right] \tag{2.28}$$

At $t = T_4$:

$$\ddot{s}_4 = -F \tag{2.29}$$

The velocity on the nose is zero therefore:

$$\dot{s}_4 = \dot{s}_3 - \frac{2FT_4}{\pi} = 0 \tag{2.30}$$

The maximum lift is specified by the designer hence:

$$s_4 = s_3 + \dot{s}_3 T_4 - F\frac{4T_4^2}{\pi^2}\left(\frac{\pi}{2} - 1\right) = L \tag{2.31}$$

***Solution of Equations for* A *and* F**. The equations for $\dot{s}_4$ and $s_4$ have two unknowns, $A$ and $F$. By substituting Eqs. (2.5), (2.12), and (2.18) into Eq. (2.30) and after some algebra, we can write:

$$\dot{s}_4 = A_0\left[T_0 + \frac{T_1}{2}\right] + A\left[\frac{T_1 + T_3}{2} + T_2\right] - \frac{2FT_4}{\pi} = 0 \tag{2.32}$$

Let:

$$\bar{A}_0 = A_0\left(T_0 + \frac{T_1}{2}\right) \tag{2.33}$$

and

$$\bar{A} = \left(\frac{T_1 + T_3}{2} + T_2\right) \tag{2.34}$$

Substituting Eqs. (2.6), (2.13) and (2.19) into (2.33) together with Eqs. (2.5), (2.12) and (2.18) into Eq. (2.32), and after further lengthy back substitutions and algebra, we can write:

$$\begin{aligned} s_4 = {} & A_0\left[\frac{T_0^2}{2} + T_0(T_1 + T_2 + T_3 + T_4) + \frac{T_1^2}{3} + \frac{T_1}{2}(T_2 + T_3 + T_4)\right] \\ & A\left[\frac{T_1^2}{6} + \frac{T_2^2}{2} + \frac{T_3^2}{3} + \frac{T_1}{2}(T_2 + T_3 + T_4) + T_2(T_3 + T_4) + \frac{T_3 T_4}{2}\right] \\ & - F\frac{4T_4^2}{\pi^2}\left(\frac{\pi}{2} - 1\right) = L \end{aligned} \tag{2.35}$$

Let:

$$\hat{A}_0 = A_0\left[\frac{T_0^2}{2} + T_0(T_1 + T_2 + T_3 + T_4) + \frac{T_1^2}{3} + \frac{T_1}{2}(T_2 + T_3 + T_4)\right] \tag{2.36}$$

and

$$\hat{A} = A\left[\frac{T_1^2}{6} + \frac{T_2^2}{2} + \frac{T_3^2}{3} + \frac{T_1}{2}(T_2 + T_3 + T_4) + T_2(T_3 + T_4) + \frac{T_3 T_4}{2}\right] \tag{2.37}$$

When simplifying lengthy algebraic equations, it is helpful to equate some expressions to new parameters. This makes the analysis simpler to follow and when writing computer code this makes for shorter expressions and reduces coding errors. By considering the individual increments of the equations the simplification process can be made more easily which results in less likelihood of terms being missed and errors made. The method given below may not be necessary for the present example, but is used in Chap. 3 where the acceleration diagram is more complex.

From Eq. (2.5):

$$dV_0^{A_0} = A_0 T_0 \tag{2.38}$$

From Eq. (2.6):

$$dS_0^{A_0} = \frac{A_0 T_0^2}{2} \tag{2.39}$$

From Eq. (2.12):

$$dV_1^{A_0} = \frac{A_0 T_1}{2} \tag{2.40}$$

$$dV_1^{A} = \frac{A T_1}{2} \tag{2.41}$$

$$dv_1 = \frac{dV_1^{A}}{A} \tag{2.42}$$

From Eq. (2.13):

$$dS_1^{A_0} = \frac{A_0 T_1^2}{3} \tag{2.43}$$

$$dS_1^{A} = \frac{A T_1^2}{6} \tag{2.44}$$

$$ds_1 = \frac{dS_1}{A} \tag{2.45}$$

From Eq. (2.18):

$$dV_2 = A T_2 \tag{2.46}$$

$$dv_2 = \frac{dV_2}{A} \tag{2.47}$$

From Eq. (2.19):

$$dS_2 = \frac{A T_2^2}{2} \tag{2.48}$$

$$ds_2 = \frac{dS_2}{A} \tag{2.49}$$

From Eq. (2.24):

$$dV_3 = \frac{A T_3}{2} \tag{2.50}$$

$$dv_3 = \frac{dV_3}{A} \tag{2.51}$$

From Eq. (2.25):

$$dS_3 = \frac{A T_3^2}{3} \tag{2.52}$$

$$ds_2 = \frac{dS_2}{A} \tag{2.53}$$

From Eq. (2.30):

$$dV_4 = \frac{-2FT_4}{\pi} \tag{2.54}$$

$$dv_4 = \frac{dV_4}{F} \tag{2.55}$$

From Eq. (2.31):

$$dS_4 = \frac{-4FT_4^2}{\pi^2}\left(\frac{\pi}{2} - 1\right) \tag{2.56}$$

$$ds_4 = \frac{dS_4}{F} \tag{2.57}$$

Let:

$$\Sigma V^{A_0} = V_0^{A_0} + V_1^{A_0} \tag{2.58}$$

Let:

$$\Sigma V^{A} = A(dv_1 + dv_2 + dv_3) \tag{2.59}$$

Let:

$$\Sigma S^{A_0} = dS_0^{A_0} + dS_1^{A_0} + dV_0^{A_0}(T_1 + T_2 + T_3 + T_4) + dV_1^{A_0}(T_2 + T_3 + T_4) \tag{2.60}$$

Let:

$$\Sigma S^{A} = A\left[ds_1^A + ds_2^A + ds_3^A + dv_1^A(T_2 + T_3 + T_4) + dv_2^A(T_3 + T_4) + dv_3^A T_4\right] \tag{2.61}$$

Equation (2.30) can be written as:

$$\dot{s}_4 = \Sigma V^{A_0} + \Sigma V^{A} - \frac{2FT_4}{\pi} \tag{2.62}$$

Equation (2.31) can be written as:

$$S_4 = \Sigma S^{A_0} + \Sigma S^{A} - \frac{4FT_4^2}{\pi^2}\left(\frac{\pi}{2} - 1\right) \tag{2.63}$$

Evaluation of Eqs. (2.59) and (2.60) confirm Eqs. (2.37) and (2.38):

$$\Sigma V^{A_0} = \bar{A}_0 = A_0\left(T_0 + \frac{T_1}{2}\right) \tag{2.64}$$

$$\Sigma V^{A} = \bar{A} = \left(\frac{T_1 + T_3}{2} + T_2\right) \tag{2.65}$$

Evaluation of Eqs. (2.66) and (2.67) confirm Eqs. (2.37) and (2.38):

$$\Sigma S^{A_0} = \hat{A}_0 = A_0\left[\frac{T_0^2}{2} + T_0(T_1 + T_2 + T_3 + T_4) + \frac{T_1^2}{3} + \frac{T_1}{2}(T_2 + T_3 + T_4)\right] \tag{2.66}$$

$$\Sigma S^{A} = \hat{A} = A\left[\frac{T_1^2}{6} + \frac{T_2^2}{2} + \frac{T_3^2}{3} + \frac{T_1}{2}(T_2 + T_3 + T_4) + T_2(T_3 + T_4) + \frac{T_3 T_4}{2}\right] \tag{2.67}$$

Substituting Eqs. (2.33) and (2.34) into Eq. (2.32):

$$\dot{s}_4 = \bar{A}_0 + A\bar{A} - \frac{2FT_4}{\pi} = 0 \tag{2.32}$$

$$F = \frac{\pi(\bar{A}_0 + A\bar{A})}{2T_4} \tag{2.68}$$

Substituting Eqs. (2.36) and (2.37) into Eq. (2.35):

$$s_4 = \hat{A}_0 + A\hat{A} - F\frac{4T_4^2}{\pi^2}\left(\frac{\pi}{2} - 1\right) = L \tag{2.69}$$

Hence:

$$A\hat{A} = L - \hat{A}_0 + \frac{\pi(\bar{A}_0 + A\bar{A})}{2T_4}\frac{4T_4^2}{\pi^2}\left(\frac{\pi}{2} - 1\right) \tag{2.70}$$

Let:

$$\hat{F} = \frac{2T_4}{\pi}\left(\frac{\pi}{2} - 1\right) \tag{2.71}$$

From Eqs. (2.70) and (2.71):

$$A = \frac{L - \hat{A}_0 + \hat{F}\bar{A}_0}{\hat{A} - \hat{F}\bar{A}} \tag{2.72}$$

$$F = \frac{\pi\left[\bar{A}_0 + \bar{A}\left(L - \hat{A} + \hat{F}\bar{A}_0\right)\right]}{2T_4\left(\hat{A} - \bar{A}\hat{F}\right)} \tag{2.73}$$

Having solved these equations for the parameters $A$ and $F$, we can compute the lift velocity, and acceleration for each section of each curve. When initially checking a program the velocity on the nose should be identically zero and the computed maximum lift should agree with the specified value.

The parameters acceleration, velocity and lift can then be obtained for each section of the curve in turn using a new loop for each section. Other errors in the program may be found by checking that the values of the parameters give continuous curves at the joints between sections. Any discontinuities will indicate where to look for an error.

# Chapter 3
# Low Jerk Cam Lift Curve

**Abstract** In Chap. 2 the derivation and integration of a simple acceleration curve, was described with the warning that it should not be used in practice. This chapter gives a smoother but analytically more complex acceleration curve, which gives the designer considerable flexibility. The four parts in the previous example has been expanded to fourteen. These parts are alternately straight lines and fifth order polynomials. The straight lines define the slope and the coordinates at the end of each part, and the first derivative of the slope is zero at the ends of the polynomial parts. Each part or interval is integrated twice to obtain the velocity and lift. Again on the nose of the cam the valve lift is known as it is specified by the designer and the velocity is zero. This again permits the solution of two equations in two unknowns. The other side of the cam is designed separately and then mirrored. To ensure a smooth transition on the nose the negative acceleration on the nose is also specified by the designer. This chapter is very repetitive in a sense, and the algebra is protracted and may be hard to follow in places. Although this acceleration curve may seem to be unnecessarily complex, in the writer's experience this sort of curve is needed to produce a good design.

## 3.1 Introduction

In Chap. 2 an elementary method for cam synthesis was described, which although simple was not suitable for use in practice. There is a need to obtain a practical cam lift curve, which will enable the designer to optimise the design and produce a cam, which will have the required characteristics and perform well. It will also be necessary to produce a cam design which can be manufactured without any undue difficulty. The cam must have the required lift and dwell while the rate of change of acceleration, the jerk, should be minimised, to ensure a smooth acceleration curve, and a stable dynamic performance of the mechanism.

J. J. Williams, *Introduction to Analytical Methods for Internal Combustion Engine Cam Mechanisms*, DOI: 10.1007/978-1-4471-4564-6_3, © Springer-Verlag London 2013

The optimisation process requires small changes in the appropriate parameters, which can be specified by the designer, and this effectively requires a very flexible acceleration diagram. The procedure required to derive such a curve may seem unnecessarily tedious and complex, but experience has shown that this procedure provides the designer with a very flexible means of valve lift curve synthesis. This is needed to permit the designer to adjust the many parameters which have to be optimised to achieve a good design.

## 3.2 A Low Jerk Cam Lift Curve

### *3.2.1 Notation*

| | |
|---|---|
| $a$ | First constant in fifth order polynomial |
| $b$ | Second constant in fifth order polynomial |
| $c$ | Third constant in fifth order polynomial |
| $d$ | Fourth constant in fifth order polynomial |
| $e$ | Fifth constant in fifth order polynomial |
| $f$ | Sixth term in fifth order polynomial |
| $A$ | Parameter quantifying acceleration |
| $A_0$ | Acceleration at end of initialramp |
| $F$ | Parameter quantifying deceleration |
| $\hat{F}$ | Parameter defined in text |
| $L$ | Maximum Lift |
| $s$ | Lift |
| $s_0$ | Lift at end of ramp, tappet clearance |
| $t$ | Time |
| $T$ | Time interval |
| $\Gamma$ | Function defined in text |
| $\Delta$ | Function defined in text |
| $\varepsilon$ | Fraction of Acceleration |
| $\lambda$ | Fraction of Deceleration |

### *3.2.2 Fifth Order Polynomial*

In order to join together sections of linearly varying acceleration, curves are needed which match the coordinates of the adjacent ends of the sections to be joined and their respective slopes and possibly higher derivatives of the acceleration as well. Cook, 2004, private communication investigated three polynomials for this task, a cubic, a fifth order, and a seventh order. A fifth order polynomial is

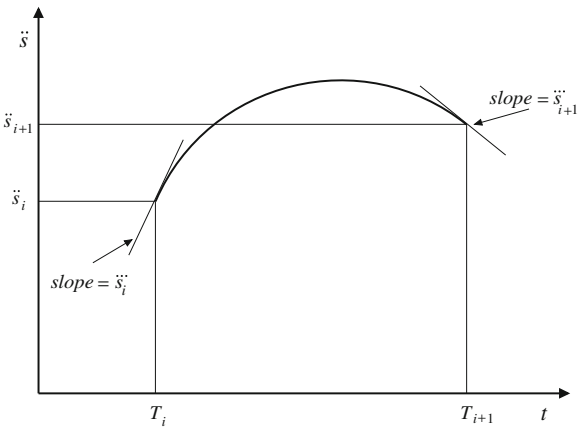


**Fig. 3.1** Fifth order polynomial

well suited to these requirements and is shown schematically in Fig. 3.1. In this section derivatives with respect to $t$ are denoted by dots, as used originally by Newton. This derivation of the method is given in full, in order to show the complexity of a practical lift curve design analysis. While it is tedious and involves a considerable amount of algebra, it is suitable for use in a program implemented on a modern personal computer, and with a suitable graphical user interface is the basis for a very useful design tool.

The derivation of a fifth order polynomial and the implementation to describe part of the acceleration curve does not involve any advanced mathematics, but it is somewhat lengthy.

Consider an interval given by: $0 \leq t \leq T_{i+1}$ and $T_i \leq T \leq T_{i+1}$

Let the acceleration be denoted by $\dddot{s}$. We can now define the acceleration over an interval from $t = T_i$ to $t = T_{i+1}$ as:

$$\ddot{s}(t) = a_{i+1} + b_{i+1}t + c_{i+1}t^2 + d_{i+1}t^3 + e_{i+1}t^4 + f_{i+1}t^5 \tag{3.1}$$

The boundary conditions can be used to evaluate the constants in the polynomial.

At $t = 0$: denote $\ddot{s}(0)$ as $\ddot{s}_i$ and at $t = T_{i+1}$: denote $\ddot{s}(T_{i+1})$ as $\ddot{s}_{i+1}$.

From Eq. (3.1), at $t = 0$:

$$a_{i+1} = \ddot{s} \tag{3.2}$$

and at $t = T_{i+1}$:

$$\ddot{s}(T_{i+1}) = a_{i+1} + b_{i+1}T_{i+1} + c_{i+1}T_{i+1}^2 + d_{i+1}T_{i+1}^3 + e_{i+1}T_{i+1}^4 + f_{i+1}T_{i+1}^5 \tag{3.3}$$

Differentiating $\ddot{s}_i$ in Eq. (3.1)

$$\dddot{s}(t) = b_{i+1} + 2c_{i+1}t + 3d_{i+1}t^2 + 4e_{i+1}t^3 + 5f_{i+1}t^4 \tag{3.4}$$

At $t = T_0$ derivative is called the jerk and it is the slope of the acceleration curve.

At $t = 0$: denote $\dddot{s}(0)$ as $\dddot{s}_i$ and at $t = T_{i+1}$: denote $\dddot{s}(T_{i+1})$ as $\dddot{s}_{i+1}$.

From Eq. (3.4), at $t = 0$:

$$b_{i+1} = \dddot{s}_i \tag{3.5}$$

and at $t = T_{i+1}$:

$$\dddot{s}(T_{i+1}) = b_{i+1} + 2c_{i+1}T_{i+1} + 3d_{i+1}T_{i+1}^2 + 4e_{i+1}T_{i+1}^3 + 5f_{i+1}T_{i+1}^4 \tag{3.6}$$

Differentiating $\dddot{s}_i$ in Eq. (3.4):

$$\ddddot{s}(t) = 2c_{i+1} + 6d_{i+1}t + 12e_{i+1}t^2 + 20f_{i+1}t^3 \tag{3.7}$$

This derivative will be called the quirk.

At $t = 0$: denote $\ddddot{s}(0)$ as $\ddddot{s}_i$ and at $t = T_{i+1}$: denote $\ddddot{s}(T_{i+1})$as $\ddddot{s}_{i+1}$

From Eq. (3.7), at $t = 0$:

$$c_{i+1} = \frac{\ddddot{s}_i}{2} \tag{3.8}$$

and at $t = T_{i+1}$:

$$\ddddot{s}(T_{i+1}) = 2c_{i+1} + 6d_{i+1}T_{i+1} + 12e_{i+1}T_{i+1}^2 + 20f_{i+1}T_{i+1}^3 \tag{3.9}$$

After some algebra, following Cook, 2004, private communication the remaining constants, $d_{i+1}, e_{i+1}$ and $f_{i+1}$ can be expressed as:

$$d_{i+1} = \frac{1}{T_{i+1}}\left[\frac{2}{T_{i+1}}\left\{\frac{5(\ddot{s}_{i+1} - a_{i+1})}{T_{i+1}} - \left(2\dddot{s}_{i+1} + 3b_{i+1}\right)\right\} + \frac{\ddddot{s}_{i+1}}{2} - 3c_{i+1}\right] \tag{3.10}$$

$$e_{i+1} = \frac{1}{T_{i+1}}\left[\frac{1}{T_{i+1}}\left\{\frac{(s_{i+1} - b_{i+1})}{T_{i+1}} - \frac{1}{2}\left(\frac{\ddddot{s}_{i+1}}{2} + 3c_{i+1}\right)\right\} - \frac{3d_{i+1}}{2}\right] \tag{3.11}$$

$$f_{i+1} = \frac{1}{5T_{i+1}}\left[\left\{\frac{1}{2T_{i+1}}\left(\frac{\ddddot{s}_{i+1}}{2} + c_{i+1}\right) - 3d_{i+1}\right\} - 3e_{i+1}\right] \tag{3.12}$$

The velocity is obtained by integrating $\ddot{s}_i$ in Eq. (3.1)

$$\dot{s}(t) = \dot{s}_i + a_{i+1}t + \frac{b_{i+1}t^2}{2} + \frac{c_{i+1}t^3}{3} + \frac{d_{i+1}t^4}{4} + \frac{e_{i+1}t^5}{5} + \frac{f_{i+1}t^6}{6} \tag{3.13}$$

and the lift is obtained by integrating $\dot{s}_i$: in Eq. (3.13)

$$s(t) = s_i + \dot{s}_i t + \frac{a_{i+1}t^2}{2} + \frac{b_{i+1}t^3}{6} + \frac{c_{i+1}t^4}{12} + \frac{d_{i+1}t^5}{20} + \frac{e_{i+1}t^6}{30} + \frac{f_{i+1}t^7}{42} \tag{3.14}$$

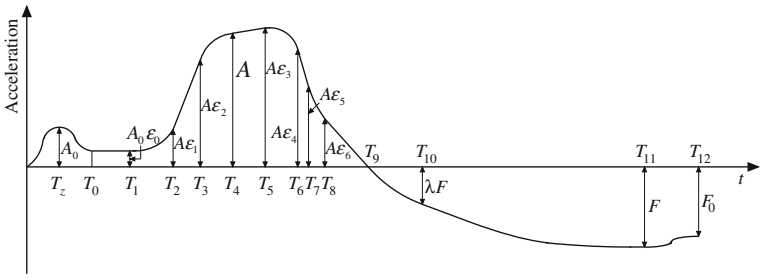


**Fig. 3.2** Low jerk acceleration diagram

In the following analysis the fifth order polynomials are referred to as fillets, after the first two sections of the first ramp, where fifth order polynomials are also used. The fifth order polynomials will be used to join together linear sections to provide a smooth transition between them. Differing forms of polynomial are used in the first two negative acceleration sections to form the acceleration curve with a fillet as the final section. The first two of these polynomial sections have indices which are chosen by the designer to help vary the curve shape and thereby optimise the use of the energy stored in the spring and maximise the speed at which cam-follower contact can be maintained. The individual sections will need to be piecewise continuous, with the same values of acceleration and cam angle at the join. The first and second derivatives of the acceleration curve will also be required to be the same at the join. These derivatives are easily quantified for the straight sections, and these boundary conditions permit the evaluation of the six constants which specify a particular fifth order polynomial. The unknown constants for the other polynomials are also evaluated from knowledge of the boundary conditions at each end.

The acceleration curve is to be made up of a series of sections which are piecewise continuously differentiable, and with second derivatives which are identically zero at the ends of sections. The diagram has been distorted for clarity. In practice the change in deceleration in the last section will usually be smaller than shown in Fig. 3.2, and the change in angle will also be smaller, as it is intended for small changes in deceleration in order to match values of deceleration exactly at the nose, for opening and closing lift curves.

## 3.3 Integration of the Acceleration

With reference to Fig. 3.2:

***The First Part of the First Ramp.*** $0 \le t \le \frac{T_0}{2} \quad 0 \le T \le \frac{T_0}{2}$ where: $\frac{T_0}{2} = T_z$

The polynomial giving the acceleration is:

$$\ddot{s}(t) = a_z + b_z t + c_z t^2 + d_z t^3 + e_z t^4 + f_z t^5 \tag{3.15}$$

Differentiating Eq. (3.15) we obtain the jerk and quirk:

$$\dddot{s}(t) = b_z + 2c_z t + 3d_z t^2 + 4e_z t^3 + 5f_z t^4 \tag{3.16}$$

$$\ddddot{s}(t) = 2c_z + 6d_z t + 12e_z t^2 + 20f_z t^3 \tag{3.17}$$

From the boundary conditions and Eqs. (3.15), (3.16), and (3.17):
At $t = 0 : \ddot{s}_0 = 0, \dddot{s}_0 = 0$, and $\ddddot{s}_0 = 0$
Hence:

$$a_z = 0 \tag{3.18}$$

$$b_z = 0 \tag{3.19}$$

$$c_z = 0 \tag{3.20}$$

At $t = T_z : \ddot{s}_z = A_0, \quad \dddot{s}_z = 0$, and $\ddddot{s}_z = 0$
Substituting these values in Eqs. (3.10), (3.11), and (3.12) we obtain:

$$d_z = \left[\left\{\frac{5(A_0 - 0)}{T_z} - 0\right\}\frac{2}{T_z} + 0\right]\frac{1}{T_z} = \frac{10A_0}{T_z^3} \tag{3.21}$$

$$e_z = \left[\left\{\frac{0}{T_z} - 0\right\}\frac{1}{T_z} - \frac{30A_0}{2T_z^3}\right]\frac{1}{T_z} = -\frac{15A_0}{T_z^4} \tag{3.22}$$

$$f_z = \left[\left\{\frac{0}{T_z} - \frac{30A_0}{T_z^3}\right\}\frac{1}{2T_z} + \frac{45A_0}{T_z^4}\right]\frac{1}{5T_z} = \frac{-3A_0}{T_z^5} + \frac{9A_0}{T_z^5} = \frac{6A_0}{T_z^5} \tag{3.23}$$

Substituting these values for the constants of the polynomials, into Eqs. (3.15), (3.16), and (3.17) gives:

$$\ddot{s} = \frac{10A_0 t^3}{T_z^3} - \frac{15A_0 t^4}{T_z^4} + \frac{6A_0 t^5}{T_z^5} \tag{3.24}$$

Differentiating Eq. (3.24) yields:

$$\dddot{s} = \frac{30A_0 t^2}{T_z^3} - \frac{60A_0 t^3}{T_z^4} + \frac{30A_0 t^4}{T_z^5} \tag{3.25}$$

$$\ddddot{s} = \frac{60A_0 t}{T_z^3} - \frac{180A_0 t^2}{T_z^4} + \frac{120A_0 t^3}{T_z^5} \tag{3.26}$$

Equation (3.21) can be integrated to give the velocity and lift:

$$\dot{s} = \frac{5A_0 t^4}{2T_z^3} - \frac{3A_0 t^5}{T_z^4} + \frac{A_0 t^6}{T_z^5} \tag{3.27}$$

$$s = \frac{A_0 t^5}{2T_z^3} - \frac{A_0 t^6}{2T_z^4} + \frac{A_0 t^7}{7T_z^5} \tag{3.28}$$

At $t = T_z = \frac{T_0}{2}$, from Eqs. (3.24), (3.25), (3.26), (3.27) and (3.28) we obtain:

$$\overset{....}{s}_z = 0 \tag{3.29}$$

$$\overset{...}{s}_z = 0 \tag{3.30}$$

$$\ddot{s}_z = 0 \tag{3.31}$$

$$\dot{s}_z = \frac{A_0 T_0}{4} \tag{3.32}$$

$$s_z = \frac{A_0 T_0^2}{28} \tag{3.33}$$

***The Second Part of the First Ramp***. $0 \le t \le T_0 \quad \frac{T_0}{2} \le T \le T_0$

The method here is similar to the previous section, and will not therefore be described in as much detail.

$$\ddot{s} = a_0 + b_0 t + c_0 t^2 + d_0 t^3 + e_0 t^4 + f_0 t^5 \tag{3.34}$$

$$\dot{s} = \dot{s}_z + a_0 t + \frac{b_0 t^2}{2} + \frac{c_0 t^3}{3} + \frac{d_0 t^4}{4} + \frac{e_0 t^5}{5} + \frac{f_0 t^6}{6} \tag{3.35}$$

$$s = s_z + \dot{s}_z t + \frac{a_0 t^2}{2} + \frac{b_0 t^3}{6} + \frac{c_0 t^4}{12} + \frac{d_0 t^5}{20} + \frac{e_0 t^6}{30} + \frac{f_0 t^7}{42} \tag{3.36}$$

Differentiating Eq. (3.31) we obtain the jerk and quirk:

$$\overset{...}{s} = b_0 + 2c_0 t + 3d_0 t^2 + 4e_0 t^3 + 5f_0 t^4 \tag{3.37}$$

and

$$\overset{....}{s} = 2c_0 + 6d_0 t + 12e_0 t^2 + 20f_0 t^3 \tag{3.38}$$

From the boundary conditions and Eqs. (3.39), (3.32), and (3.33):
At $t = 0 : \ddot{s}_z = A_0, \overset{...}{s}_z = 0, \overset{....}{s}_z = 0$ Hence:

$$a_0 = A_0 \tag{3.39}$$

$$b_0 = 0 \tag{3.40}$$

$$c_0 = 0 \tag{3.41}$$

At $t = T_0 : \ddot{s}_0 = A_0 \varepsilon_0, \quad \overset{...}{s}_0 = 0, \quad \overset{....}{s}_0 = 0$

Substituting these values in Eqs. (3.10), (3.11), and (3.12) we obtain:

$$d_0 = \left[\left\{\frac{5(A_0\varepsilon_0 - A_0)}{T_z} - 0\right\}\frac{2}{T_z} + 0\right]\frac{1}{T_z} = \frac{10A_0(\varepsilon_0 - 1)}{T_z^3} \tag{3.42}$$

$$e_0 = \left[0 - \frac{15A_0(\varepsilon_0 - 1)}{T_z^3}\right]\frac{1}{T_z} = \frac{-15A_0(\varepsilon_0 - 1)}{T_z^4} \tag{3.43}$$

$$\begin{aligned} f_0 &= \left[\left\{\frac{0}{T_z} - \frac{30A_0(\varepsilon_0 - 1)}{T_z^3}\right\}\frac{1}{2T_z} + \frac{45A_0(\varepsilon_0 - 1)}{T_z^4}\right]\frac{1}{5T_z} \\ &= \frac{-3A_0(\varepsilon_0 - 1)}{T_z^5} + \frac{9A_0(\varepsilon_0 - 1)}{T_z^5} = \frac{6A_0(\varepsilon_0 - 1)}{T_z^5} \end{aligned} \tag{3.44}$$

Substituting $\dot{s}_z, s_z, a_0, b_0, c_0, d_0, e_0$ and $f_0$ into Eqs. (3.34), (3.35), (3.36), (3.37), and (3.38) we can write:

$$\ddot{s} = A_0 + \frac{10A_0(\varepsilon_0 - 1)t^3}{T_z^3} + \frac{15A_0(1 - \varepsilon_0)t^4}{T_z^4} + \frac{6A_0(\varepsilon_0 - 1)t^5}{T_z^5} \tag{3.45}$$

$$\dot{s} = \dot{s}_z + A_0 t + \frac{5A_0(\varepsilon_0 - 1)t^4}{2T_z^3} + \frac{3A_0(1 - \varepsilon_0)t^5}{T_z^4} + \frac{A_0(\varepsilon_0 - 1)t^6}{T_z^5} \tag{3.46}$$

$$s = s_z + \dot{s}_z t + \frac{A_0 t^2}{2} + \frac{A_0(\varepsilon_0 - 1)t^5}{2T_z^3} + \frac{A_0(1 - \varepsilon_0)t^6}{2T_z^4} + \frac{A_0(\varepsilon_0 - 1)t^7}{7T_z^5} \tag{3.47}$$

$$\dddot{s} = \frac{30A_0(\varepsilon_0 - 1)t^2}{T_z^3} + \frac{60A_0(1 - \varepsilon_0)t^3}{T_z^4} + \frac{30A_0(\varepsilon_0 - 1)t^4}{T_z^5} \tag{3.48}$$

$$\ddddot{s} = \frac{60A_0(\varepsilon_0 - 1)t}{T_z^3} + \frac{180A_0(1 - \varepsilon_0)t^2}{T_z^4} + \frac{120A_0(\varepsilon_0 - 1)t^3}{T_z^5} \tag{3.49}$$

At $T = T_0$ and after some simplification we recover the boundary conditions:

$$\ddot{s}_0 = A_0\varepsilon_0 \tag{3.50}$$

$$\dddot{s}_0 = 0 \tag{3.51}$$

$$\ddddot{s}_0 = 0 \tag{3.52}$$

This is a check on the previous equations, and:

$$\dot{s}_0 = \frac{A_0 T_0(2 + \varepsilon_0)}{4} \tag{3.53}$$

$$s_0 = \frac{A_0 T_0^2}{4}\left(1 + \frac{\varepsilon_0}{7}\right) \tag{3.54}$$

***Second Ramp, Constant Acceleration.*** $\ddot{s} = A_0\varepsilon_0 \quad 0 \le t \le T_1, \quad T_0 \le T \le T_1$

Over the interval $T_0 \le T \le T_1$:

$$\dddot{s} = 0 \tag{3.55}$$

$$\ddot{s} = 0 \tag{3.56}$$

$$\ddot{s} = A_0\varepsilon_0 \tag{3.57}$$

$$\dot{s} = \dot{s}_0 + A_0\varepsilon_0 t \tag{3.58}$$

$$s = s_0 + \dot{s}_0 t + \frac{A_0\varepsilon_0 t^2}{2} \tag{3.59}$$

At $t = T_1$:

$$\ddot{s}_1 = A_0\varepsilon_0 \tag{3.60}$$

$$\dot{s}_1 = \frac{A_0 T_0}{4}(2 + \varepsilon_0) + A_0\varepsilon_0 T_1 \tag{3.61}$$

$$s_1 = \frac{A_0 T_0^2}{4}\left(1 + \frac{\varepsilon_0}{7}\right) + \frac{A_0 T_0 T_1 (2 + \varepsilon_0)}{4} + \frac{A_0\varepsilon_0 T_1^2}{2} \tag{3.62}$$

From Eq. (3.56) as the lift at the end of the ramp $s_1$ is specified by the designer we can write:

$$A_0 = \frac{s_1}{\frac{T_0^2}{4}\left(1 + \frac{\varepsilon_0}{7}\right) + \frac{T_0 T_1 (2+\varepsilon_0)}{4} + \frac{T_1^2 \varepsilon_0}{2}} \tag{3.63}$$

The value of $A_0$ will be needed later.

***First Fillet.*** $0 \le t \le T_2 \quad T_1 \le T \le T_2$

The method for the fillet is similar to that used for the first two parts of the first ramp. The polynomial for this section of the acceleration curve and the associated equations for velocity, lift, jerk and quirk are given by:

$$\ddot{s} = a_2 + b_2 t + c_2 t^2 + d_2 t^3 + e_2 t^4 + f_2 t^5 \tag{3.64}$$

$$\dot{s} = \dot{s}_2 + a_2 t + \frac{b_2 t^2}{2} + \frac{c_2 t^3}{3} + \frac{d_2 t^4}{4} + \frac{e_2 t^5}{5} + \frac{f_2 t^6}{6} \tag{3.65}$$

$$s = s_1 + \dot{s}_1 t + \frac{a_2 t^2}{2} + \frac{b_2 t^3}{6} + \frac{c_2 t^4}{12} + \frac{d_2 t^5}{20} + \frac{e_2 t^6}{30} + \frac{f_2 t^7}{42} \tag{3.66}$$

$$\dddot{s} = b_2 + 2c_2 t + 3d_2 t^2 + 4e_2 t^3 + 5f_2 t^4 \tag{3.67}$$

$$\dddot{s} = 2c_2 + 6d_2 t + 12e_2 t^2 + 20f_2 t^3 \tag{3.68}$$

At $t = 0, T = T_1 : \dddot{s} = 0$, and $\ddddot{s} = 0$
From Fig. 3.2:

$$a_2 = A_0\varepsilon_0 \tag{3.69}$$

Substituting the boundary conditions into Eqs. (3.67) and (3.68) yields:

$$b_2 = 0 \tag{3.70}$$

$$c_2 = 0 \tag{3.71}$$

Hence from Eqs. (3.7), (3.8) and (3.9):

$$d_2 == \frac{10(A\varepsilon_1 - A_0\varepsilon_0)}{T_2^3} - \frac{4A(\varepsilon_2 - \varepsilon_1)}{T_2^2 T_3} \tag{3.72}$$

$$e_2 = \frac{7A(\varepsilon_2 - \varepsilon_1)}{T_2^3 T_3} \frac{-15(A\varepsilon_1 - A_0\varepsilon_0)}{T_2^4} \tag{3.73}$$

$$f_2 = \frac{6(A\varepsilon_1 - A_0\varepsilon_0)}{T_2^5} - \frac{3A(\varepsilon_2 - \varepsilon_1)}{T_2^4 T_3} \tag{3.74}$$

At $t = T_2 : \ddot{s}_2 = A\varepsilon_1$
Hence by substitution in Eqs. (3.65) and (3.66) we obtain:

$$\dot{s}_2 = \dot{s}_1 + \frac{(A_0\varepsilon_0 + A\varepsilon_1)T_2}{2} - \frac{A(\varepsilon_2 - \varepsilon_1)T_2^2}{10T_3} \tag{3.75}$$

$$s_2 = s_1 + \dot{s}_1 T_2 + \frac{5A_0\varepsilon_0 T_2^2}{14} + \frac{A\varepsilon_1 T_2^2}{7} - \frac{4A(\varepsilon_2 - \varepsilon_1)T_2^3}{105T_3} \tag{3.76}$$

***Linear Increase in Acceleration.*** $0 \le t \le T_3,\ T_2 \le T \le T_3$
From inspection of Fig. 3.2 the acceleration is given by:

$$\ddot{s} = A\varepsilon_1 + \frac{A(\varepsilon_2 - \varepsilon_1)t}{T_3} \tag{3.77}$$

Progressively differentiating Eq. (3.77) gives the slope of the line, the jerk, and then the quirk.

$$\dddot{s} = \frac{A(\varepsilon_2 - \varepsilon_1)}{T_3} \tag{3.78}$$

$$\ddddot{s} = 0 \tag{3.79}$$

Integrating Eq. (3.77) gives the velocity curve:

$$\dot{s} = \dot{s}_2 + A\varepsilon_1 t + \frac{A(\varepsilon_2 - \varepsilon_1)t^2}{2T_3} \tag{3.80}$$

Integrating Eq. (3.80) yields the lift curve:

$$s = s_2 + \dot{s}_2 t + \frac{A\varepsilon_1 t^2}{2} + \frac{A(\varepsilon_2 - \varepsilon_1)t^3}{6T_3} \tag{3.81}$$

At $t = T_3 : s_3 = A\varepsilon_2$ Hence from (3.80):

$$\dot{s}_3 = \dot{s}_2 + \frac{A(\varepsilon_1 + \varepsilon_2)T_3}{2} \tag{3.82}$$

and from (3.81):

$$s_3 = s_2 + \dot{s}_2 T_3 + AT_3^2\left(\frac{\varepsilon_1}{3} + \frac{\varepsilon_2}{6}\right) \tag{3.83}$$

***Second Fillet.*** $0 \le t \le T_4, T_3 \le T \le T_4$

This section is very similar to that for the first fillet, but with differing boundary conditions.

The derivation is therefore given without detailed explanation.

$$\ddot{s} = a_4 + b_4 t + c_4 t^2 + d_4 t^3 + e_4 t^4 + f_4 t^5 \tag{3.84}$$

$$\dot{s} = \dot{s}_3 + a_4 t + \frac{b_4 t^2}{2} + \frac{c_4 t^3}{3} + \frac{d_4 t^4}{4} + \frac{e_4 t^5}{5} + \frac{f_4 t^6}{6} \tag{3.85}$$

$$s = s_3 + \dot{s}_3 t + \frac{a_4 t^2}{2} + \frac{b_4 t^3}{6} + \frac{c_4 t^4}{12} + \frac{d_4 t^5}{20} + \frac{e_4 t^6}{30} + \frac{f_4 t^7}{42} \tag{3.86}$$

$$\dddot{s} = b_4 + 2c_4 t + 3d_4 t^2 + 4e_4 t^3 + 5f_4 t^4 \tag{3.87}$$

$$\ddddot{s} = 2c_4 + 6d_4 t + 12e_4 t^2 + 20f_4 t^3 \tag{3.88}$$

At: $t = T_3 : \ddot{s} = A\varepsilon_2, \dddot{s} = \frac{a(\varepsilon_2 - \varepsilon_1)}{T_3}, \ddddot{s} = 0$ At: $t = T_4 : \ddot{s} = A, \dddot{s} = \frac{A(\varepsilon_3 - 1)}{T_5}, \ddddot{s} = 0$

Hence:

$$a_4 = A\varepsilon_2 \tag{3.89}$$

$$b_4 = \frac{A(\varepsilon_2 - \varepsilon_3)}{T_3} \tag{3.90}$$

$$c_4 = 0 \tag{3.91}$$

$$d_4 = A\left[\frac{10(1 - \varepsilon_2)}{T_4^3} - \frac{4(\varepsilon_3 - 1)}{T_4^2 T_5} - \frac{6(\varepsilon_2 - \varepsilon_1)}{T_3 T_4^2}\right] \tag{3.92}$$

$$e_4 = A\left[\frac{7(\varepsilon_3 - 1)}{T_4^3 T_5} + \frac{8(\varepsilon_3 - 1)}{T_3 T_4^3} - \frac{15(1 - \varepsilon_2)}{T_4^4}\right] \tag{3.93}$$

$$f_4 = A\left[\frac{6(1 - \varepsilon_2)}{T_4^5} - \frac{3(\varepsilon_3 - 1)}{T_4^4 T_5} - \frac{3(\varepsilon_2 - \varepsilon_1)}{T_3 T_4^4}\right] \tag{3.94}$$

At:$t = T_4$:

$$\dot{s}_4 = \dot{s}_3 + A\left[\frac{(\varepsilon_2 - \varepsilon_1)T_4^2}{10T_3} + \frac{(1 + \varepsilon_2)T_4}{2} - \frac{(\varepsilon_3 - 1)T_4^2}{10T_5}\right] \tag{3.95}$$

and from (3.95):

$$s_4 = s_3 + \dot{s}_3 T_4 + A\left[\frac{\varepsilon_2 T_4^2}{2} + \frac{13(\varepsilon_2 - \varepsilon_1)T_4^3}{210T_3} - \frac{4(\varepsilon_3 - 1)T_4^3}{105T_3} + \frac{(1 - \varepsilon_2)T_4^2}{7}\right] \tag{3.96}$$

***Linear Acceleration.*** $0 \le t \le T_5$, $T_4 \le T \le T_5$

In this section $\varepsilon_3$ can be greater than, equal to, or less than 1. If the minimum radius of curvature is rather small on a concave flank a value of $\varepsilon_3$ greater than 1 can result in an increase in minimum radius. This section is very similar to the previous linear section and will not have a detailed explanation.

From inspection of Fig. 3.2:

$$\dddot{\dddot{s}} = 0 \tag{3.97}$$

$$\dddot{s} = \frac{A(\varepsilon_3 - 1)}{T_5} \tag{3.98}$$

$$\ddot{s} = A + \frac{A(\varepsilon_3 - 1)t}{T_5} \tag{3.99}$$

Integrating Eq. (3.99) yields:

$$\dot{s} = \dot{s}_4 + At + \frac{A(\varepsilon_3 - 1)t^2}{2T_5} \tag{3.100}$$

Integrating Eq. (3.100) yields the lift curve:

$$s = s_4 + \dot{s}_4 t + \frac{At^2}{2} + \frac{A(\varepsilon_3 - 1)t^3}{6T_5} \tag{3.101}$$

At $t = T_5$:

$$\dot{s}_5 = \dot{s}_4 + \frac{A(\varepsilon_3 + 1)T_5}{2} \tag{3.102}$$

$$s = s_4 + \dot{s}_4 T_5 + \frac{AT_5^2}{2} + \frac{A(\varepsilon_3 - 1)T_5^2}{6} \tag{3.103}$$

***Third Fillet.*** $0 \le t \le T_6,\ T_5 \le T \le T_6$

$$\ddot{s} = a_6 + b_6 t + c_6 t^2 + d_6 t^3 + e_6 t^4 + f_6 t^5 \tag{3.104}$$

$$\dot{s} = \dot{s}_5 + a_6 t + \frac{b_6 t^2}{2} + \frac{c_6 t^3}{3} + \frac{d_6 t^4}{4} + \frac{e_6 t^5}{5} + \frac{f_6 t^6}{6} \tag{3.105}$$

$$s = s_5 + \dot{s}_5 t + \frac{a_6 t^2}{2} + \frac{b_6 t^3}{6} + \frac{c_6 t^4}{12} + \frac{d_6 t^5}{20} + \frac{e_6 t^6}{30} + \frac{f_6 t^7}{42} \tag{3.106}$$

$$\dddot{s} = b_6 + 2c_6 t + 3d_6 t^2 + 4e_6 t^3 + 5f_6 t^4 \tag{3.107}$$

$$\ddddot{s} = 2c_6 + 6d_6 t + 12e_6 t^2 + 20f_6 t^3 \tag{3.108}$$

At $t = 0, T = T_5 : \ddot{s}_5 = A\varepsilon_3, \quad \dddot{s}_5 = \frac{A(\varepsilon_3 - 1)}{T_5}, \ddddot{s}_5 = 0,$
At $t = T_6, T = T_6 : \ddot{s}_6 = A\varepsilon_4, \dddot{s}_6 = \frac{A(\varepsilon_5 - \varepsilon_4)}{T_7}, \ddddot{s}_6 = 0$
Hence:

$$a_6 = A\varepsilon_3 \tag{3.109}$$

$$b_6 = \frac{A(\varepsilon_3 - 1)}{T_5} \tag{3.110}$$

$$c_6 = 0 \tag{3.111}$$

$$d_6 = \frac{A}{T_6^2}\left[\frac{10(\varepsilon_4 - \varepsilon_3)}{T_6} - \frac{4(\varepsilon_5 - \varepsilon_4)}{T_7} - \frac{6(\varepsilon_3 - 1)}{T_5}\right] \tag{3.112}$$

$$e_6 = \frac{A}{T_6^3}\left[\frac{7(\varepsilon_5 - \varepsilon_4)}{T_7} + \frac{8(\varepsilon_3 - 1)}{T_5} - \frac{15(\varepsilon_4 - \varepsilon_3)}{T_6}\right] \tag{3.113}$$

$$f_6 = \frac{A}{T_6^4}\left[\frac{6(\varepsilon_4 - \varepsilon_3)}{T_6} - \frac{3(\varepsilon_5 - \varepsilon_4)}{T_7} - \frac{3(\varepsilon_5 - 1)}{T_5}\right] \tag{3.114}$$

Hence:

$$\dot{s}_6 = \dot{s}_5 + A\left[\varepsilon_3 T_6 + T_6^2\left\{\frac{\varepsilon_3 - 1}{10T_5} + \frac{\varepsilon_4 - \varepsilon_3}{2T_6} - \frac{\varepsilon_5 - \varepsilon_4}{10T_7}\right\}\right] \tag{3.115}$$

$$s_6 = s_5 + \dot{s}_5 T_6 + A\left[\frac{\varepsilon_3 T_6^2}{2} + T_6^3\left\{\frac{13(\varepsilon_3 - 1)}{210T_5} + \frac{\varepsilon_4 - \varepsilon_3}{7T_6} - \frac{4(\varepsilon_5 - \varepsilon_4)}{105T_7}\right\}\right] \tag{3.116}$$

***Linear Decrease in Acceleration.*** $0 \le t \le T_7, T_6 \le T \le T_7$

At $t = 0, T = T_6 : \ddot{s}_6 = A\varepsilon_4, \quad \dddot{s}_6 = -\frac{A(\varepsilon_4 - \varepsilon_5)}{T_7}, \quad \ddddot{s}_6 = 0,$

At $t = T_7, T = T_7 : \ddot{s}_7 = A\varepsilon_5, \quad \dddot{s}_7 = -\frac{A(\varepsilon_4 - \varepsilon_5)}{T_7}, \quad \ddddot{s}_7 = 0$

$$\ddddot{s} = 0 \tag{3.117}$$

$$\dddot{s} = \frac{A(\varepsilon_4 - \varepsilon_5)}{T_7} \tag{3.118}$$

$$\ddot{s} = A + \frac{A(\varepsilon_3 - 1)t}{T_7} \tag{3.119}$$

Integrating Eq. (3.119):

$$\dot{s} = \dot{s}_6 + A\varepsilon_4 t - \frac{A(\varepsilon_4 - \varepsilon_5)t^2}{2T_7} \tag{3.120}$$

Integrating Eq. (3.100) yields the lift curve:

$$s = s_6 + \dot{s}_6 t + A\left[\frac{\varepsilon_4 t^2}{2} + \frac{(\varepsilon_5 - \varepsilon_4)t^3}{6T_7}\right] \tag{3.121}$$

At $t = T_7$:

$$\dot{s}_7 = \dot{s}_6 + \frac{AT_7(\varepsilon_4 - \varepsilon_5)}{2} \tag{3.122}$$

$$s_7 = s_6 + \dot{s}_6 T_7 + AT_7^2\left[\frac{\varepsilon_4}{2} + \frac{(\varepsilon_5 - \varepsilon_4)}{6}\right] \tag{3.123}$$

***Fourth Fillet.*** $0 \le t \le T_8, T_7 \le T \le T_8$

$$\ddot{s} = a_8 + b_8 t + c_8 t^2 + d_8 t^3 + e_8 t^4 + f_8 t^5 \tag{3.124}$$

$$\dot{s} = \dot{s}_7 + a_8 t + \frac{b_8 t^2}{2} + \frac{c_8 t^3}{3} + \frac{d_8 t^4}{4} + \frac{e_8 t^5}{5} + \frac{f_8 t^6}{6} \tag{3.125}$$

$$s = s_7 + \dot{s}_7 t + \frac{a_8 t^2}{2} + \frac{b_8 t^3}{6} + \frac{c_8 t^4}{12} + \frac{d_8 t^5}{20} + \frac{e_8 t^6}{30} + \frac{f_8 t^7}{42} \tag{3.126}$$

$$\dddot{s} = b_8 + 2c_8 t + 3d_8 t^2 + 4e_8 t^3 + 5f_8 t^4 \tag{3.127}$$

$$\ddddot{s} = 2c_8 + 6d_8 t + 12e_8 t^2 + 20f_8 t^3 \tag{3.128}$$

At $t = 0, T = T_7 : \ddot{s}_7 = A\varepsilon_5, \dddot{s}_7 = \frac{A(\varepsilon_5 - \varepsilon_4)}{T_7}, \ddddot{s}_7 = 0$

At $t = T_8, T = T_8 : \ddot{s}_8 = A\varepsilon_6, \dddot{s}_8 = -\frac{A\varepsilon_6}{T_9}, \ddddot{s}_8 = 0$

Hence:

$$a_8 = A\varepsilon_5 \tag{3.129}$$

$$b_8 = \frac{A(\varepsilon_5 - \varepsilon_4)}{T_7} \tag{3.130}$$

$$c_8 = 0 \tag{3.131}$$

$$d_8 = \frac{A}{T_8^2}\left[\frac{10(\varepsilon_6 - \varepsilon_5)}{T_8} - \frac{4\varepsilon_6}{T_9} - \frac{6(\varepsilon_5 - \varepsilon_4)}{T_7}\right] \tag{3.132}$$

$$e_8 = \frac{A}{T_8^3}\left[-\frac{7\varepsilon_4}{T_9} + \frac{8(\varepsilon_5 - \varepsilon_4)}{T_7} - \frac{15(\varepsilon_6 - \varepsilon_5)}{T_8}\right] \tag{3.133}$$

$$f_8 = \frac{A}{T_6^4}\left[\frac{6(\varepsilon_6 - \varepsilon_5)}{T_8} - \frac{3\varepsilon_6}{T_9} - \frac{3(\varepsilon_5 - \varepsilon_4)}{T_7}\right] \tag{3.134}$$

$$\dot{s}_8 = \dot{s}_7 + A\left[T_8\frac{\varepsilon_5 + \varepsilon_6}{2} + \frac{T_8^2}{10}\left\{\frac{\varepsilon_5 - \varepsilon_4}{T_7} + \frac{\varepsilon_6}{T_9}\right\}\right] \tag{3.135}$$

Hence after some simplification:

$$s_8 = s_7 + \dot{s}_7 T_8 + A\left[T_8^2\left\{\frac{\varepsilon_5}{2} - \frac{\varepsilon_6 - \varepsilon_5}{7}\right\} + T_8^3\left\{\frac{4\varepsilon_6}{105T_9} + \frac{13(\varepsilon_5 - \varepsilon_4)}{210T_7}\right\}\right] \tag{3.136}$$

***Linear Decrease in Acceleration.*** $0 \le t \le T_9,\ T_8 \le T \le T_9$

At $t = 0, T = T_8 : \ddot{s}_9 = 0, \quad \dddot{s}_8 = -\frac{A\varepsilon_6}{T_9}, \ddddot{s}_8 = 0$

At $t = T_9, T = T_9 : \ddot{s}_9 = 0, \quad \dddot{s}_9 = -\frac{A\varepsilon_6}{T_9}, \ddddot{s}_9 = 0$

$$\ddddot{s} = 0 \tag{3.137}$$

$$\dddot{s} = -\frac{A\varepsilon_6}{T_9} \tag{3.138}$$

$$\ddot{s} = A\varepsilon_6 - \frac{A\varepsilon_6 t}{T_9} \tag{3.139}$$

$$\dot{s} = \dot{s}_8 + A\varepsilon_6 t - \frac{A\varepsilon_6 t^2}{2T_9} \tag{3.140}$$

$$s = s_8 + \dot{s}_8 t + \frac{A\varepsilon_6 t^3}{6T_9} \tag{3.141}$$

At $t = T_9$:

$$\dot{s}_9 = \dot{s}_8 + \frac{A\varepsilon_6 T_9}{2} \tag{3.142}$$

$$s_9 = s_8 + \dot{s}_8 T_9 + \frac{A\varepsilon_6 T_9^2}{6} \tag{3.143}$$

To define the boundary conditions for the Fifth Fillet we need the slope, $\dddot{s}_{10}$, at $T_{10}$, and in order to calculate the slope at $T_{10}$ we need to consider the Polynomial section first.

***Polynomial.*** $0 \le t \le T_{11}, T_{10} \le T \le T_{11}$

This section is intended to permit the designer to optimise the use of the energy stored in the spring to maintain contact at as high a speed as possible. The two indices, $p$ and $q$, which are specified by the designer can be real with both indices differing in value and greater than 1.

We define the acceleration by:

$$\ddot{s} = a_{11} + b_{11}t + c_{11}t^p + d_{11}t^q \tag{3.144}$$

$$\dddot{s} = b_{11} + pc_{11}t^{p-1} + qd_{11}t^{q-1} \tag{3.145}$$

$$\ddddot{s} = p(p-1)c_{11}t^{p-2} + q(q-1)d_{11}t^{q-2} \tag{3.146}$$

At $t = 0$, $T = T_{10}$ : $\ddot{s}_{10} = -\lambda F, \dddot{s}_{10} = b_{11} \neq 0, \ddddot{s}_{10} = 0$

$$a_{11} = -\lambda F \tag{3.147}$$

At $t = T_{11}$, $T = T_{11}$ : $\ddot{s}_{11} = -F, \dddot{s} = 0, \ddddot{s} = 0$

$$\ddot{s}_{11} = -\lambda F + b_{11}T_{11} + c_{11}T_{11}^p + d_{11}T_{11}^q = -F \tag{3.148}$$

$$\dddot{s}_{11} = b_{11} + pc_{11}T_{11}^{p-1} + qd_{11}T_{11}^{q-1} = 0 \tag{3.149}$$

Eliminating $b_{11}$ we can write:

$$c_{11} = \frac{F(1-\lambda)}{T_{11}^p(p-1)} - \frac{d_{11}T_{11}^{q-p}(q-1)}{(p-1)} \tag{3.150}$$

$$\ddddot{s}_{11} = p(p-1)c_{11}T_{11}^{p-2} + q(q-1)d_{11}T_{11}^{q-2} = 0 \tag{3.151}$$

$$c_{11} = -\frac{d_{11}q(q-1)T_{11}^{q-p}}{p(p-1)} \tag{3.152}$$

Eliminating $c_{11}$ we can obtain:

$$d_{11} = \frac{F(1-\lambda)p}{T_{11}^q(q-1)(p-q)} \tag{3.153}$$

Substituting for $d_{11}$:

$$c_{11} = \frac{-F(1-\lambda)q}{T_{11}^{p}(p-1)(p-q)} \tag{3.154}$$

Substituting for $c_{11}$ and $d_{11}$:

$$b_{11} = \frac{-F(1-\lambda)pq}{T_{11}(p-1)(q-1)} = \dddot{s}_{10} \tag{3.155}$$

***Fifth Fillet.*** $0 \le t \le T_{10},\ T_9 \le T \le T_{10}$

$$\ddot{s} = a_{10} + b_{10}t + c_{10}t^2 + d_{10}t^3 + e_{10}t^4 + f_{10}t^5 \tag{3.156}$$

$$\dot{s} = \dot{s}_9 + a_{10}t + \frac{b_{10}t^2}{2} + \frac{c_{10}t^3}{3} + \frac{d_{10}t^4}{4} + \frac{e_{10}t^5}{5} + \frac{f_{10}t^6}{6} \tag{3.157}$$

$$s = s_9 + \dot{s}_9 t + \frac{a_{10}t^2}{2} + \frac{b_{10}t^3}{6} + \frac{c_{10}t^4}{12} + \frac{d_{10}t^5}{20} + \frac{e_{10}t^6}{30} + \frac{f_{10}t^7}{42} \tag{3.158}$$

$$\dddot{s} = b_{10} + 2c_{10}t + 3d_{10}t^2 + 4e_{10}t^3 + 5f_{10}t^4 \tag{3.159}$$

$$\ddddot{s} = 2c_{10} + 6d_{10}t + 12e_{10}t^2 + 20f_{10}t^3 \tag{3.160}$$

At $t = 0, T = T_9 : \ddot{s}_9 = 0, \dddot{s}_9 = \frac{-A\varepsilon_6}{T_9}, \ddddot{s}_9 = 0$
At $t = T_{10},\ T = T_{10} : \ddot{s}_{10} = -\lambda F, \dddot{s}_{10} = b_{11}, \ddddot{s}_{10} = 0$
Hence:

$$a_{10} = 0 \tag{3.161}$$

$$b_{10} = \frac{-A\varepsilon_6}{T_9} \tag{3.162}$$

$$c_{10} = 0 \tag{3.163}$$

$$d_{10} = -\frac{10\lambda F}{T_{10}^3} - \frac{4b_{11}}{T_{10}^2} + \frac{6A\varepsilon_6}{T_9 T_{10}^2} \tag{3.164}$$

$$e_{10} = \frac{7b_{11}}{T_{10}^3} - \frac{8A\varepsilon_6}{T_9 T_{10}^3} + \frac{15\lambda F}{T_{10}^4} \tag{3.165}$$

$$f_{10} = -\frac{6\lambda F}{T_{10}^5} - \frac{4b_{11}}{T_{10}^4} + \frac{3A\varepsilon_6}{T_9 T_{10}^4} \tag{3.166}$$

$$\dot{s}_{10} = \dot{s}_9 - \frac{A\varepsilon_6 T_{10}^2}{10T_9} - \frac{\lambda F T_{10}}{2} + \frac{F(1-\lambda)pqT_{10}^2}{10T_{11}(p-1)(q-1)} \tag{3.167}$$

Hence after some simplification:

$$s_{10} = s_9 + \dot{s}_9 T_{10} - \frac{13A\varepsilon_6 T_{10}^3}{210T_9} - \frac{\lambda F T_{10}^2}{7} + \frac{4F(1-\lambda)pqT_{10}^3}{105T_{11}(p-1)(q-1)} \tag{3.168}$$

If $T_8 = T_9 = 0$ then: $\dddot{s}_7 = \dddot{s}_9 = \frac{A\varepsilon_4}{T_7}$

$$a_{10} = 0 \tag{3.169}$$

$$b_{10} = \frac{-A\varepsilon_6}{T_7} \tag{3.170}$$

$$c_{10} = 0 \tag{3.171}$$

$$d_{10} = -\frac{10\lambda F}{T_{10}^3} - \frac{4b_{11}}{T_{10}^2} + \frac{6A\varepsilon_6}{T_7 T_{10}^2} \tag{3.172}$$

$$e_{10} = \frac{7b_{11}}{T_{10}^3} - \frac{8A\varepsilon_6}{T_7 T_{10}^3} + \frac{15\lambda F}{T_{10}^4} \tag{3.173}$$

$$f_{10} = -\frac{6\lambda F}{T_{10}^5} - \frac{4b_{11}}{T_{10}^4} + \frac{3A\varepsilon_6}{T_7 T_{10}^4} \tag{3.174}$$

$$\dot{s}_{10} = \dot{s}_9 - \frac{A\varepsilon_6 T_{10}^2}{10T_7} - \frac{\lambda F T_{10}}{2} + \frac{F(1-\lambda)pqT_{10}^2}{10T_{11}(p-1)(q-1)} \tag{3.175}$$

Hence after some simplification:

$$s_{10} = s_9 + \dot{s}_9 T_{10} - \frac{13A\varepsilon_6 T_{10}^3}{210T_7} - \frac{\lambda F T_{10}^2}{7} + \frac{4F(1-\lambda)pqT_{10}^3}{105T_{11}(p-1)(q-1)} \tag{3.176}$$

***Polynomial.*** $t \le T \le T_{11}$, $T_{10} \le T \le T_{11}$

Integrating Eq. (3.144)

$$\dot{s}_{11} = \dot{s}_{10} + a_{11}t + \frac{b_{11}t^2}{2} + \frac{c_{11}t^{p+1}}{p+1} + \frac{d_{11}t^{q+1}}{q+1} \tag{3.177}$$

$$s_{11} = s_{10} + \dot{s}_{10}t + \frac{a_{11}t^2}{2} + \frac{b_{11}t^3}{6} + \frac{c_{11}t^{p+2}}{(p+1)(p+2)} + \frac{d_{11}t^{q+2}}{(q+1)(q+2)} \tag{3.178}$$

Recall that $a_{11}, b_{11}, c_{11}$ and $d_{11}$ have already been determined and are given by Eqs. (3.146), (3.154), (3.153), and (3.152) respectively. Substituting these values into Eqs. (3.175) and (3.176) and after some simplification we obtain:

$$\dot{s}_{11} = \dot{s}_{10} - \lambda F T_{11} - F(1-\lambda)T_{11} \left[\frac{pq}{2(p-1)(q-1)} + \frac{q}{(p-q)(p-1)(p+1)} - \frac{p}{(q-1)(p-q)(q+1)}\right] \tag{3.179}$$

$$s_{11} = s_{10} + \dot{s}_{10} T_{11} - \frac{\lambda F T_{11}^2}{2} - F(1-\lambda) T_{11}^2 \left[ \frac{pq}{6(p-1)(q-1)} + \frac{q}{(p-q)(p-1)(p+1)(p+2)} - \frac{p}{(q-1)(p-q)(q+1)(q+2)} \right] \tag{3.180}$$

***Sixth Fillet.*** $t \le T \le T_{12},\ T_{11} \le T \le T_{12}$

$$\ddot{s} = a_{12} + b_{12} t + c_{12} t^2 + d_{12} t^3 + e_{12} t^4 + f_{12} t^5 \tag{3.181}$$

$$\dot{s} = \dot{s}_{11} + a_{12} t + \frac{b_{12} t^2}{2} + \frac{c_{12} t^3}{3} + \frac{d_{12} t^4}{4} + \frac{e_{12} t^5}{5} + \frac{f_{12} t^6}{6} \tag{3.182}$$

$$s = s_{11} + \dot{s}_{11} t + \frac{a_{12} t^2}{2} + \frac{b_{12} t^3}{6} + \frac{c_{12} t^4}{12} + \frac{d_{12} t^5}{20} + \frac{e_{12} t^6}{30} + \frac{f_{12} t^7}{42} \tag{3.183}$$

$$\dddot{s} = b_{12} + 2c_{12} t + 3d_{12} t^2 + 4e_{12} t^3 + 4f_{12} t^4 \tag{3.184}$$

$$\ddddot{s} = 2c_{12} + 6d_{12} t + 12e_{12} t^2 + 20f_{12} t^3 \tag{3.185}$$

At $t = 0,\ T = T_{11} : \ddot{s}_{11} = -F, \dddot{s}_{11} = 0, \ddddot{s}_{11} = 0$
At $t = T_{12}, T = T_{12} : \ddot{s}_{12} = -F_0, \dddot{s}_{12} = 0, \ddddot{s}_{12} = 0$

$$a_{12} = -F \tag{3.186}$$

$$b_{12} = 0 \tag{3.187}$$

$$c_{12} = 0 \tag{3.188}$$

$$d_{12} = \frac{10(F - F_0)}{T_{12}^3} \tag{3.189}$$

$$e_{12} = -\frac{15(F - F_0)}{T_{12}^4} \tag{3.190}$$

$$f_{12} = \frac{6(F - F_0)}{T_{12}^5} \tag{3.191}$$

$$\dot{s}_{12} = \dot{s}_{11} - \frac{(F + F_0) T_{12}}{2} \tag{3.192}$$

$$s_{12} = s_{11} + \dot{s}_{11} T_{12} - \frac{T_{12}^2}{7} \left[ \frac{5F}{2} - F_0 \right] \tag{3.193}$$

## 3.4 Calculation of the Parameters A and F

In order to determine the two parameters, A and F, we need to solve two simultaneous equations: The first equates the velocity on the nose, $\dot{s}_{12}$, to zero, and the second equates the lift, $s_{12}$, to the specified lift, L.

The increments in velocity and lift over each section of the curve have been determined.

We denote the increments in velocity by $dV_i$, the increments in lift by $dS_i$, the terms which are functions of $A_0$ as $dV_i^{A_0}$ and $dS_i^{A_0}$, and the terms which are functions of $F_0$ as $dV_i^{F_0}$ and $dS_i^{F_0}$. Where terms are functions of $A$ or $F$, and there are also terms which are functions of another parameter, they are denoted as $dV^A$, $dS^A$, $dV^F$, and $dS^F$ to avoid any ambiguity and to improve clarity.

At $T = T_0$, from Eq. (3.53)

$$dV_0^{A_0} = \frac{A_0 T_0 (2 + \varepsilon_0)}{4} \tag{3.194}$$

and from Eq. (3.54)

$$dS_0^{A_0} = \frac{A_0 T_0^2}{4}\left(1 + \frac{\varepsilon_0}{7}\right) \tag{3.195}$$

At $T = T_1$, from Eq. (3.61)

$$dV_1^{A_0} = A_0 \varepsilon_0 T_1 \tag{3.196}$$

and from Eq. (3.62)

$$dS_1^{A_0} = \frac{A_0 T_0 T_1 (2 + \varepsilon_0)}{4} + \frac{A_0 T_1^2 \varepsilon_0}{2} \tag{3.197}$$

NB $dS_1^{A_0}$ is specified by the cam designer.

At $T = T_2$ from Eq. (3.75):

$$dV_2^{A_0} = \frac{A_0 \varepsilon_0 T_2}{2} \tag{3.198}$$

and

$$dV_2 = A\left[\frac{\varepsilon_0 T_2}{2} - \frac{(\varepsilon_2 - \varepsilon_1) T_2^2}{10 T_3}\right] \tag{3.199}$$

and

$$dv_2 = \frac{dV_2}{A} \tag{3.200}$$

From Eq. (3.76):

$$dS_2^{A_0} = \frac{5A_0\varepsilon_0 T_2^2}{14} \tag{3.201}$$

and

$$dS_2^A = A\left[\frac{\varepsilon_1 T_2^2}{7} - \frac{4(\varepsilon_2 - \varepsilon_1)T_2^3}{105T_3}\right] \tag{3.202}$$

and

$$ds_2 = \frac{dS_2^A}{A} \tag{3.203}$$

At $T = T_3$ from Eq. (3.82):

$$dV_3 = A\left[\frac{(\varepsilon_1 + \varepsilon_2)T_3}{2}\right] \tag{3.204}$$

and

$$dv_3 = \frac{dV_3}{A} \tag{3.205}$$

From Eq. (3.83):

$$dS_3 = A\left[\left\{\frac{\varepsilon_1}{2} + \frac{\varepsilon_2 - \varepsilon_1}{6}\right\}T_3^2\right] \tag{3.206}$$

and

$$ds_3 = \frac{dS_3}{A} \tag{3.207}$$

At $T = T_4$ from Eq. (3.94):

$$dV_4 = A\left[\frac{(1 + \varepsilon_2)T_4}{2} + \frac{(\varepsilon_2 - \varepsilon_1)T_4^2}{10T_3} - \frac{(\varepsilon_3 - 1)T_4^2}{10T_5}\right] \tag{3.208}$$

and

$$dv_4 = \frac{dV_4}{A} \tag{3.209}$$

From Eq. (3.95):

$$dS_4 = A\left[\frac{\varepsilon_2 T_4^2}{2} + \frac{13(\varepsilon_2 - \varepsilon_1)T_4^3}{210T_3} + \frac{(1 - \varepsilon_2)T_4^2}{7} - \frac{4(\varepsilon_3 - 1)T_4^3}{105T_5}\right] \tag{3.210}$$

and

$$ds_4 = \frac{dS_4}{A} \tag{3.211}$$

At $T = T_5$: from Eq. (3.101):

$$dV_5 = A\left[\frac{(\varepsilon_3 - 1)T_5}{2}\right] \tag{3.212}$$

and

$$dv_5 = \frac{dV_5}{A} \tag{3.213}$$

From Eq. (3.102):

$$dS_5 = A\left[\frac{T_5^2}{2} + \frac{(\varepsilon_3 - 1)T_5^2}{6}\right] \tag{3.214}$$

and

$$ds_5 = \frac{dS_5}{A} \tag{3.215}$$

At $T = T_6$: from Eq. (3.114):

$$dV_6 = A\left[\varepsilon_3 T_6 + \frac{(\varepsilon_3 - 1)T_6^2}{10T_5} + \frac{(\varepsilon_4 - \varepsilon_3)T_6}{2} - \frac{(\varepsilon_5 - \varepsilon_4)T_6^2}{10T_7}\right] \tag{3.216}$$

and

$$dv_6 = \frac{dV_6}{A} \tag{3.217}$$

From Eq. (3.115)

$$dS_6 = A\left[\frac{\varepsilon_3 T_6^2}{2} + \frac{13(\varepsilon_3 - 1)T_6^3}{210T_5} + \frac{(\varepsilon_4 - \varepsilon_3)T_6^2}{7} - \frac{4(\varepsilon_5 - \varepsilon_4)T_6^3}{105T_7}\right] \tag{3.218}$$

and

$$ds_6 = \frac{dS_6}{A} \tag{3.219}$$

At $T = T_7$ from Eq. (3.121):

$$dV_7 = A\left[\frac{(\varepsilon_4 + \varepsilon_5)T_7}{2}\right] \tag{3.220}$$

and

$$dv_7 = \frac{dV_7}{A} \tag{3.221}$$

From Eq. (3.122):

$$dS_7 = A\left[\left\{\frac{\varepsilon_4}{2} + \frac{(\varepsilon_5 - \varepsilon_4)}{6}\right\}T_7^2\right] \tag{3.222}$$

and

$$ds_7 = \frac{dS_7}{A} \tag{3.223}$$

At $T = T_8$ from Eq. (3.134):

$$dV_8 = A\left[\frac{(\varepsilon_5 + \varepsilon_6)T_8}{2} + \frac{T_8^2}{10}\left\{\frac{(\varepsilon_5 - \varepsilon_4)}{T_7} + \frac{\varepsilon_6}{T_9}\right\}\right] \tag{3.224}$$

and

$$dv_8 = \frac{dV_8}{A} \tag{3.225}$$

From Eq. (3.135):

$$dS_8 = A\left[\left\{\frac{\varepsilon_5}{2} + \frac{(\varepsilon_6 - \varepsilon_5)}{7}\right\}T_8^2 + \left\{\frac{4\varepsilon_6}{105T_9} + \frac{13(\varepsilon_5 - \varepsilon_4)}{210T_7}\right\}T_8^3\right] \tag{3.226}$$

and

$$ds_8 = \frac{dS_8}{A} \tag{3.227}$$

At $T = T_9$ from Eq. (3.141):

$$dV_9 = A\left[\frac{\varepsilon_6 T_9}{2}\right] \tag{3.228}$$

and

$$dv_9 = \frac{dV_9}{A} \tag{3.229}$$

$$dS_9 = A\left[\frac{\varepsilon_6 T_9^2}{3}\right] \tag{3.230}$$

$$ds_9 = \frac{dS_9}{A} \tag{3.231}$$

At $T = T_{10}$ from Eq. (3.165):

$$dV_{10}^A = A\left[\frac{-\varepsilon_6 T_{10}^2}{10T_9}\right] \tag{3.232}$$

and

$$dv_{10}^{A} = \frac{dV_{10}^{A}}{A} \tag{3.233}$$

and

$$dV_{10}^{F} = F\left[\frac{-\lambda T_{10}}{2} + \frac{pq(1-\lambda)T_{10}^{2}}{10(p-1)(q-1)T_{11}}\right] \tag{3.234}$$

and

$$dv_{10}^{F} = \frac{dV_{10}^{F}}{F} \tag{3.235}$$

From Eq. (3.166):

$$dS_{10}^{A} = A\left[\frac{-13\varepsilon_6 T_{10}^{3}}{210T_9}\right] \tag{3.236}$$

and

$$ds_{10}^{A} = \frac{dS_{10}^{A}}{A} \tag{3.237}$$

and

$$dS_{10}^{F} = F\left[\frac{-\lambda T_{10}^{2}}{7} + \frac{4pq(1-\lambda)T_{10}^{3}}{105(p-1)(q-1)T_{11}}\right] \tag{3.238}$$

and

$$ds_{10}^{F} = \frac{dS_{10}^{F}}{F} \tag{3.239}$$

If $T_8 = T_9 = 0$ then:

$$dV_8 = dv_8 = 0 \tag{3.240}$$

$$dV_9 = dv_9 = 0 \tag{3.241}$$

From Eq. (3.173):

$$dV_{10}^{A} = A\left[\frac{-\varepsilon_4 T_{10}^{2}}{10T_7}\right] \tag{3.242}$$

$$dv_{10}^{A} = \frac{dV_{10}^{A}}{A} \tag{3.243}$$

From Eq. (3.174):

$$dS_{10}^{A} = A\left[\frac{-13\varepsilon_4 T_{10}^3}{210T_7}\right] \tag{3.244}$$

$$ds_{10}^{A} = \frac{dS_{10}^{A}}{A} \tag{3.245}$$

At $T = T_{11}$:

$$dV_{11} = F\left[\left\{-\lambda - \frac{pq(1-\lambda)}{2(q-1)(p-1)} - \frac{q(1-\lambda)}{(p-1)(p-q)(p+1)} + \frac{p(1-\lambda)}{(q-1)(p-q)(q+1)}\right\}T_{11}\right] \tag{3.246}$$

$$dv_{11} = \frac{dV_{11}}{F} \tag{3.247}$$

$dS_{11} =$

$$F\left[\left\{\frac{-\lambda}{2} - \frac{pq(1-\lambda)}{6(q-1)(p-1)} - \frac{q(1-\lambda)}{(p-q)(p-1)(p+1)(p+2)} + \frac{p(1-\lambda)}{(q-1)(p-q)(q+1)(q+2)}\right\}T_{11}^2\right] \tag{3.248}$$

$$ds_{11} = \frac{dS_{11}}{F} \tag{3.249}$$

At $T = T_{12}$:

$$dV_{12} = F\left[\frac{-T_{12}}{2}\right] \tag{3.250}$$

$$dv_{12} = \frac{dV_{12}}{F} \tag{3.251}$$

$$dV_{12}^{F_0} = \frac{-F_0 T_{12}}{2} \tag{3.252}$$

$$dS_{12} = F\left[\frac{-5T_{12}^2}{14}\right] \tag{3.253}$$

$$ds_{12} = \frac{dS_{12}}{F} \tag{3.254}$$

$$dS_{12}^{F_0} = \frac{-F_0 T_{12}^2}{7} \tag{3.255}$$

Let:

$$\begin{aligned}\Sigma S^{A_0} = {} & dS_0^{A_0} + dS_1^{A_0} + dS_2^{A_0} + dV_0^{A_0} \\ & [T_1 + T_2 + T_3 + T_4 + T_5 + T_6 + T_7 + T_8 + T_9 + T_{10} + T_{11} + T_{12}] + \\ & dV_1^{A_0}[T_2 + T_3 + T_4 + T_5 + T_6 + T_7 + T_8 + T_9 + T_{10} + T_{11} + T_{12}] + \\ & dV_2^{A_0}[T_3 + T_4 + T_5 + T_6 + T_7 + T_8 + T_9 + T_{10} + T_{11} + T_{12}]\end{aligned} \tag{3.256}$$

Let

$$\Sigma V^A = dv_2 + dv_3 + dv_4 + dv_5 + dv_6 + dv_7 + dv_8 + dv_9 + dv_{10}^A \tag{3.257}$$

Let

$$\Sigma V^F = dv_{10}^F + dv_{11} + dv_{12} \tag{3.258}$$

Let

$$\begin{aligned}\Sigma S^A = {} & ds_2 + ds_3 + ds_4 + ds_5 + ds_6 + ds_7 + ds_8 + ds_9 + ds_{10}^A \\ & + dv_2[T_3 + T_4 + T_5 + T_6 + T_7 + T_8 + T_9 + T_{10} + T_{11} + T_{12}] \\ & + dv_3[T_4 + T_5 + T_6 + T_7 + T_8 + T_9 + T_{10} + T_{11} + T_{12}] \\ & + dv_4[T_5 + T_6 + T_7 + T_8 + T_9 + T_{10} + T_{11} + T_{12}] \\ & + dv_5[T_6 + T_7 + T_8 + T_9 + T_{10} + T_{11} + T_{12}] \\ & + dv_6[T_7 + T_8 + T_9 + T_{10} + T_{11} + T_{12}] + dv_7[T_8 + T_9 + T_{10} + T_{11} + T_{12}] \\ & + dv_8[T_9 + T_{10} + T_{11} + T_{12}] + dv_9[T_{10} + T_{11} + T_{12}] + dv_{10}^A[T_{11} + T_{12}]\end{aligned} \tag{3.259}$$

Let

$$\Sigma S^F = ds_{10}^F + ds_{11} + ds_{12} + dv_{10}^F[T_{11} + T_{12}] + dv_{11}T_{12} \tag{3.260}$$

Let

$$\Sigma V^{A_0} = dV_0^{A_0} + dV_1^{A_0} + dV_2^{A_0} \tag{3.261}$$

Let

$$V^0 = \Sigma V^{A_0} + dV_{12}^{F_0} \tag{3.262}$$

Let

$$S^0 = \Sigma S_1^{A_0} + dS_{12}^{F_0} \tag{3.263}$$

The velocity on the nose, $T = T_{12}$, is zero. Therefore:

$$V^0 + A\Sigma V^A + F\Sigma V^F = 0 \tag{3.264}$$

and the cam lift, L, is given by:

$$S^0 + A\Sigma S^A + F\Sigma S^F = L \tag{3.265}$$

Equations (3.264) and (3.265) are two simultaneous equations in two unknowns, $A$ and $F$. To eliminate $F$ we divide Eq. (3.264) by $\Sigma V^F$

$$\frac{V^0}{\Sigma V^F} + \frac{A\Sigma V^A}{\Sigma V^F} = -F \tag{3.266}$$

and divide Eq. (3.265) by $\Sigma S^F$

$$\frac{V^0}{\Sigma V^F} + \frac{A\Sigma V^A}{\Sigma V^F} = \frac{S^0}{\Sigma S^F} + \frac{A\Sigma S^A}{\Sigma S^F} - \frac{L}{\Sigma S^F} \tag{3.267}$$

Let

$$\Delta = \frac{V^0}{\Sigma V^F} \tag{3.268}$$

and

$$\Gamma = \frac{\Sigma V^A}{\Sigma V^F} \tag{3.269}$$

Equation (3.267) can now be written:

$$\Sigma S^F(\Delta + A\Gamma) = S^0 + A\Sigma V^A - L \tag{3.270}$$

Hence:

$$A = \frac{L + \Delta\Sigma S^F - S^0}{\Sigma S^A - \Gamma\Sigma S^F} \tag{3.271}$$

and Eq. (3.266) can be written as:

$$F = -\Delta - A\Gamma \tag{3.272}$$

With a knowledge of the unknowns, $A$ and $F$ the equations for Lift, Velocity, Acceleration, Jerk and Quirk can be evaluated.

A choice of design values which produce a satisfactory design is only arrived at after some familiarisation with the method, and achieving the required result is an iterative process. An example of possible values to obtain a satisfactory design is given in Appendix 1.

### *3.4.1 Note: Minimisation of Maximum Valve Velocity*

The sections $T_7 \leq T \leq T_8$ and $T_8 \leq T \leq T_9$ are included to permit the designer to reduce the maximum valve velocity while achieving maximum valve lift, when high maximum velocity results in the tappet diameter becoming too large to fit into

the available space. This can occur for flat translating followers and curved translating followers with large radii of curvature. It will also reduce the maximum pressure angle for curved translating followers of small radii, which will slightly reduce the maximum transverse force. If desired the parameter $\varepsilon_6$ can be set to zero giving a period of constant maximum velocity. Frequently a small value of $\varepsilon_6$ will give a better result.

In the case of a curved swinging follower these two sections can usually be omitted and then the jerk at $T_9$ should be equated to the jerk at $T_7$ i.e. $\dddot{s}_9 = \dddot{s}_7$. These two sections permit the designer more freedom, and the optimal procedure can be found with experimentation and experience.

It may be thought that the design process could be programmed as a constrained optimisation in many dimensions. However in practice there is a need for experience and judgement to ensure a viable design.

# Chapter 4
# Flat Translating Follower

**Abstract** The previous chapter gives a method for producing a valve acceleration curve together with the corresponding valve velocity and lift. In this chapter these data are used to compute the information needed to design and manufacture the analytically simplest useable cam mechanism, which is a flat translating follower. Equations are derived for the torque, shape, curvature, entrainment velocity, contact force and stress, and the maximum speed at which cam–follower contact can be achieved. The data needed is the cam base circle radius, and the valve acceleration, velocity and lift.

## 4.1 Introduction

For automotive use the flat translating follower offers several advantages to the engine designer. The cams are always convex and can therefore be ground with a large diameter grinding wheel. This is easier and cheaper. The inverted bucket tappet is relatively cheap and simple to manufacture and analytically this cam–follower combination is the simplest of those of practical interest. For a high performance and high speed engine the inertia of the follower may well be higher than for other mechanisms, and high lift cams of small base circle radius tend to have a small nose radius which may cause tribological problems, giving premature wear and causing scuffing during the running-in process.

J. J. Williams, *Introduction to Analytical Methods for Internal Combustion Engine Cam Mechanisms*, DOI: 10.1007/978-1-4471-4564-6_4, 

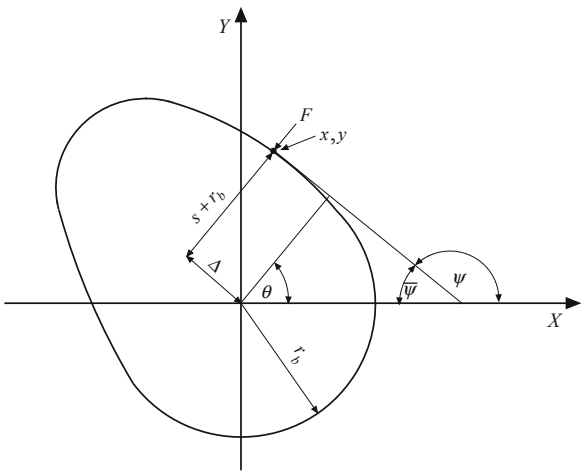


**Fig. 4.1** Flat follower cam mechanism

## 4.2 Analytical Method

The diagram used for analysis is frequently the most difficult part of the problem. Firstly the mechanism has to be drawn in a simple form which permits the relevant parameters required for the analysis to be identified. This may seem obvious, but the correct identification of these parameters is essential if the method of analysis is to be determined. It is helpful to invert the mechanism, that is to say rather than have a rotating cam, the cam is kept stationary and the follower rotates in the opposite direction. The mechanism of current interest is shown in Fig. 1.4, and Fig. 4.1 is to be used for the analysis. Here the angle of follower rotation is shown increasing in an anticlockwise direction. This therefore is for a cam which is rotating clockwise relative to the follower. This procedure will be used for analysing all the cam mechanisms which are considered.

The flat translating follower is the simplest mechanism to be considered, but the diagram is worth some initial consideration. The follower is in tangential contact with the cam at $x$, $y$ and the contact force, $F$ acts in the direction of motion of the follower. The pressure angle is defined as that between the direction of motion of the follower and that of the contact force, and is therefore zero for this mechanism.

## 4.3 Notation

$F$ Force
$r_b$ Base circle radius
$s$ Valve lift
$t$ Time

$T$ Cam torque
$V_c$ Cam velocity
$V_e$ Entrainment velocity
$V_f$ Follower velocity
$V_s$ Sliding velocity
$x$ Coordinate
$y$ Coordinate
$\delta$ Distance around cam
$\Delta$ Distance defined in text
$\theta$ Angle of cam rotation
$\rho$ Radius of curvature
$\psi$ Angle of tangent to cam
$\omega$ Angular velocity

## 4.4 Cam Shape and Torque

In the previous two chapters integration and differentiation were always with respect to one variable, time, and higher derivatives were frequently considered. It was therefore easier to use Newton's notation. In this and subsequent chapters involving cam mechanisms, where derivatives of more than one variable are involved, and therefore Leibnitz's notation will be used.

Recall that the cam and follower shown schematically in Fig. 4.1 have the follower shown rotated anticlockwise by angle $\theta$ rather than showing the cam rotated clockwise by an angle $\theta$. The lift at angle $\theta$ is $S$ and the base circle radius is $r_b$. With notation of Fig. 4.1

Let the cam force at the point of contact $x$, $y$ be $F$. Consider an infinitesimal rotation of the cam, $d\theta$ and a corresponding displacement of the follower $ds$. The pressure angle for a follower of this type is always zero, i.e. the cam force is always parallel to the direction of motion of the follower. The distance from the line of action of the cam force to the centre of rotation of the cam is $\Delta$. The work done is given by

$$Fds = F\Delta d\theta \tag{4.1}$$

Hence

$$\Delta = \frac{ds}{d\theta} \tag{4.2}$$

Note that the maximum value of $\Delta$ occurs when the valve velocity, $\frac{ds}{d\theta}$ is a maximum. The minimum follower diameter is therefore dependent upon the maximum valve velocity. One limitation on the design of high lift cams of short

dwell is therefore the space available to fit in a sufficiently large follower. The cam torque is given by

$$T = F\frac{ds}{d\theta} \tag{4.3}$$

And the coordinates of the point of contact are given by

$$x = (r_b + s)\cos\theta - \frac{ds}{d\theta}\sin\theta \tag{4.4}$$

$$y = (r_b + s)\sin\theta + \frac{ds}{d\theta}\cos\theta \tag{4.5}$$

## 4.5 Cam Curvature

The radius of curvature, $\rho$ of this type of follower is of interest to the cam designer mainly for computing other parameters associated with the tribology of the cam and follower, such as the contact stress and the entrainment velocity. Recall that the sum of the internal angles of a triangle is $\pi$. From Fig. 4.1:

$$\bar{\psi} = \frac{\pi}{2} - \theta \tag{4.6}$$

Differentiating Eq. (4.6) with respect to $\theta$

$$\frac{d\bar{\psi}}{d\theta} = -1 \tag{4.7}$$

From Eq. (4.6):

$$\cos\bar{\psi} = \cos\left(\frac{\pi}{2} - \theta\right) = \sin\theta \tag{4.8}$$

$$\sin\bar{\psi} = \sin\left(\frac{\pi}{2} - \theta\right) = \cos\theta \tag{4.9}$$

Differentiating Eqs. (4.4) and (4.5) with respect to $\theta$

$$\frac{dx}{d\theta} = -(r_b + s)\sin\theta - \frac{d^2s}{d\theta^2}\sin\theta \tag{4.10}$$

$$\frac{dy}{d\theta} = (r_b + s)\cos\theta + \frac{d^2s}{d\theta^2}\cos\theta \tag{4.11}$$

With notation of Fig. 4.1, at $x$, $y$ as $\theta$, $y$ and the distance, $\delta$, and around the cam increase but $x$ and $\bar{\psi}$ decrease. Recall Sect. 1.8.2:

$$\cos\bar{\psi} = -\frac{dx}{d\delta} \tag{1.1}$$

$$\sin\bar{\psi} = \frac{dy}{d\delta} \tag{1.2}$$

and

$$\rho = -\frac{d\delta}{d\bar{\psi}} \tag{1.3}$$

where $\rho$ is the radius of curvature at the point of contact $x$, $y$.

From Eqs. (4.7), (4.8), (1.2) and (1.3):

$$\rho\sin\theta = -\frac{dx}{d\theta} \tag{4.12}$$

From Eqs. (4.7) (4.9) (1.1) and (1.3):

$$\rho\cos\theta = \frac{dy}{d\theta} \tag{4.13}$$

From both Eqs. (4.10) and (4.12), and Eqs. (4.11) and (4.13):

$$\rho = r_b + s + \frac{d^2s}{d\theta^2} \tag{4.14}$$

## 4.6 Entrainment Velocity

The contact between cam and follower is heavily loaded, and the integrity of the components is dependent upon the existence of an oil film whose thickness should be greater than the surface roughness. The growth of an oil film requires the entrainment of oil in the contact area.

With notation of Fig. 4.1, the point of contact at zero lift will be at the centre of the follower. As the cam rotates the distance of the contact from the centre is given by

$$\Delta = \frac{ds}{d\theta} \tag{4.2}$$

Let the angular velocity of the cam be $\frac{d\theta}{dt} = \omega$ rad/s. The velocity $V_f$ of the contact point with respect to the follower is:

$$V_f = \frac{d\Delta}{dt} = \frac{d\Delta}{d\theta}\frac{d\theta}{dt} = \frac{d\Delta}{d\theta}\omega = \frac{d^2s}{d\theta^2}\omega \tag{4.15}$$

The velocity $V_c$ of the contact point relative to the cam is:

$$V_c = \frac{d\delta}{dt} = \frac{d\delta}{d\theta}\frac{d\theta}{dt} = \frac{d\delta}{d\theta}\omega \tag{4.16}$$

From Eqs. (4.7) and (1.3)

$$\rho = \frac{d\delta}{d\theta} \tag{4.17}$$

From Eqs. (4.16) and (4.17):

$$V_c = \rho\omega \tag{4.18}$$

The sliding velocity is given by

$$V_s = V_c - V_f \tag{4.19}$$

And the entrainment velocity is:

$$V_e = V_c + V_f \tag{4.20}$$

## 4.7 Contact Force and Stress

Recall Sect. 1.12 Contact stresses.

$$\rho^* = \rho_C \tag{4.21}$$

The pressure angle is zero for a flat follower and therefore Eq. (1.38) can be written as

$$F_C = F_V \tag{4.22}$$

Equation (1.45) can therefore be written as:

$$\sigma_{Hz} = \left[\frac{P^* E^*}{\pi \rho_C}\right]^{\frac{1}{2}} \tag{4.23}$$

## 4.8 Maximum Speed to Maintain Cam–Follower Contact

Recall Sect. 1.14, where Newton's notation is used, the maximum speed to maintain contact is shown to be:

$$N = \frac{60}{\pi}\sqrt{\frac{-F_S}{\ddot{s}M_E}} \tag{1.36}$$

# Chapter 5
# Curved Translating Radial Follower

**Abstract** This chapter considers a curved translating follower and is similar to Chap. 4, but whereas the pressure angle is always zero for a flat translating follower, this analysis involves the determination of the pressure angle, as well as the other data also required for a flat follower.

## 5.1 Introduction

The curved translating radial follower has been used in the past in racing engines, for example, the Miller Straight Eight [1], which raced in the early 1920s. With a suitable choice of follower radius, a convex cam of high lift and short dwell will have a larger nose radius and require a smaller follower, than the corresponding flat follower. Roller followers have a small radius to reduce mass and care must be taken to ensure that the pressure angle is not too large or the follower may stick in the guide.

## 5.2 Notation

$E^*$ Contact modulus
$F_C$ Cam force
$F_V$ Valve force
$P^*$ Force per unit width of line contact
$r_b$ Base circle radius
$r_f$ Follower radius
$s$ Valve lift
$t$ Time

J. J. Williams, *Introduction to Analytical Methods for Internal Combustion Engine Cam Mechanisms*, DOI: 10.1007/978-1-4471-4564-6_5, © Springer-Verlag London 2013

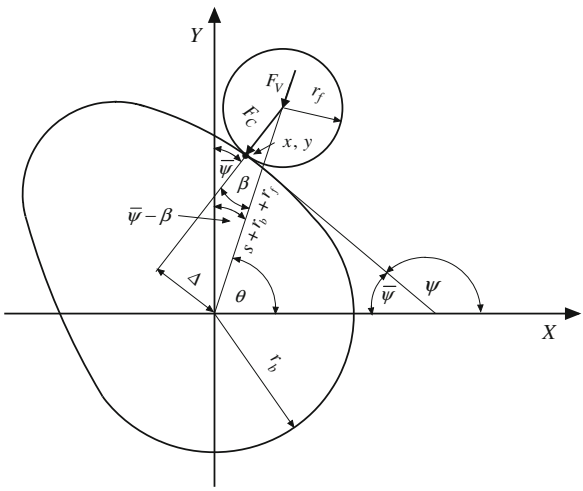


**Fig. 5.1** Curved translating follower cam mechanism

$T$ Cam torque
$V_c$ Cam velocity
$V_e$ Entrainment velocity
$V_f$ Follower velocity
$V_s$ Sliding velocity
$x$ Coordinate
$y$ Coordinate
$\beta$ Pressure angle
$\delta$ Distance around cam
$\Delta$ Distance defined in text
$\theta$ Angle of cam rotation
$\rho$ Radius of curvature
$\bar{\psi}$ Angle of tangent to cam
$\omega$ Angular velocity

## 5.3 Pressure Angle

For convenience the cam and follower shown schematically in Fig. 5.1 have the follower shown rotated anti-clockwise by angle $\theta$ rather than showing the cam rotated clockwise by an angle $\theta$. Let the lift at angle $\theta$ be $s$ and the base circle radius be$r_b$. As mentioned in Sect. 4.4, in this and subsequent chapters involving cam mechanisms, the derivatives of more than one variable will be involved, and therefore Leibnitz's notation will be used.

With notation of Fig. 5.1

$$\Delta = (s + r_b + r_f)\sin\beta \tag{5.1}$$

Let the contact force at the point of contact $x, y$ be $F_C$. Consider an infinitesimal rotation of the cam, $d\theta$ and a corresponding displacement of the follower $ds$. The work done by the cam is:

$$F_C\,\Delta\,d\theta = F_C(s + r_b + r_f)\sin\beta\,d\theta \tag{5.2}$$

Work done on follower is $F_C\cos\beta\,ds$
Equating the work, and from Eqs. (5.1) and (5.2):

$$F_C(s + r_b + r_f)\sin\beta\,d\theta = F_C\cos\beta\,ds \tag{5.3}$$

From which:

$$\tan\beta = \frac{ds/d\theta}{s + r_b + r_f} \tag{5.4}$$

*Note* Since the pressure angle, $\beta$ is now known the cam torque, can now be determined.

$$T = F_C(s + r_b + r_f)\sin\beta \tag{5.5}$$

## 5.4 Cam Shape

With notation of Fig. 5.1, the coordinates $x, y$ of the contact points are given by

$$x = (s + r_b + r_f)\cos\theta - r_f\sin\bar{\psi} \tag{5.6}$$

$$y = (s + r_b + r_f)\sin\theta - r_f\cos\bar{\psi} \tag{5.7}$$

where

$$\bar{\psi} = \beta - \theta + \frac{\pi}{2} \tag{5.8}$$

## 5.5 Cam Curvature

Differentiating Eq. (5.4) with respect to $\theta$

$$\frac{d\beta}{d\theta} = \frac{\left\{(s + r_b + r_f)\frac{d^2s}{d\theta^2} - \left[\frac{ds}{d\theta}\right]^2\right\}}{(s + r_b + r_f)^2\sec^2\beta} \tag{5.9}$$

At $x, y$ as $y$, and $\theta$ increase, the distance, $\delta$ around the cam increases but $x$ and $\bar{\psi}$ decrease. Recall from Sect. 1.8.2:

$$\cos\bar{\psi} = -\frac{dx}{d\delta} \tag{1.1}$$

and

$$\sin\bar{\psi} = \frac{dy}{d\delta} \tag{1.2}$$

and

$$\rho = -\frac{d\delta}{d\bar{\psi}} \tag{1.6}$$

From Eqs. (1.1) and (1.6)

$$\rho\cos\bar{\psi} = \frac{dx}{d\bar{\psi}} \tag{1.7}$$

From Eqs. (1.2) and (1.6)

$$\rho\sin\bar{\psi} = -\frac{dy}{d\bar{\psi}} \tag{1.8}$$

Differentiating Eqs. (5.6) and (5.7) with respect to $\bar{\psi}$

$$\frac{dx}{d\bar{\psi}} = \frac{ds}{d\bar{\psi}}\cos\theta - \left(s + r_b + r_f\right)\sin\theta\frac{d\theta}{d\bar{\psi}} - r_f\cos\bar{\psi} \tag{5.10}$$

$$\frac{dy}{d\bar{\psi}} = \frac{ds}{d\bar{\psi}}\sin\theta + \left(s + r_b + r_f\right)\sin\theta\frac{d\theta}{d\bar{\psi}} + r_f\sin\bar{\psi} \tag{5.11}$$

Differentiating Eq. (5.8) with respect to $\theta$:

$$\frac{d\bar{\psi}}{d\theta} = \frac{d\beta}{d\theta} - 1 \tag{5.12}$$

From Eqs. (1.7) and (5.10) and multiplying both sides by $\frac{d\bar{\psi}}{d\theta}$:

$$\rho\cos\bar{\psi}\frac{d\bar{\psi}}{d\theta} = \frac{ds}{d\bar{\psi}}\frac{d\bar{\psi}}{d\theta}\cos\theta - \left(s + r_b + r_f\right)\sin\theta\frac{d\theta}{d\bar{\psi}}\frac{d\bar{\psi}}{d\theta} - r_f\cos\bar{\psi}\frac{d\bar{\psi}}{d\theta} \tag{5.13}$$

From Eqs. (5.12) and (5.13):

$$\left(\frac{d\beta}{d\theta} - 1\right)\rho\cos\bar{\psi} = \frac{ds}{d\theta}\cos\theta - \left(s + r_b + r_f\right)\sin\theta - r_f\cos\bar{\psi}\left(\frac{d\beta}{d\theta} - 1\right) \tag{5.14}$$

Equation (5.14) can be simplified to give

$$\rho = \frac{\frac{ds}{d\theta}\cos\theta - \left(s + r_b + r_f\right)\sin\theta}{\left(\frac{d\beta}{d\theta} - 1\right)\cos\bar{\psi}} - r_f \tag{5.15}$$

From Eqs. (1.8) and (5.11) and multiplying both sides by $\frac{d\bar{\psi}}{d\theta}$

$$-\rho\sin\bar{\psi}\frac{d\bar{\psi}}{d\theta} = \frac{ds}{d\bar{\psi}}\frac{d\bar{\psi}}{d\theta}\sin\theta + \left(s + r_b + r_f\right)\cos\theta\frac{d\theta}{d\bar{\psi}}\frac{d\bar{\psi}}{d\theta} + r_f\sin\bar{\psi}\frac{d\bar{\psi}}{d\theta} \tag{5.16}$$

From Eqs. (5.12) and (5.16):

$$-\rho\sin\bar{\psi}\left(\frac{d\beta}{d\theta} - 1\right) = \frac{ds}{d\theta}\sin\theta + \left(s + r_b + r_f\right)\cos\theta\frac{d\theta}{d\theta} + r_f\sin\bar{\psi}\left(\frac{d\beta}{d\theta} - 1\right) \tag{5.17}$$

Equation (5.17) can be simplified to give:

$$\rho = \frac{-\frac{ds}{d\theta}\sin\theta - \left(s + r_b + r_f\right)\cos\theta}{\left(\frac{d\beta}{d\theta} - 1\right)\sin\bar{\psi}} - r_f \tag{5.18}$$

## 5.6 Entrainment Velocity

Unless the follower is a roller follower, the contact between cam and follower is heavily loaded and the integrity of the components is dependent upon the existence of an oil film whose thickness should be greater than the surface roughness. The growth of an oil film requires the entrainment of oil in the contact area.

Let the angular velocity of the cam be $\frac{d\theta}{dt} = \omega$ rad/s. The velocity $V_f$ of the contact point with respect to the follower is:

$$V_f = r_f\frac{d\beta}{d\theta}\frac{d\theta}{dt} = r_f\frac{d\beta}{d\theta}\omega \tag{5.19}$$

where $\frac{d\beta}{d\theta}$ is given by Eq. (5.9).

The velocity: $V_c$ of the contact point relative to the cam is

$$V_c = \rho\frac{d\bar{\psi}}{d\theta}\frac{d\theta}{dt} = \rho\frac{d\bar{\psi}}{d\theta}\omega \tag{5.20}$$

$\frac{d\bar{\psi}}{d\theta}$ can be evaluated from Eqs. (5.9) and (5.12)

The sliding velocity $V_s$ is given by

$$V_s = V_c - V_f \tag{5.21}$$

And the entrainment $V_e$ velocity by

$$V_e = V_c + V_f \tag{5.22}$$

## 5.7 Contact Force and Stress

From Fig. 5.1: equilibrium of the follower gives:

$$F_C \cos\beta = F_V \tag{5.23}$$

hence

$$F_C = \frac{F_V}{\cos\beta} \tag{5.24}$$

Recall from Sect. 1.12.3 that the effective radius of curvature, $\rho^*$, for a curved follower and a convex and a concave cam is given by:

$$\rho^* = \left| \frac{\rho_C \rho_F}{\rho_C + \rho_F} \right| \tag{5.25}$$

The contact stress is given by

$$\sigma_{Hz} = \left[ \frac{P^* E^*}{\pi \rho^*} \right]^{\frac{1}{2}} \tag{5.26}$$

## 5.8 Engine Speed for Zero Contact Force Between Cam and Follower

Recall from Sect. 1.14 that the spring force $F_S$ is given by

$$F_S = k(s_0 + s) \tag{5.27}$$

At an engine speed of N rpm the camshaft speed is $\frac{N}{2}\frac{360}{60} = 3N^\circ/s = 3N\frac{\pi}{180} = \frac{\pi N}{60}$ rad/s.

Using Newton's notation the total valve force is

$$F_V = \ddot{s}\left(\frac{\pi N}{60}\right)^2 M_E + F_S \tag{5.28}$$

If the contact force between cam and follower, $F_C = 0$ then $F_V = 0$, hence

$$F_S = -\ddot{s}\left(\frac{\pi N}{60}\right)^2 M_E \tag{1.29}$$

Hence the maximum speed to maintain contact is:

$$N = \frac{60}{\pi}\sqrt{\frac{-F_S}{\ddot{s}M_E}} \tag{1.35}$$

*Note* This speed should only be computed when the valve acceleration is negative, as the number whose square root is required must be positive.

## Reference

1. Dees ML (1981) The Miller dynasty, Cam drawing. Barnes Publishing Inc., Scarsdale, pp 169, ISBN 0-914822-28-1

# Chapter 6
# Offset Curved Translating Follower

**Abstract** The offset curved translating follower analysed in this chapter is a little more complex than the radial curved translating follower considered in Chap. 5. Once a diagram for the mechanism has been drawn the analysis follows and is straight forward. The equations simplify to those obtained in Chap. 5 for zero offset.

## 6.1 Introduction

As mentioned in Chap. 5 a curved translating follower with a suitable choice of follower radius, can result in a convex cam of high lift and short dwell, which will have a larger nose radius and require a smaller follower, than the corresponding flat follower. However, care must be taken to ensure that the pressure angle is not too large or the follower may stick in the guide. The offset curved translating follower can be used to reduce the pressure angle and consequent transverse loading.

## 6.2 Notation

| | |
|---|---|
| $e$ | Offset |
| $F_C$ | Cam force |
| $F_V$ | Valve force |
| $r_b$ | Base circle radius |
| $r_f$ | Follower radius |
| $s$ | Valve lift |
| $t$ | Time |

J. J. Williams, *Introduction to Analytical Methods for Internal Combustion Engine Cam Mechanisms*, DOI: 10.1007/978-1-4471-4564-6_6, 

$T$ Cam torque
$V_c$ Cam velocity
$V_e$ Entrainment velocity
$V_f$ Follower velocity
$V_s$ Sliding velocity
$x$ Coordinate
$y$ Coordinate
$\beta$ Pressure angle
$\delta$ Distance around cam
$\Delta$ Distance defined in text
$\theta$ Angle of cam rotation
$\rho$ Radius of curvature
$\bar{\psi}$ Angle of tangent to cam
$\omega$ Angular velocity

For convenience the cam and follower shown schematically in Fig. 6.1 have the follower shown rotated anti-clockwise by angle $\theta$ rather than showing the cam rotated clockwise by an angle, $\theta$. Let the lift at angle $\theta$ be $s$, the base circle radius be $r_b$ and the offset be $e$. This figure may need some thought in order to permit the reader to comprehend it fully.

## 6.3 Pressure Angle

As mentioned previously in this and subsequent chapters involving cam mechanisms, the derivatives of more than one variable are involved, Leibnitz's notation will be used.

With notation of Fig. 6.1:

$$d = \left[\left(r_b + r_f\right)^2 - e^2\right]^{0.5} \tag{6.1}$$

The torque arm of the cam force,$F_C$is given by:

$$\Delta = (d + s + e\tan\beta)\sin\beta - \frac{e}{\cos\beta} \tag{6.2}$$

The cam torque $T$ is given by

$$T = F_C\,\Delta \tag{6.3}$$

For an infinitesimal rotation of the cam, $d\theta$, and corresponding change in lift, $ds$, the work done by the cam is, $F_C\left[(d + s + e\tan\beta)\sin\beta - \frac{e}{\cos\beta}\right]d\theta$ and the work done on the follower is $F_V\,ds$.

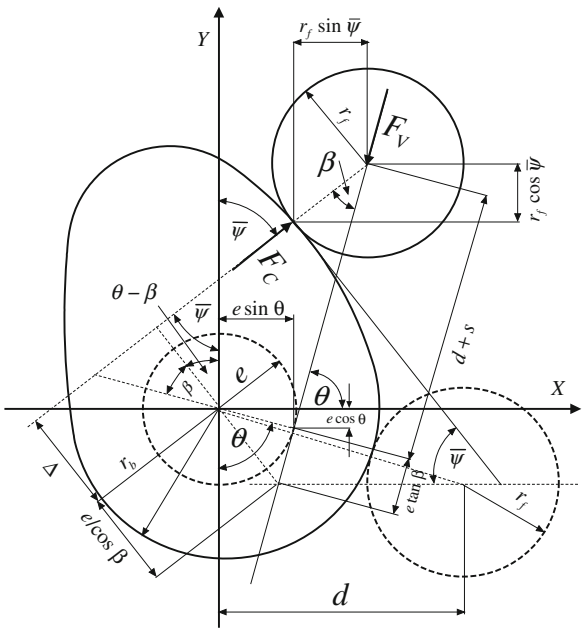


**Fig. 6.1** Offset curved translating follower cam mechanism

Now

$$F_V = F_C \cos\beta \tag{6.4}$$

We can therefore write:

$$F_C \cos\beta \, ds = F_C \left[ (d + s + e\tan\beta)\sin\beta - \frac{e}{\cos\beta} \right] d\theta \tag{6.5}$$

Hence:

$$\frac{ds}{d\theta} = \frac{(d + s + e\tan\beta)\sin\beta - \frac{e}{\cos\beta}}{\cos\beta} \tag{6.6}$$

Simplifying:

$$\frac{ds}{d\theta} = (d + s)\tan\beta + \frac{e\left(\sin^2\beta - 1\right)}{\cos^2\beta} \tag{6.7}$$

$$\frac{ds}{d\theta} + e = (d + s)\tan\beta \tag{6.8}$$

From Eq. (6.8) the pressure angle, $\beta$ is given by

$$\tan\beta = \frac{\left(\frac{ds}{d\theta} + e\right)}{(s + d)} \tag{6.9}$$

*Note* Since the pressure angle, $\beta$ is now known the cam torque $T = F_C \cdot \Delta$ can now be computed.

## 6.4 Cam Shape

The coordinates $x, y$ of the contact points are given by

$$x = (d+s)\cos\theta + e\sin\theta - r_f \sin\bar{\psi} \tag{6.10}$$

$$y = (d+s)\sin\theta - e\cos\theta - r_f \cos\bar{\psi} \tag{6.11}$$

## 6.5 Cam Curvature

Differentiating Eq. (6.9) w.r.t. $\theta$:

$$\frac{d\beta}{d\theta} = \frac{(d+s)\frac{d^2s}{d\theta^2} - \left(\frac{ds}{d\theta} + e\right)\frac{ds}{d\theta}}{(d+s)^2 \sec^2\beta} \tag{6.12}$$

From Sect. 1.8.2, recall that:

$$\frac{dx}{d\bar{\psi}} = \rho\cos\bar{\psi} \tag{1.7}$$

and

$$\frac{dy}{d\bar{\psi}} = -\rho\sin\bar{\psi} \tag{1.8}$$

Differentiating Eqs. (6.10) and (6.11) w.r.t. $\bar{\psi}$:

$$\frac{dx}{d\bar{\psi}} = \frac{ds}{d\bar{\psi}}\cos\theta - (d+s)\sin\theta\frac{d\theta}{d\bar{\psi}} + e\cos\theta\frac{d\theta}{d\bar{\psi}} - r_f\cos\bar{\psi} \tag{6.13}$$

$$\frac{dy}{d\bar{\psi}} = \frac{ds}{d\bar{\psi}}\sin\theta + (d+s)\cos\theta\frac{d\theta}{d\bar{\psi}} + e\sin\theta\frac{d\theta}{d\bar{\psi}} + r_f\sin\bar{\psi} \tag{6.14}$$

With notation of Fig. 6.1:

$$\bar{\psi} = \beta + \frac{\pi}{2} - \theta \tag{6.15}$$

Differentiating Eq. (6.15) w.r.t. $\theta$:

$$\frac{d\bar{\psi}}{d\theta} = \frac{d\beta}{d\theta} - 1 \tag{6.16}$$

From Eqs. (1.7), (6.13) and (6.16):

$$\rho = \frac{\frac{ds}{d\theta}\cos\theta - (d+s)\sin\theta + e\cos\theta}{\left(\frac{d\beta}{d\theta} - 1\right)\cos\bar{\psi}} - r_f \tag{6.17}$$

From Eqs. (1.8), (6.14) and (6.16):

$$\rho = -\frac{\frac{ds}{d\theta}\sin\theta + (d+s)\cos\theta + e\sin\theta}{\left(\frac{d\beta}{d\theta} - 1\right)\sin\bar{\psi}} - r_f \tag{6.18}$$

where $\frac{d\beta}{d\theta}$ is given by Eq. (6.12).

## 6.6 Entrainment Velocity

Let the angular velocity of the cam be $\frac{d\theta}{dt} = \omega$ rad/s.

The velocity of the contact point with respect to the cam is:

$$V_c = \rho\frac{d\bar{\psi}}{d\theta}\frac{d\theta}{dt} = \rho\frac{d\bar{\psi}}{d\theta}\omega \tag{6.19}$$

We can evaluate $\frac{d\bar{\psi}}{d\theta}$ from Eqs. (6.12) and (6.16):

The follower velocity is:

$$V_f = r_f\frac{d\beta}{d\theta}\frac{d\theta}{dt} = r_f\frac{d\beta}{d\theta}\omega \tag{6.20}$$

where $\frac{d\beta}{d\theta}$ is given by Eq. (6.12).

The entrainment velocity is:

$$V_e = V_c + V_f \tag{6.21}$$

and the sliding velocity is:

$$V_s = V_c - V_f \tag{6.22}$$

## 6.7 Contact Force and Stress

From Fig. 6.1 equilibrium of the follower requires that:

$$F_C \cos\beta = F_V \tag{6.23}$$

Hence

$$F_C = \frac{F_V}{\cos\beta} \tag{6.24}$$

Recall from Sect. 1.12.3 that the effective radius of curvature, $\rho^*$, for a curved follower and a convex and a concave cam is given by:

$$\rho^* = \left| \frac{\rho_C \rho_F}{\rho_C + \rho_F} \right| \tag{1.27}$$

The contact stress is given by:

$$\sigma_{Hz} = \left[ \frac{P^* E^*}{\pi \rho^*} \right]^{\frac{1}{2}} \tag{6.25}$$

## 6.8 Engine Speed for Zero Contact Force

Recall from Sect. 1.14 that the spring force $F_S$ is given by

$$F_S = k(s_0 + s) \tag{1.15}$$

At an engine speed of $N$ rpm the camshaft speed is $\frac{N}{2}\frac{360}{60} = 3N^\circ/s$ $= 3N\frac{\pi}{180} = \frac{\pi N}{60}$ rad/s.

Using Newton's notation the total valve force is:

$$F_V = \ddot{s}\left(\frac{\pi N}{60}\right)^2 M_E + F_S \tag{6.26}$$

If the contact force between cam and follower, $F_C = 0$ then $F_V = 0$.

Hence:

$$F_S = -\ddot{s}\left(\frac{\pi N}{60}\right)^2 M_E \tag{1.34}$$

Hence the maximum speed to maintain contact is:

$$N = \frac{60}{\pi}\sqrt{\frac{-F_S}{\ddot{s} M_E}} \tag{1.35}$$

*Note* This speed should only be computed when the valve acceleration is negative, as the number whose square root is required must be positive.

# Chapter 7
# Curved Finger Follower

**Abstract** The curved finger follower analysed in this chapter is more complex, both in obtaining a suitable diagram and analytically. The kinematics also considers the effect of a radial valve angle and the correct sign for the pressure angle. The kinetics of this mechanism involves rigid body motion and requires a complex diagram, which requires careful consideration. Similar but more complex equations for the design and manufacture of the cam are again derived from first principles.

## 7.1 Introduction

This cam mechanism has an asymmetrical cam shape even for a symmetrical valve lift curve. When building the engine and timing the cam the reference point is the nose of the cam, the point of maximum lift. It will be found that the point on the cam diametrically opposite the nose is not the point of contact at 180° of cam rotation from the nose. This is due to the asymmetry of the mechanism. For convenience the cam coordinates are computed as functions of $\theta$, the angle from the positive $x$-axis.

## 7.2 Notation

$F_C$ Cam force
$L$ Maximum valve lift
$r_a$ Distance from camshaft axis to centre of follower pivot
$r_b$ Base circle radius

J. J. Williams, *Introduction to Analytical Methods for Internal Combustion Engine Cam Mechanisms*, DOI: 10.1007/978-1-4471-4564-6_7, © Springer-Verlag London 2013

$r_f$ Follower radius
$r_r$ Distance from follower pivot to centre of curvature of follower
$s$ Valve lift
$t$ Time
$T$ Cam torque
$V_c$ Velocity of contact point relative to cam
$V_f$ Velocity of contact point relative to followerfollower
$x$ Coordinate
$y$ Coordinate
$\alpha$ Angle defined in text
$\beta$ Pressure angle
$\beta_0$ Pressure angle on base circle
$\delta$ Peripheral distance around cam
$\Delta$ Moment arm of contact force about camshaft axis
$\theta$ Angle of cam rotation
$\rho$ Radius of curvature of cam
$\phi$ Angle of follower rotation
$\phi_0$ Initial angular position of follower on base circle
$\bar{\phi}$ Angle defined in text
$\bar{\psi}$ Angle of tangent to cam at point of contact
$\omega$ Angular velocity of camshaft

## 7.3 Pressure Angle

As mentioned previously, in this and subsequent chapters involving cam mechanisms, the derivatives of more than one variable will be involved, and therefore Leibnitz's notation will be used. It is worth considering Fig. 7.1 and noting the parameters of interest. Identification of these parameters together with the correct diagram is essential if a mechanism is to be analysed. For convenience the cam mechanism shown schematically in Fig. 7.1 has the follower shown rotated anticlockwise by angle $\theta$, rather than showing the cam rotated clockwise by an angle $\theta$. The pressure angle for a swinging curved follower is the angle of the line of action of the contact force to the normal to the line from the centre of the follower pivot to the centre of curvature of the follower. Note that for this mechanism the pressure angle on the base circle, $\beta_0 > 0$. This will be proved in Sect. 7.3.1.

Let the follower lift at angle $\theta$ be $\phi$, the distance from cam centre to follower pivot be $r_a$, the distance from pivot to the centre of curvature of the follower be $r_r$, and the base circle radius be $r_b$.

With the notation of Fig. 7.1

$$\Delta = r_r \cos\beta - r_a \cos(\bar{\phi} + \beta) \tag{7.1}$$

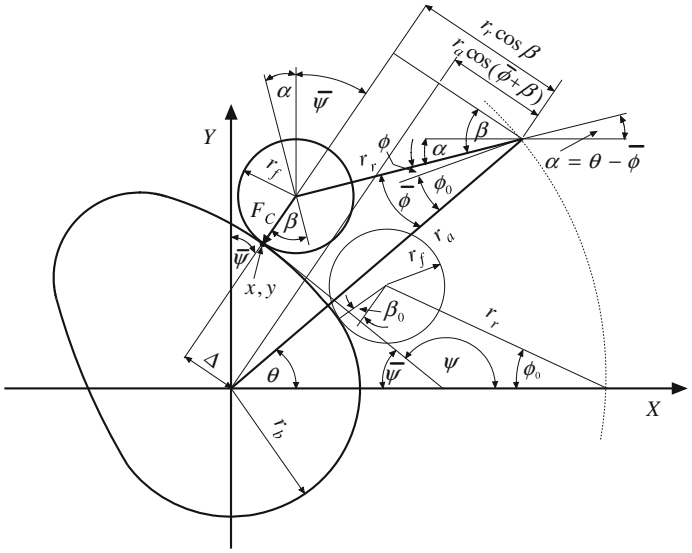


**Fig. 7.1** Curved finger follower cam mechanism

where

$$\bar{\phi} = \phi + \phi_0 \tag{7.2}$$

$$\cos\phi_0 = \frac{r_a^2 + r_r^2 - \left(r_b + r_f\right)^2}{2r_a r_r} \tag{7.3}$$

Let the cam force at the point of contact $(x, y)$ be $F_C$. Consider an infinitesimal rotation $d\theta$ of the cam, and a corresponding displacement $d\phi$ of the follower.

The work done by the cam is

$$F_C \Delta d\theta = F_C\left[r_r \cos\beta - r_a \cos\left(\bar{\phi} + \beta\right)\right] d\theta \tag{7.4}$$

The work done on the follower is

$$F_C r_r \cos\beta d\phi$$

Equating the work done, we obtain

$$F_C r_r \cos\beta d\phi = F_C\left[r_r \cos\beta - r_a \cos\left(\bar{\phi} + \beta\right)\right] d\theta \tag{7.5}$$

Hence:

$$r_r\left[1 - \frac{d\phi}{d\theta}\right] = r_a\left[\cos\bar{\phi} - \sin\bar{\phi}\tan\beta\right] \tag{7.6}$$

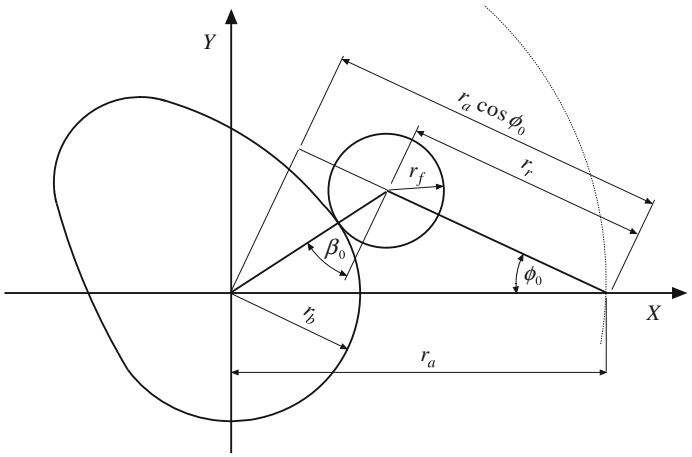


**Fig. 7.2** Positive pressure angle

This can be rearranged to give:

$$\tan \beta = \cot \bar{\phi} - \frac{r_r \left[1 - \frac{d\phi}{d\theta}\right]}{r_a \sin \bar{\phi}} \tag{7.7}$$

It can be seen from Eq. (7.7) that the sign of the pressure angle is not simply dependent on the sign of the valve velocity, unlike a curved translating follower. A negative pressure angle is shown in Fig. 7.3.

### *7.3.1 Correct Sign for Pressure Angle*

A typical pressure angle for a cam with a swinging curved follower is shown in Fig. 1.7 and can be positive or negative. It is therefore helpful to know how to identify the sign of the pressure angle. Figure 7.1 shows the follower on the base circle as shown in Fig. 7.2

On the base circle:

$$\theta = \phi = \frac{d\phi}{d\theta} = 0 \tag{7.8}$$

and

$$\bar{\phi} = \phi + \phi_0 = \phi_0 \tag{7.9}$$

Therefore Eq. (7.7) can be written as

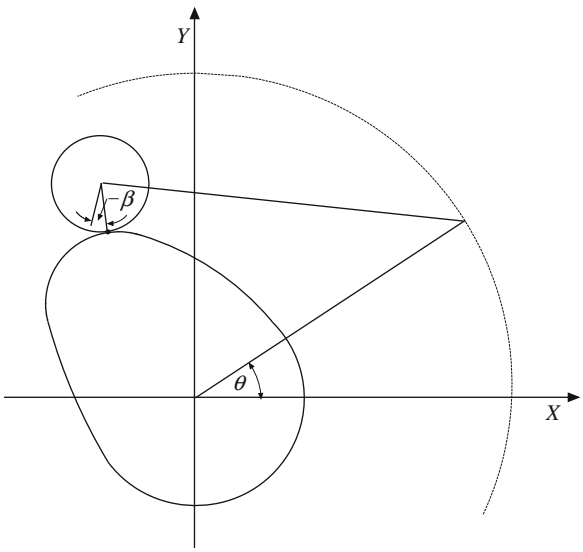


**Fig. 7.3** Negative pressure angle

$$\tan \beta_0 = \cot \phi_0 - \frac{r_r}{r_a \sin \bar{\phi}} \tag{7.10}$$

$$\tan \beta_0 = \frac{1}{\sin \phi_0} \left[ \cos \phi_0 - \frac{r_r}{r_a} \right] \tag{7.11}$$

As $0 < \bar{\phi} < \pi$ it follows that $\sin \phi_0 > 0$. If $\tan \beta_0 > 0$ then $\beta_0 > 0$ and from Eq. (7.11) this requires that

$$r_a \cos \phi_0 > r_r \tag{7.12}$$

From examination of Fig. 7.2 it is clear that inequality (7.12) is satisfied, and therefore $\beta_0 > 0$. It follows that in Fig. 7.1 we also have $\beta_0 > 0$.

It should be noted that in Fig. 1.7 the pressure angle on the base circle is negative. This is due to the differing geometry which tends to be used in practice, where the follower radius $r_f$, is somewhat larger than shown in Fig. 7.2. When designing a follower the extreme pressure angles of the follower contact surface should be comfortably larger than those computed for the initial cam design, to allow for any manufacturing errors and possible fitting of another cam with higher extreme valve velocities and consequent larger extreme pressure angles.

It is sometimes preferable to produce diagrams where the pressure angle is positive, as this is less likely to lead to errors in any subsequent analysis. A negative pressure angle is shown in Fig. 7.3. If it is more convenient to use a diagram with a negative pressure angle such as Fig. 7.6, it is worthwhile also drawing another with a positive pressure angle to check other angles have been obtained correctly as in Fig. 7.7.

## 7.4 Cam Shape

With the notation of Fig. 7.1

$$\alpha = \theta - \bar{\phi} \tag{7.13}$$

$$\bar{\psi} = \beta - \alpha \tag{7.14}$$

$$x = r_a \cos\theta - r_r \cos\alpha - r_f \sin\bar{\psi} \tag{7.15}$$

$$y = r_a \sin\theta - r_r \sin\alpha - r_f \cos\bar{\psi} \tag{7.16}$$

## 7.5 Cam Curvature

Recall Eqs. (1.1) and (1.2) derived in Sect. 1.8.2.

$$\cos\bar{\psi} = -\frac{dx}{d\delta} \tag{1.1}$$

and

$$\sin\bar{\psi} = \frac{dx}{d\delta} \tag{1.2}$$

Recall that:

$$\rho = \frac{d\delta}{d\bar{\psi}} \tag{1.3}$$

From Eqs. (1.1) and (1.3):

$$\rho\cos\bar{\psi} = \frac{dx}{d\bar{\psi}} \tag{1.4}$$

From Eqs. (1.2) and (1.3):

$$\rho \sin \bar{\psi} = -\frac{dy}{d\bar{\psi}} \tag{1.5}$$

Differentiating Eq. (7.7) with respect to $\theta$, and after some simplification:

$$\frac{d\beta}{d\theta} = \left[\frac{r_r}{r_a}\left\{\sin \bar{\phi}\frac{d^2\phi}{d\theta^2} + \left(1 - \frac{d\phi}{d\theta}\right)\cos \bar{\phi}\frac{d\phi}{d\theta}\right\} - \frac{d\phi}{d\theta}\right]\frac{\cos^2 \beta}{\sin^2 \bar{\phi}} \tag{7.17}$$

Differentiating Eq. (7.13) with respect to $\bar{\psi}$

$$\frac{d\alpha}{d\bar{\psi}} = \frac{d\theta}{d\bar{\psi}} - \frac{d\phi}{d\bar{\psi}} \tag{7.18}$$

Differentiating Eqs. (7.13) and (7.14) with respect to $\theta$:

$$\frac{d\bar{\psi}}{d\theta} = \frac{d\beta}{d\theta} - 1 + \frac{d\phi}{d\theta} \tag{7.19}$$

Differentiating Eq. (7.15) with respect to $\bar{\psi}$:

$$\frac{dx}{d\bar{\psi}} = -r_a \sin\theta \frac{d\theta}{d\bar{\psi}} + r_r \sin\alpha \frac{d\alpha}{d\bar{\psi}} - r_f \cos\bar{\psi} \tag{7.20}$$

Differentiating Eq. (7.16) with respect to $\bar{\psi}$

$$\frac{dy}{d\bar{\psi}} = r_a \cos\theta \frac{d\theta}{d\bar{\psi}} - r_r \cos\alpha \frac{d\alpha}{d\bar{\psi}} + r_f \sin\bar{\psi} \tag{7.21}$$

From Eqs. (1.4), (7.18) and (7.20)

$$\rho = \frac{\left[-r_a \sin\theta + r_r \sin\alpha\left(1 - \frac{d\phi}{d\theta}\right)\right]\frac{d\theta}{d\bar{\psi}}}{\cos\bar{\psi}} - r_f \tag{7.22}$$

From Eqs. (1.5), (7.18) and (7.21)

$$\rho = \frac{\left[-r_a \cos\theta + r_r \cos\alpha\left(1 - \frac{d\phi}{d\theta}\right)\right]\frac{d\theta}{d\bar{\psi}}}{\sin\bar{\psi}} - r_f \tag{7.23}$$

$\bar{\psi}$ is given by Eq. (7.14), and $\frac{d\bar{\psi}}{d\theta}$ by Eqs. (7.17) and (7.19).

## 7.6 Entrainment Velocity

Let the angular velocity of the cam be $\frac{d\theta}{dt} = \omega$ rad/s. Recall that $\bar{\psi}$ decreases as $\theta$ increases. The velocity of the contact point with respect to the cam is therefore:

$$V_c = \rho \frac{d\bar{\psi}}{d\theta}\frac{d\theta}{dt} = \rho \frac{d\bar{\psi}}{d\theta}\omega \tag{7.24}$$

The follower velocity is

$$V_f = r_f \frac{d\beta}{d\theta}\frac{d\theta}{dt} = r_f \frac{d\beta}{d\theta}\omega \tag{7.25}$$

where $\frac{d\beta}{d\theta}$ is given by Eq. (7.17).
The sliding velocity is

$$V_f - V_c = \left[r_f \frac{d\beta}{d\theta} - \rho \frac{d\bar{\psi}}{d\theta}\right]\omega \tag{7.26}$$

The entrainment velocity is

$$V_f + V_c = \left[r_f \frac{d\beta}{d\theta} + \rho \frac{d\bar{\psi}}{d\theta}\right]\omega \tag{7.27}$$

## 7.7 Kinematics for Curved Finger Follower

### *7.7.1 Notation*

| | |
|---|---|
| $B$ | Distance from follower pivot to camshaft axis perpendicular to valve axis |
| $C$ | Distance from follower pivot to camshaft axis parallel to valve axis |
| $D$ | Effective length of follower |
| $L$ | Maximum valve lift |
| $r_a$ | Distance from centre of cam to centre of follower pivot |
| $r_b$ | Base circle radius |
| $r_f$ | Follower radius |
| $r_r$ | Distance from follower pivot to centre of curvature of follower |
| $s$ | Valve lift |
| $\lambda$ | Fraction of total lift when follower centre line is perpendicular to valve axis |
| $\xi$ | Radial valve angle |
| $\theta$ | Angle of cam rotation |
| $\phi$ | Angle of follower rotation |
| $\phi_0$ | Initial angular position of follower on base circle |
| $\bar{\phi}$ | Angle defined in text |
| $\psi_0$ | Angle defined in text |

Fast combustion is essential for good performance, and this is very dependent upon the shape of the combustion chamber, which can be improved by inclining the valves in two perpendicular directions. The radial valve angle, $\xi$, is in a plane

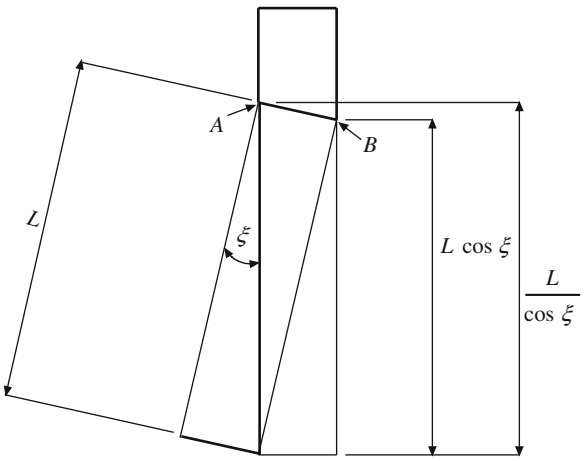


**Fig. 7.4** Effect of radial valve angle

normal to the camshaft axis and this helps the combustion chamber shape to approximate more closely to hemispherical.

In many designs this angle is zero to save complication and expense. However, if $\xi > 0$ then this needs to be considered in the analysis.

Following Cook (2003, private communication), and with notation of Fig. 7.4, the point A is an initial point of contact between cam and follower. As the valve opens the point A on the cam moves along the follower to the point B. The valve opens a distance, $L$, but the corresponding cam lift is $\frac{L}{\cos \xi}$.

The cam mechanism has been redrawn to suit the analysis and permit greater clarity. It is shown in Fig. 7.5.

$$D \sin \psi_0 = \frac{\lambda L}{\cos \xi} \tag{7.28}$$

Hence

$$\psi_0 = \sin^{-1} \frac{\lambda L}{D \cos \xi} \tag{7.29}$$

where $L$ is the maximum valve lift, $\lambda L$ is the valve lift when the follower centre line is perpendicular to the valve axis, and $D$ is the effective follower length.

Note that $s$ the valve lift at cam angle $\theta$. From consideration of Fig. 7.5

$$s - \lambda L = D \sin(\phi - \psi_0) \cos \xi \tag{7.30}$$

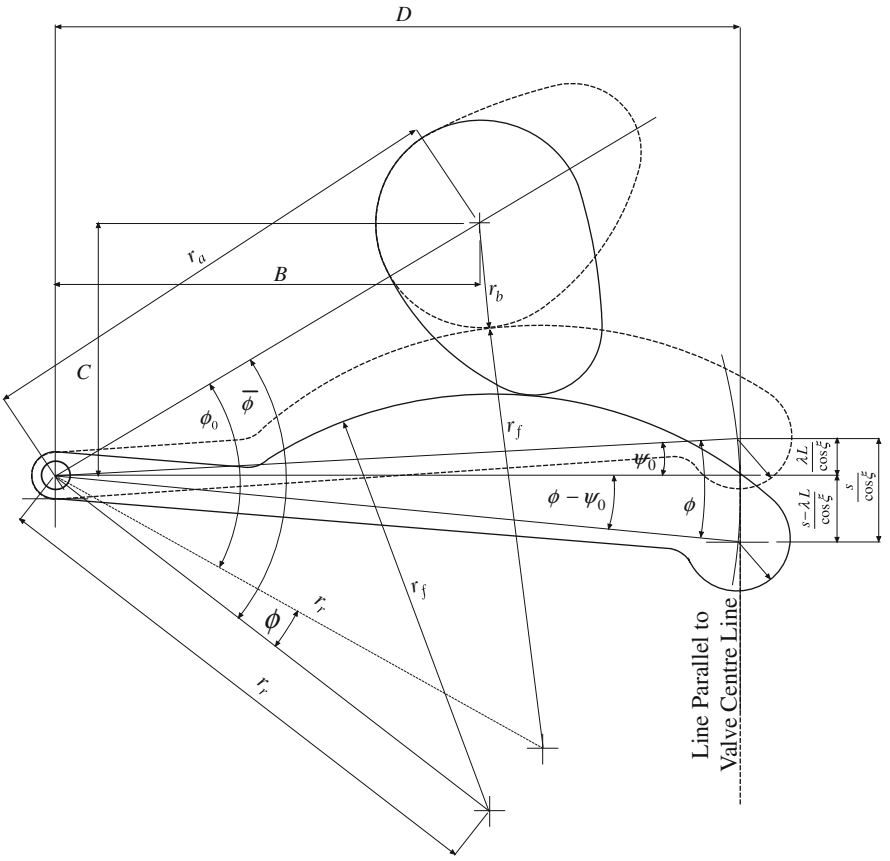


**Fig. 7.5** Follower kinematics

and

$$\phi_0 = \cos^{-1}\left[\frac{r_r^2 + r_a^2 - \left(r_b + r_f\right)^2}{2r_a r_r}\right] \tag{7.31}$$

$$\phi - \psi_0 = \sin^{-1}\left[\frac{s - \lambda L}{D\cos\xi}\right] \tag{7.32}$$

Differentiating Eq. (7.30) w.r.t. $\theta$

$$\frac{ds}{d\theta} = D\cos(\phi - \psi_0)\cos\xi\frac{d\phi}{d\theta} \tag{7.33}$$

Hence

$$\frac{d\phi}{d\theta} = \frac{ds}{d\theta} \frac{1}{D\cos(\phi - \psi_0)\cos\xi} \tag{7.34}$$

Differentiating Eq. (7.34) w.r.t. $\theta$:

$$\frac{d^2\phi}{d\theta^2} = \frac{D\cos(\phi - \psi_0)\cos\xi \frac{d^2s}{d\theta^2} + \frac{ds}{d\theta} D\cos\xi \sin(\phi - \psi_0)\frac{d\phi}{d\theta}}{D^2\cos^2(\phi - \psi_0)\cos^2\xi} \tag{7.35}$$

From Eqs. (7.34) and (7.35):

$$\frac{d^2\phi}{d\theta^2} = \frac{d^2s}{d\theta^2} \frac{1}{D\cos(\phi - \psi_0)\cos\xi} + \left[\frac{ds}{d\theta}\right]^2 \frac{\sin(\phi - \psi_0)}{D^2\cos^3(\phi - \psi_0)\cos^2\xi} \tag{7.36}$$

## 7.8 Kinetics for Curved Finger Follower

### 7.8.1 Notation

| | |
|---|---|
| $D$ | Effective length of follower |
| $E^*$ | Contact modulus |
| $F_C$ | Cam force |
| $F_{P_X}$ | Pivot force in X-direction |
| $F_{P_Y}$ | Pivot force in Y-direction |
| $F_S$ | Spring force |
| $F_V$ | Valve force |
| $I_p$ | Polar moment of inertia about pivot |
| $M_E$ | Mass of follower, valve, shim, cotters, top spring retainer and effective spring mass |
| $M_F$ | Mass of follower |
| $N$ | Rotational speed of engine in rpm |
| $P^*$ | Force per unit width of line contact |
| $k$ | Spring stiffness |
| $r_a$ | Distance from centre of cam to centre of follower pivot |
| $r_b$ | Base circle radius |
| $r_f$ | Follower radius |
| $r_g$ | Distance from pivot to centre of gravity of follower |
| $r_r$ | Distance from follower pivot to centre of curvature of follower |
| $\ddot{s}$ | Valve acceleration in m / radian$^2$ |
| $\beta$ | Pressure angle |
| $\theta$ | Angle of cam rotation |

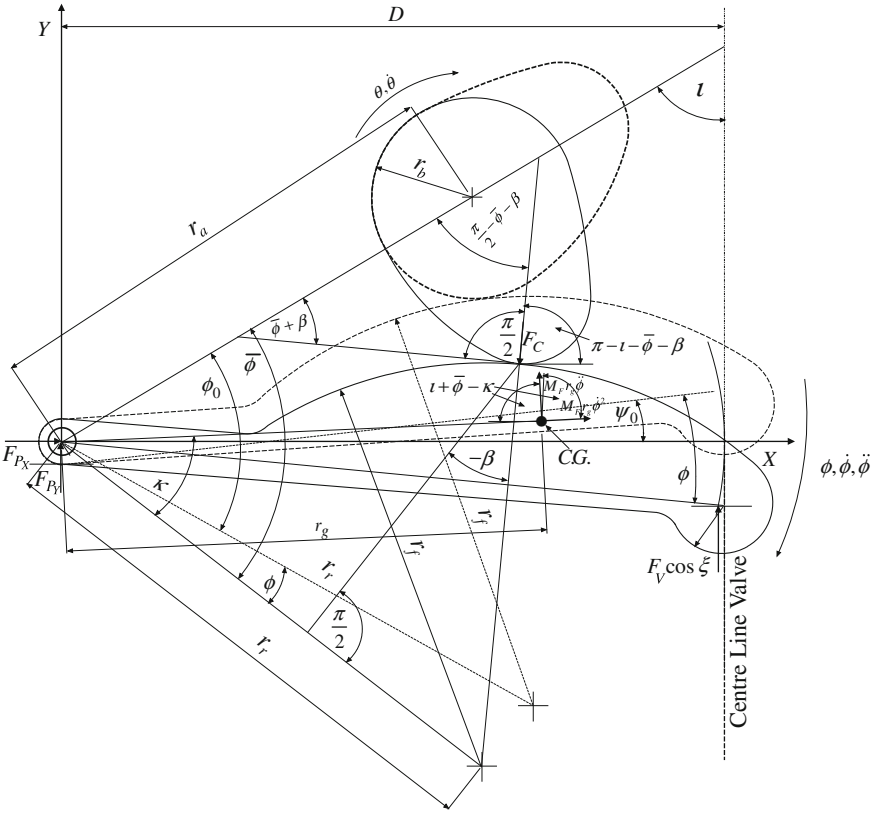


**Fig. 7.6** Follower kinetics

- $\iota$ Angle between line through centre of pivot and cam axis, and valve centre line
- $\kappa$ Angle between line through centre of pivot and centre of gravity of follower, and line through centre of pivot and centre of curvature of follower
- $\lambda$ Fraction of total lift when follower centre line is perpendicular to valve axis
- $\xi$ Radial valve angle
- $\rho$ Radius of curvature
- $\phi$ Angle of follower rotation
- $\ddot{\phi}$ Angular acceleration of follower in radian/radian$^2$
- $\phi_0$ Initial angular position of follower on base circle
- $\bar{\phi}$ Angle defined in Eq. 7.1 and shown in Fig. 7.6

With notation of Fig. 7.6, where the pressure angle, $\beta$, is negative and the cam rotates with: constant angular velocity, $\dot{\theta} = \omega$.

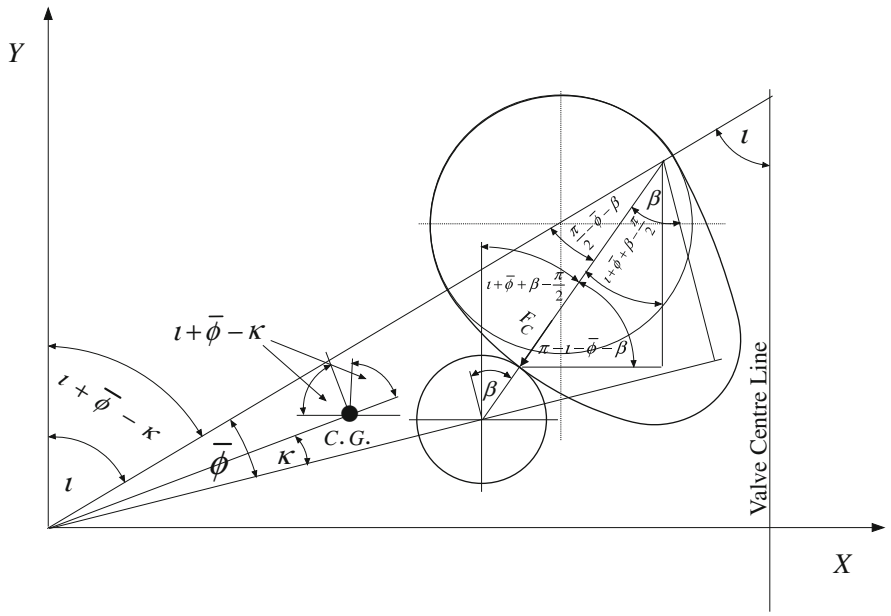


**Fig. 7.7** Angles for kinetics with positive pressure angle

Using Newton's notation to denote derivatives with respect to time, and taking moments about the follower pivot:

$$F_C r_r \cos\beta = I_p \ddot{\phi}\left[\frac{\pi N}{60}\right]^2 + F_V D \cos\xi \cos(\phi - \psi_0) \tag{7.37}$$

From Eq. (7.37):

$$F_C = \frac{I_p \ddot{\phi}\left[\frac{\pi N}{60}\right]^2 + F_V D \cos\xi \cos(\phi - \psi_0)}{r_r \cos\beta} \tag{7.38}$$

Resolving forces in the $X$-direction:

$$F_{P_X} = -F_C \cos\left(\iota + \bar{\phi} + \beta\right) + m_F r_g \ddot{\phi} \cos(\iota + \bar{\phi} - \kappa) - m_F r_g \dot{\phi}^2 \sin(\iota + \bar{\phi} - \kappa) \tag{7.39}$$

Resolving forces in the $Y$-direction:

$$\begin{aligned} F_{P_Y} + F_V \cos\xi = {} & F_C \sin\left(\iota + \bar{\phi} + \beta\right) - m_F r_g \ddot{\phi} \sin\left(\iota + \bar{\phi} - \kappa\right) \\ & - m_F r_g \dot{\phi}^2 \cos\left(\iota + \bar{\phi} - \kappa\right) \end{aligned} \tag{7.40}$$

From Eq. (7.40):

$$F_{P_Y} = F_C \sin\left(\imath + \bar{\phi} + \beta\right) - F_V \cos\xi - m_F r_g \ddot{\phi} \sin\left(\imath + \bar{\phi} - \kappa\right) - m_F r_g \dot{\phi}^2 \cos\left(\imath + \bar{\phi} - \kappa\right) \tag{7.41}$$

### 7.8.2 Contact Stress

Recall from Sect. 1.12. that the effective radius of curvature, $\rho^*$, for a curved follower and a convex and a concave cam is given by

$$\rho^* = \left|\frac{\rho_C \rho_F}{\rho_C + \rho_F}\right| \tag{1.27}$$

And the contact stress is given by

$$\sigma_{Hz} = \left[\frac{P^* E^*}{\pi \rho^*}\right]^{\frac{1}{2}} \tag{1.28}$$

### 7.8.3 Maximum Speed to Maintain Cam–Follower Contact for Curved Finger Follower

With reference to Sects. 1.14, 1.15 and 5.8, if the cam force is zero then from Eq. (7.37):

$$I_p \ddot{\phi} \left[\frac{\pi N}{60}\right]^2 + F_V D \cos\xi \cos(\phi - \psi_0) = 0 \tag{7.42}$$

$$F_V = \ddot{s} M_E \left[\frac{\pi N}{60}\right]^2 + F_S \tag{7.43}$$

From Eqs. (7.42) and (7.43)

$$I_P \ddot{\phi} \left[\frac{\pi N}{60}\right]^2 + \left\{F_S + \ddot{s} M_E \left[\frac{\pi N}{60}\right]^2\right\} D \cos(\phi - \psi_0) \cos\xi = 0 \tag{7.44}$$

After some algebra Eq. (7.44) can be written

$$N = \frac{60}{\pi} \left[\frac{-F_s}{\frac{I_P \ddot{\phi}}{D \cos(\phi - \psi_0) \cos\xi} + \ddot{s} M_E}\right]^{\frac{1}{2}} \tag{7.45}$$

# Chapter 8
# Asymmetric Cam Mechanisms

**Abstract** The offset rotating follower and the finger follower may both present problems in manufacture, which will not occur for a radial translating follower. Some CNC cam grinding machines and inspection machines are designed only for radial translating followers and will only accept data for this type of cam mechanism. If these machines accept data in $x \sim y$ format then there is no problem. If $x \sim y$ data is not acceptable it is necessary to transform the cam shape data into that for a radial translating curved follower. Methods for achieving this are described in this chapter. As the finger follower is more widely used for automotive purposes this mechanism is considered first, followed by the offset translating follower. Both the cam mechanisms considered in Chaps. 6 and 7 will have asymmetric cam shapes even for a symmetric valve lift curve. This means that the cam shape for a given valve lift differs if the direction of cam rotation changes, or if the follower is moved to the opposite side. The two possibilities, for a finger follower, have been described in the literature as leading and trailing, and towards and away. The latter terminology is used here.

## 8.1 Introduction

In Chaps. 6 and 7 the offset curved translating follower and the curved finger follower were analysed, but no consideration was given to manufacture or any other consequences of the asymmetry. In this chapter a solution is given to a potential problem with grinding and inspecting cams if the relevant machine does not accept cam shape data in $x \sim y$ coordinates.

Some CNC cam grinding machines and inspection machines require data for a radially translating follower with a flat translating follower as a special case. The cam lift data therefore requires transformation into a form acceptable to the CNC

J. J. Williams, *Introduction to Analytical Methods for Internal Combustion Engine Cam Mechanisms*, DOI: 10.1007/978-1-4471-4564-6_8, 

machine. If the machine will accept the cam shape in $x \sim y$ or $r \sim \theta$ format, then this procedure will not be required.

The method of cam lift transformation from an asymmetric cam mechanism to a radially translating follower mechanism requires data to be stored in computer memory to considerable *precision* if a sufficiently *accurate* cam lift curve is to be computed.

The curved finger follower is more widely used than the offset translating follower and therefore the finger follower will be considered first.

## 8.2 Curved Finger Follower

### *8.2.1 Notation*

$r_a$ Distance from centre of cam to centre of follower pivot
$r_b$ Base circle radius
$r_f$ Follower radius
$r_r$ Distance from follower pivot to centre of curvature of follower
$s^*$ Valve lift as a function of $\theta^*$
$\tilde{s}^*$ Valve lift as a function of $\tilde{\theta}^*$
$\hat{s}$ Valve lift as a function of $\hat{\theta}$
$x$ Coordinate of contact point at $\theta$
$y$ Coordinate of contact point at $\theta$
$\hat{x}$ Coordinate of contact point at $\hat{\theta}$
$\hat{y}$ Coordinate of contact point at $\hat{\theta}$
$\alpha$ Angle defined in text
$\beta$ Pressure angle as a function of $\theta$
$\beta_0$ Pressure angle on base circle
$\beta$ Pressure angle for finger follower as a function of $\theta$
$\beta^*$ Pressure angle for radial translating follower as a function of $\theta^*$
$\theta$ Angle of finger follower cam rotation
$\theta^*$ Angle of radially translating follower cam rotation
$\tilde{\theta}^*$ Angle of radially translating follower cam rotation
$\bar{\theta}$ Angle defined in text
$\hat{\theta}$ Angle of radially translating follower cam rotation
$\phi$ Angle of follower rotation
$\phi_0$ Initial angular position of follower on base circle
$\bar{\phi}$ Angle defined in text
$\psi$ Angle defined in text
$\bar{\psi}$ Angle of tangent to cam at point of contact as a function of $\theta$ and $\theta^*$
$\hat{\psi}$ Angle of tangent to cam at point of contact as a function of $\hat{\theta}$

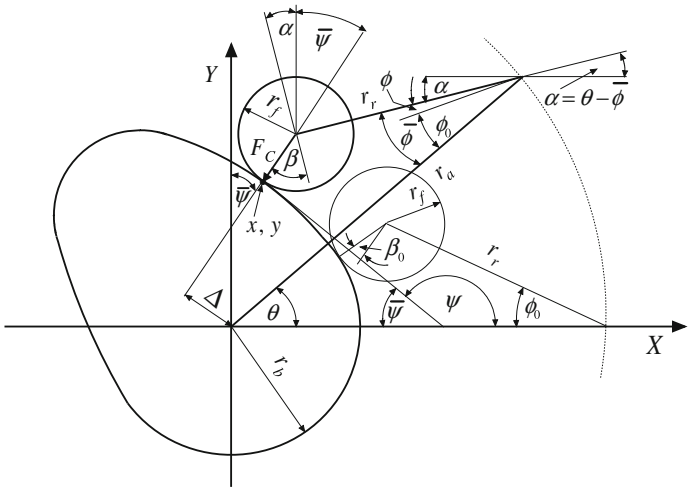


**Fig. 8.1** Curved finger follower mechanism

## *8.2.2 Transformation to Radially Translating Curved Follower*

If we have obtained a cam shape for a cam with a curved finger follower of constant radius as shown schematically in Fig. 8.1, and either the available CNC cam grinding machine or the cam inspection machine or both will not accept data in $x \sim y$ coordinates then the data will need to be transformed into the lift curve for a cam with a radially translating follower with the same follower radius.

This curved finger follower was analysed in Chap. 7. With notation of Fig. 8.1, we have lift data for a curved finger follower where, $r_a$, $r_b$, $r_f$ and $r_r$ have been prescribed by the designer. The previously computed data consists of the cam lift, $s$, and the angle, $\bar{\phi}$ which are functions of cam rotation angle, $\theta$ which is in equally incremented steps, where

$$\bar{\phi} = \phi_0 + \phi. \tag{8.1}$$

The curved translating follower has been analysed in Chap. 5 and is shown in Fig. 8.2. In the two cases the cams shown have the same shape, the follower is shown at the same point of contact and the two followers have equal radii. However, the angle of cam rotation, $\theta$ for the two mechanisms is not the same. The cam shape for the curved finger follower has been computed for equal increments of angle of rotation, but the corresponding contact points on the curved translating follower have increments of angle of rotation which will not be equal, but may be larger or smaller than those for the finger follower.

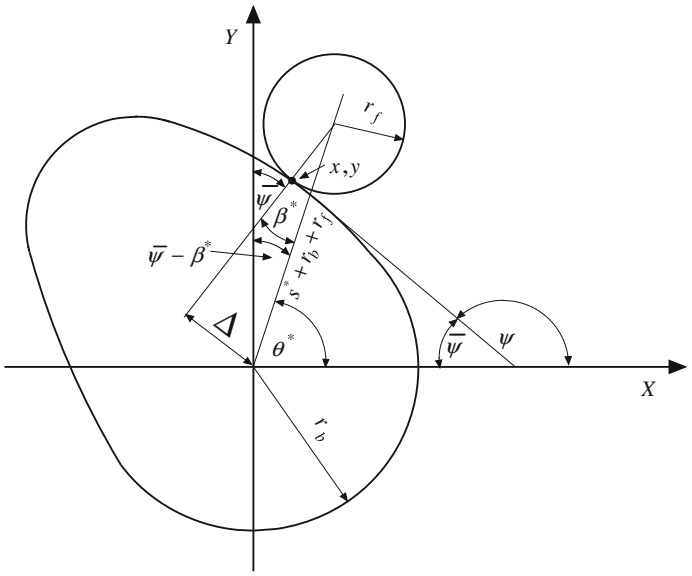


**Fig. 8.2** Curved translating follower with same contact point

In Fig. 8.2 the parameters, $r_b$, and $r_f$ are the same as those for the finger follower in Fig. 8.1 and as the cams are of the same shape, but the pressure angle, $\beta^*$ at the same contact point differs from that for the finger follower, $\beta$.

Figures 8.1 and 8.2 are shown superposed in Fig. 8.3. The two angles of cam rotation differ but need to be related. The angle of cam rotation for the curved finger follower remains as $\theta$, and that for the translating follower becomes $\theta^*$ and the associated cam lift is $s^*$. With notation of Fig. 8.3 the angle $\theta^*$ is given by

$$\theta^* = \theta + \bar{\theta} \tag{8.2}$$

In order to obtain the angle, $\theta^*$, the angle, $\bar{\theta}$ can be obtained from:

$$\tan \bar{\theta} = \frac{r_r \sin \bar{\phi}}{r_a - r_r \cos \bar{\phi}} \tag{8.3}$$

and

$$\left(s^* + r_b + r_f\right) \sin \theta = r_r \sin \bar{\phi} \tag{8.4}$$

Equation (8.4) can be rewritten as:

$$s^* = \frac{r_r \sin \bar{\phi}}{\sin \theta} - r_b - r_f \tag{8.5}$$

Note that although the angle, $\theta$, is in equal increments, $\bar{\theta}$ is not and therefore $\theta^*$ is not. In order to align the values of $\theta$ and $\theta^*$ which have initially been computed

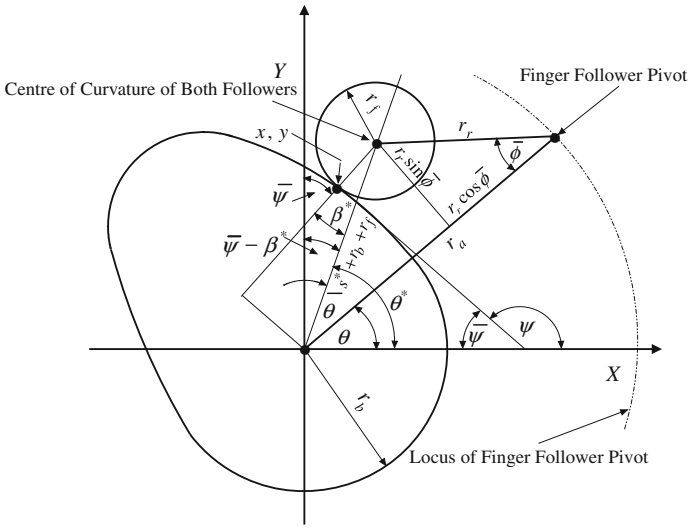


**Fig. 8.3** Combination of finger follower and translating follower mechanisms

from differing origins, due to the differing mechanisms, we can equate the value of $\theta^*$ at maximum lift to 180°, and adjust the other values of $\theta^*$ and $s^*$ accordingly, to obtain a new set of lift data, $\tilde{s}^*$ and $\tilde{\theta}^*$. If $\tilde{\theta}^* < 0$ then add 360° to those values of $\tilde{\theta}^*$, and if $\tilde{\theta}^* > 360°$ then subtract 360° from those values of $\tilde{\theta}^*$.

As the angle of cam rotation, $\theta^*$ does not increase in equal increments, it follows that $\tilde{\theta}^*$ does not either. Some camshaft measuring machines, will only accept lift data in equal increments of cam rotation angle. A new set of the lift data $\tilde{s}^*$, denoted by $\hat{s}$, where $\hat{s}$ is for equal increments of cam angle denoted by $\hat{\theta}$, which can be computed using cubic spline interpolation, a procedure which is well documented [1, 2].

Using these data, where $\hat{s}$, is a function of equally spaced values of $\hat{\theta}$, the cam shape can be determined from consideration of Fig. 8.4. Recall Eqs. (5.6) and (5.7) which can be rewritten as:

$$\hat{x} = \left(\hat{s} + r_b + r_f\right)\cos\hat{\theta} - r_f \sin\hat{\psi} \tag{8.6}$$

$$\hat{y} = \left(\hat{s} + r_b + r_f\right)\sin\hat{\theta} - r_f \cos\hat{\psi} \tag{8.7}$$

where

$$\hat{\psi} = \hat{\beta} + \frac{\pi}{2} - \hat{\theta} \tag{8.8}$$

The pressure angle, $\hat{\beta}$ is given by

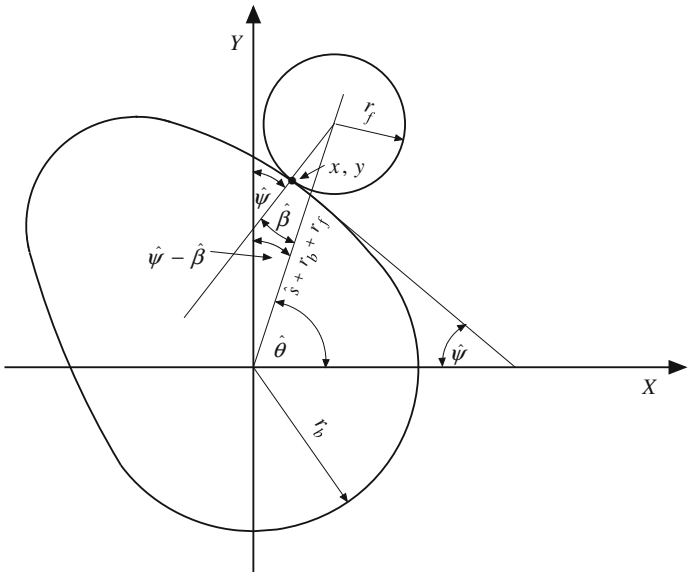


**Fig. 8.4** Curved translating follower with lift data for corresponding finger follower

$$\tan \hat{\beta} = \frac{d\hat{s}/d\hat{\theta}}{\hat{s} + r_b + r_f} \tag{8.9}$$

We can obtain approximate, but sufficiently accurate values of the velocity, $d\hat{s}/d\hat{\theta}$ from first differences of the lift, $\hat{s}$. This is often the method employed by the relevant grinding or measuring machine to compute the cam shape, and is described in Appendix 2. An approximate check on the resulting cam shape, $\hat{x} \sim \hat{y}$ computed using Eqs. (8.6) and (8.7) can be compared with that for the finger follower cam, $x \sim y$, which can be obtained from Eqs. (7.15) and (7.16), by superposing the two cam shapes.

## 8.3 Offset Translating Curved Follower

### *8.3.1 Notation*

| | |
|---|---|
| $A$ | Parameter in quadratic equation |
| $B$ | Parameter in quadratic equation |
| $C$ | Parameter in quadratic equation |
| $d$ | Length defined in text |
| $e$ | Follower offset |

$r_b$ Base circle radius
$r_f$ Follower radius
$s$ Valve lift as a function of $\theta$
$\bar{s}$ Valve lift as a function of $\bar{\theta}$
$s^*$ Valve lift as a function of $\theta^*$
$\tilde{s}^*$ Valve lift as a function of $\tilde{\theta}^*$
$\hat{s}$ Valve lift as a function of $\hat{\theta}$
$x$ Coordinate of contact point at $\theta$
$y$ Coordinate of contact point at $\theta$
$\hat{x}$ Coordinate of contact point at $\hat{\theta}$
$\hat{y}$ Coordinate of contact point at $\hat{\theta}$
$\alpha$ Angle defined in text
$\beta$ Pressure angle as a function of $\theta$
$\bar{\beta}$ Angle defined in text
$\hat{\beta}$ Pressure angle as a function of $\hat{\theta}$
$\theta$ Angle of finger follower cam rotation
$\theta^*$ Angle of radially translating follower cam rotation
$\tilde{\theta}^*$ Angle of radially translating follower cam rotation
$\bar{\theta}$ Angle defined in text
$\hat{\theta}$ Angle defined in text
$\tilde{\theta}$ Angle defined in text
$\psi$ Angle defined in text
$\bar{\psi}$ Angle of tangent to cam at point of contact as a function of $\theta$
$\hat{\psi}$ Angle of tangent to cam at point of contact as a function of $\hat{\theta}$

### *8.3.2 Transformation to Radially Translating Curved Follower*

The basic method of solution is the same as for the curved finger follower. The offset translating curved follower has been considered in Chap. 6 and is shown in Fig. 8.5. As it is again an asymmetric mechanism the same problems may arise in manufacture as with the curved finger follower. The cam shape for the offset translating curved follower has been computed for equal increments of angle of rotation but for the corresponding contact points on the radial translating follower the increments of angle of rotation will not be equal, but may be larger or smaller than for the offset follower.

Figures 8.2 and 8.5 are shown superposed in Fig. 8.6. The two angles of cam rotation differ but need to be related. The angle of cam rotation for the offset follower remains as $\theta$, and that for the translating follower is $\theta^*$. With notation of Fig. 8.6, the parameters, $r_b$, and $r_f$ are the same for both mechanisms, and the

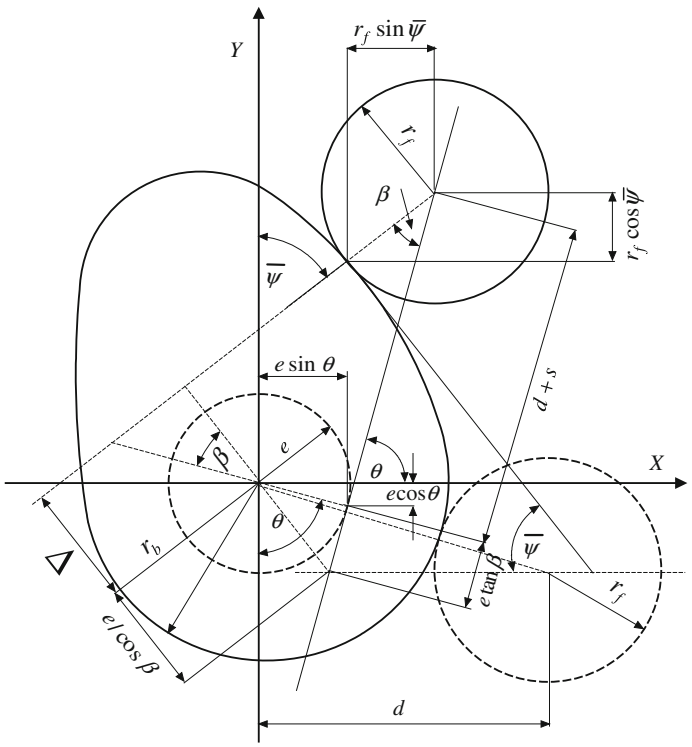


**Fig. 8.5** Offset curved translating follower mechanism

respective pressure angles, at the same contact point are $\beta$ and $\bar{\beta}$. The valve lift, $s$ is known for the offset cam. The corresponding valve lift for the radial cam is denoted by $\bar{s}$, where

$$\left(\bar{s} + r_b + r_f\right)^2 = e^2 + (d+s)^2 \tag{8.10}$$

where

$$d = \left[\left(r_b + r_f\right)^2 + e^2\right]^{0.5} \tag{6.1}$$

Equation (8.10) can be written as a quadratic equation in the unknown lift, $\bar{s}$ where

$$A\bar{s}^2 + B\bar{s} + C = 0 \tag{8.11}$$

and

$$A = 1 \tag{8.12}$$

$$B = 2\left(r_b + r_f\right) \tag{8.13}$$

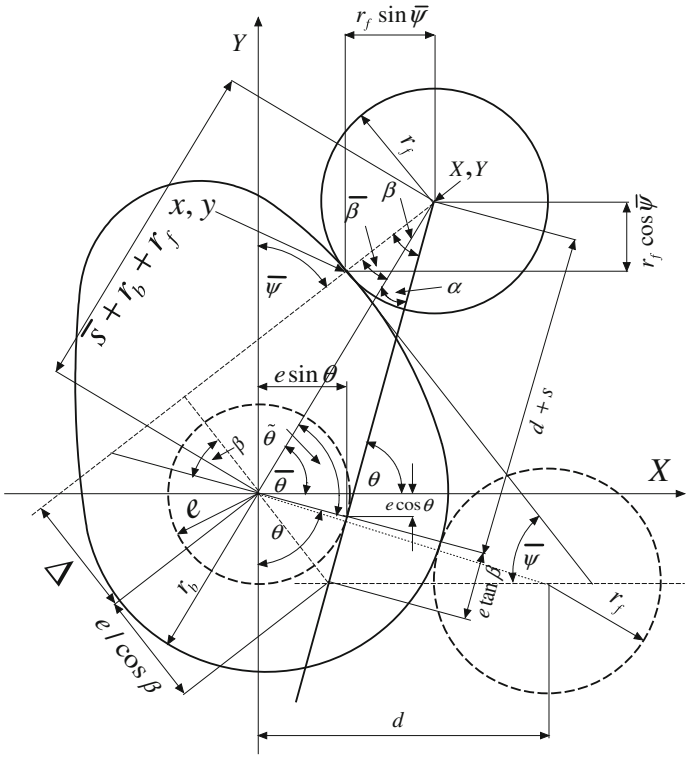


**Fig. 8.6** Combination of radial and offset curved finger follower mechanisms

$$C = r_b^2 + r_f^2 + e^2 + d^2 + s^2 + 2\left(r_b r_f + ds\right) \tag{8.14}$$

Since $\bar{s} \geq 0$:

$$\bar{s} = \frac{-B + \sqrt{B^2 - 4AC}}{2A} \tag{8.15}$$

Hence with knowledge of $\bar{s}$ the angle $\tilde{\theta}$ can be evaluated:

$$\tilde{\theta} = \cos^{-1}\left[\frac{e^2 + \left(\bar{s} + r_b + r_f\right)^2 - (d+s)^2}{2e\left(\bar{s} + r_b + r_f\right)}\right] \tag{8.16}$$

$$\bar{\theta} = \tilde{\theta} - \left(\frac{\pi}{2} - \theta\right) \tag{8.17}$$

$$\bar{\theta} = \tilde{\theta} + \theta - \frac{\pi}{2} \tag{8.18}$$

$$\alpha = \frac{\pi}{2} - \tilde{\theta} \tag{8.19}$$

$$\bar{\beta} = \beta - \alpha \tag{8.20}$$

As before although the angle, $\theta$ is in equal increments but $\bar{\theta}$ is not. In order to align the values of $\theta$ and $\theta^*$ which have initially been computed from differing origins, due to the differing mechanisms, we can equate the value of $\theta^*$ at maximum lift to 180°, and adjust the other values of $\theta^*$ and $s^*$ accordingly, to obtain a new set of lift data, $\tilde{s}^*$ and $\tilde{\theta}^*$. If $\tilde{\theta}^* < 0$ then add 360° to those values of $\tilde{\theta}^*$, and if $\tilde{\theta}^* > 360°$ then subtract 360° from those values.

Again whereas angle $\theta$ increases in equal increments, angle $\tilde{\theta}^*$ does not. Some camshaft measuring machines, will only accept lift data in equal increments of cam rotation angle. A new set of the lift data, $\hat{s}$ where $\hat{s}$ is for equal increments of camshaft angle, $\hat{\theta}$ can now be computed using cubic spline interpolation, [1, 2].

With reference to Fig. 8.4 we can again determine the pressure angle, $\hat{\beta}$ from Eq. (8.9). By using central differences to compute the valve velocity, $d\hat{s}/d\hat{\theta}$ it is then possible to obtain $\hat{\psi}$ from Eq. (8.8). Using these new data, the cam shape can be determined from Eqs. (8.6) and (8.7). As in Sect. 8.2.2, we can obtain approximate, but sufficiently accurate values of the velocity, $d\hat{s}/d\hat{\theta}$ from first differences of the lift, $\hat{s}$. This is often the method employed by the relevant grinding or measuring machine to compute the cam shape, and is described in Appendix 2. An approximate check on the resulting cam shape, $\hat{x} \sim \hat{y}$ computed using Eqs. (8.6) and (8.7) can be compared with that for the finger follower cam, $x \sim y$, which can be obtained from Eqs. (7.15) and (7.16), by superposing the two cam shapes.

## 8.4 Unequally Spaced Contact Points

The radially translating point follower mechanism shown in Fig. 8.7 has the point of contact, $x$, $y$ at an angle $\theta$. As the camshaft rotates in equal increments, $\delta\theta$, the angular spacing between the points $x$, $y$ is also in equal increments $\delta\theta$. Such a mechanism is clearly of very limited use for tribological reasons.

For other mechanisms both symmetric and asymmetric, these equal increments in spacing of the contact point $x$, $y$ only occur while the follower is in contact with the base circle. One consequence of this is that if the cam shape data is required in $r$, $\theta$, format the increments in $\theta$ will be unequal, apart from the contact points on the base circle. If the manufacturing data is required in equal increments of $\theta$ this can again be obtained accurately using cubic spline interpolation, [1, 2].

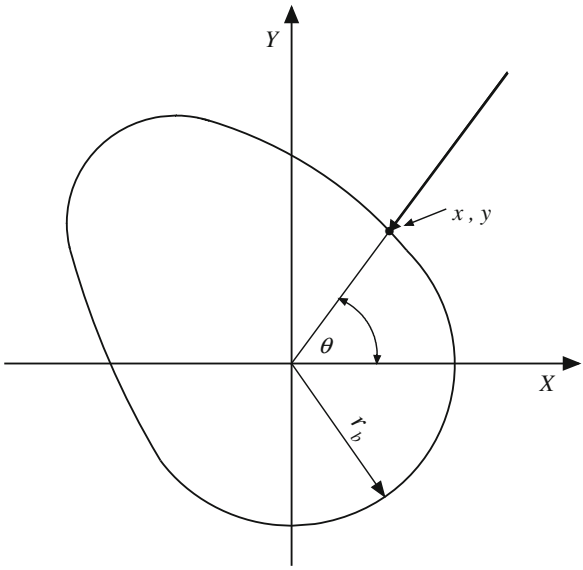


**Fig. 8.7** Translating point follower mechanism

## 8.5 Further Consequences of Asymmetry

### *8.5.1 Towards and Away*

In the case of a flat translating follower a symmetric valve lift curve produces a symmetric cam shape, so even if the direction of cam rotation is reversed, the valve motion remains the same. Matters are more complex for a swinging follower, where the cam shape will not be symmetric.

The arguments advanced below are not mathematical but may be more easily comprehended if the reader has access to a cylinder head with a cam shaft and finger followers fitted which can be viewed from either end. If such a visual aid is not available the reader may find that a diagram of a finger follower cam mechanism drawn on a transparent material, which can be viewed from both sides is helpful.

Figure 8.8a, b shows the two possibilities for asymmetric cam mechanisms. Consider initially a cam whose valve lift curve is symmetric. The two cases are sometimes referred to as leading and trailing cams, or towards and away.

When the direction of rotation of the cam and the follower are the same as the lift increases, the rotation is said to be *towards* the pivot. When the direction of rotation of the cam and the follower are in opposite directions as the lift increases, the rotation is said to be *away* from the pivot.

Suppose viewed from the driven end a cam with a symmetric valve lift curve rotates clockwise and rotation is *towards* the follower pivot. If the cam were to rotate anticlockwise then the valve motion would remain unchanged but rotation would be *away* from the follower pivot. If the cam is viewed from the opposite end

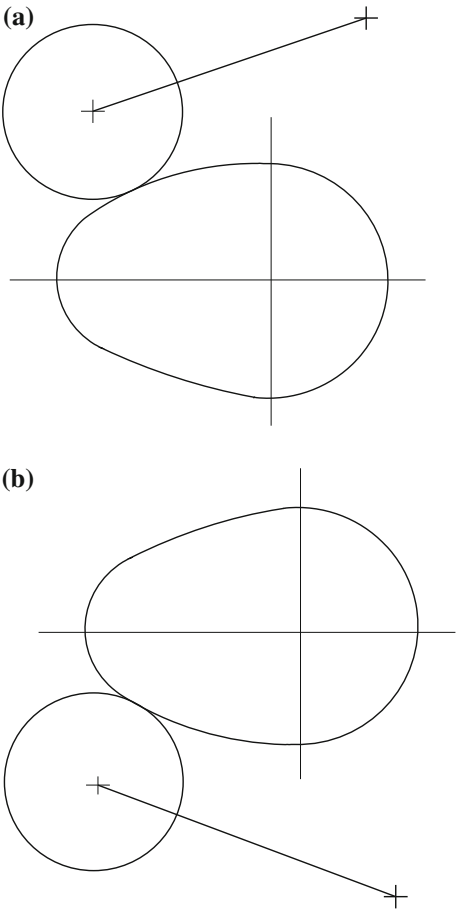


**Fig. 8.8** **a** Clockwise *towards* cam, anticlockwise *away* cam. **b** Clockwise *away* cam, anticlockwise *towards* cam

of the shaft the apparent direction of motion is reversed and a mirror image of the cam shape is observed. It follows from symmetry considerations that the *away* cam is the mirror image of the *towards* cam, however this only applies for a symmetric valve lift curve.

The analysis given previously is for a clockwise towards cam, but depending upon requirements there may be a need for an away cam and/or an anticlockwise cam. It is therefore possible to obtain any of the other three possibilities using the clockwise towards program result. The cam synthesis is in two parts which meet at the nose. The closing part is obtained by mirroring the data which is initially for the opening side about the nose. The complete acceleration curve is obtained by joining the two pieces together.

A clockwise *towards* cam shape, and associated data, can be initially synthesised from the valve lift data using the opening cam data followed by the closing side data. If the valve lift curve is produced with the closing side data followed by the opening side data, then this will result in an anticlockwise *away*

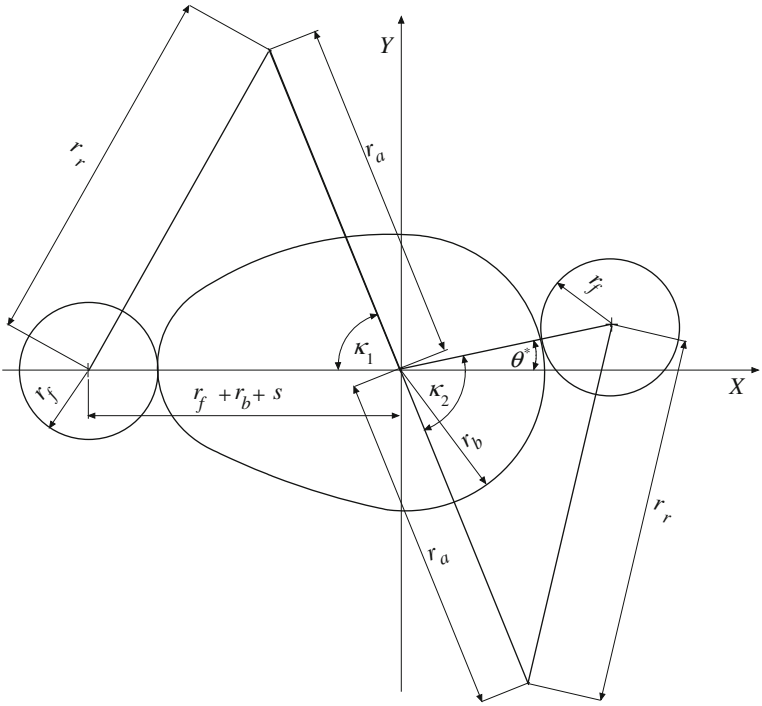


**Fig. 8.9** Contact point at 180° of cam rotation from nose

cam. The corresponding cam for the opposite direction of rotation can then be obtained by mirroring the cam shape.

## *8.5.2 Alignment of the Cam Shape Data*

In the case of a symmetric mechanism such as a translating flat follower the position of the follower after 180° of cam rotation from the nose is on a line from the nose through the cam axis. With notation of Fig. 8.9, it can be seen that this is not the case for a curved finger follower, where the point of contact on the base circle is seen to be at an angle of $\theta^*$ to the cam axis.

$$\kappa_1 = \cos^{-1}\left[\frac{r_a^2 + \left(r_f + r_b + s\right)^2 + r_r^2}{2r_a\left(r_f + r_b + s\right)}\right] \tag{8.21}$$

$$\kappa_2 = \cos^{-1}\left[\frac{r_a^2 + \left(r_f + r_b\right)^2 + r_r^2}{2r_a\left(r_f + r_b\right)}\right] \tag{8.22}$$

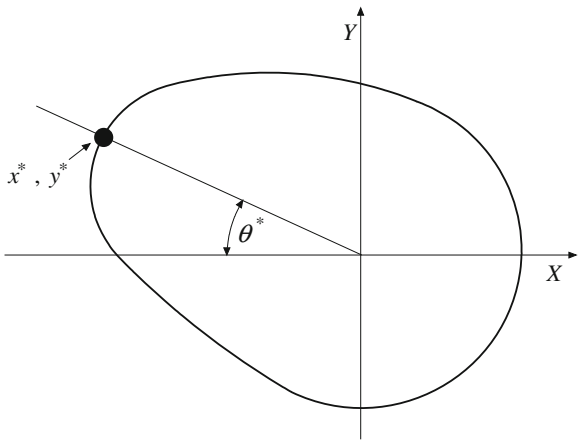


**Fig. 8.10** Typical cam shape as computed

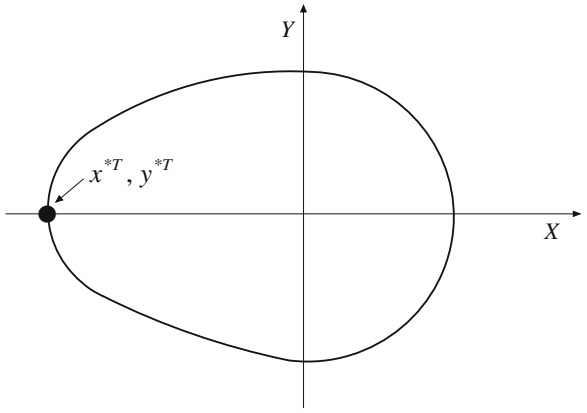


**Fig. 8.11** Transform of shape to position the nose on the $X$-axis

$$\theta^* = \kappa_2 - \kappa_1 \tag{8.23}$$

One consequence of this is that the computed cam shape when displayed on the screen will tend to look like the cam shown in Fig. 8.10. Another is that if two finger follower mechanisms are to be used together where the angles $\theta^*$ for the two mechanisms differ as when used in some desmodromic cam mechanisms, it is best to time the cam shape data at the nose to ensure the correct relative timing of the cams.

For each point $x(\theta)$, $y(\theta)$ we can obtain a new point $x^T(\theta)$, $y^T(\theta)$ as shown in Fig. 8.11.

With notation of Fig. 8.10, the line from the origin to the nose at $x^*$, $y^*$ is inclined at an angle $\theta^*$ to the $X$-axis. We can transform the cam shape to bring the nose to lie on the $X$-axis.

$$\tan \theta^* = -\frac{y^*}{x^*} \tag{8.24}$$

We can obtain the new cam shape using the transformation:

$$x^T(\theta) = x(\theta)\cos\theta^* - y(\theta)\sin\theta^* \tag{8.25}$$

$$y^T(\theta) = x(\theta)\sin\theta^* + y(\theta)\cos\theta^* \tag{8.26}$$

To obtain a mirror image of the cam shape shown in Fig. 8.11 we can multiply all values of $y^T(\theta)$ by $-1$.

## References

1. Curtis AR, Powell MJD (1967) Using cubic splines to approximate functions, of one variable to prescribed accuracy AERE R-5602, January 1967
2. Press WH et al (1996) Numerical recipes in Pascal, chapter 3. Cambridge University Press, Cambridge. ISBN: 0-521-37516-9

# Chapter 9
# Camshaft Torques

**Abstract** At high engine speeds the inertia loads caused by the high accelerations of the valves as they open and close generate camshaft torques which can excite torsional oscillations of the camshafts. If the valve timing, and for V engines, the V-angle are such that the torques from each camshaft tend to reinforce one another, then these torques can be significant. Any resulting torsional vibrations can cause valve timing errors at certain engine speeds, especially in the cylinders remote from the camshaft drive train. This can result in valve and piston collisions which can result in the destruction of the engine. To damp these vibrations the engine designer needs to ascertain the magnitude of the torques for the engine orders associated with the largest harmonic components. To do this the camshaft torques need to be computed and then analysed. This harmonic analysis can be achieved with a personal computer and the Fast Fourier Transform. This chapter describes the method of computing the camshaft torques and adding them together and gives examples of the results of the Fourier analysis, which show the effect of valve timing and V-angle on the magnitude of the resulting constituent engine orders for a V8 engine.

## 9.1 Introduction

High speed internal combustion engines develop high inertia loads and this includes the camshaft torques developed while opening and closing the valves.

For certain combinations of engine configuration and valve timing these torques can result in significant torsional vibration. V-8 engines can be particularly prone to this problem, whose magnitude is dependent on the way the torques generated by individual camshafts interact with one another. This effect is very dependent upon the V-angle and the valve timing, which affect the way the torques from

J. J. Williams, *Introduction to Analytical Methods for Internal Combustion Engine Cam Mechanisms*, DOI: 10.1007/978-1-4471-4564-6_9, © Springer-Verlag London 2013

differing camshafts add together. The constituent frequencies of the exciting torques are at certain integer multiples, n, of the camshaft speed.

For a four stroke V8 these integer values, n, or orders will be 4, 8, 12, 16 etc. The eighth order is usually the largest component. The magnitude of the higher orders rapidly decreases, and after the eighth, the fourth, or the twelfth order is usually the next largest component. These generalisations are not always the case, and in one example given below the sixteenth order is the second largest component.

The use of reactive rotating pendulum dampers, to damp the torsional vibrations caused by these oscillatory torques will be considered in the next chapter. The damping of the lower harmonics is easier as the precision required to manufacture the components can preclude the damping of higher orders. Significant wear of the moving parts can cause the damper to exacerbate rather than solve the problem, and this is worse for the smaller dimensions associated with higher orders such as the twelfth and especially the sixteenth.

## 9.2 Valve Timing and the Addition of Torques

The V8 engine configuration is particularly prone to vibration induced by camshaft torques, and will be used to illustrate the problem. In the present example the engine is assumed to have four valves per cylinder and twin overhead camshafts. At certain combinations of valve timing and V-angle these torques can combine to cause large periodic torques which may result in serious vibration problems. When the engine speed is such that one of the dominant component frequencies coincides with one of the natural torsional frequencies of the engine assembly, the resonant response may result in rapid fatigue failure of a component at or near a node where shear stresses will be largest or if the camshaft timing relative to the crankshaft changes sufficiently then this can result in valve-piston contact, which can result in destruction of the engine.

As an initial example an engine is considered with the inlet valves timed to be fully open at 118° ATDC, and the exhaust valves timed to be fully open at 124° BTDC. The V-angle is 82°. The cylinders in one bank fire every 90 camshaft degrees.

Relevant simple computer code is given in Appendix 7.

### *9.2.1 Inlet Cam Torque*

*Note* In these figures the angles shown are in crankshaft degrees. (Figs 9.1, 9.2).

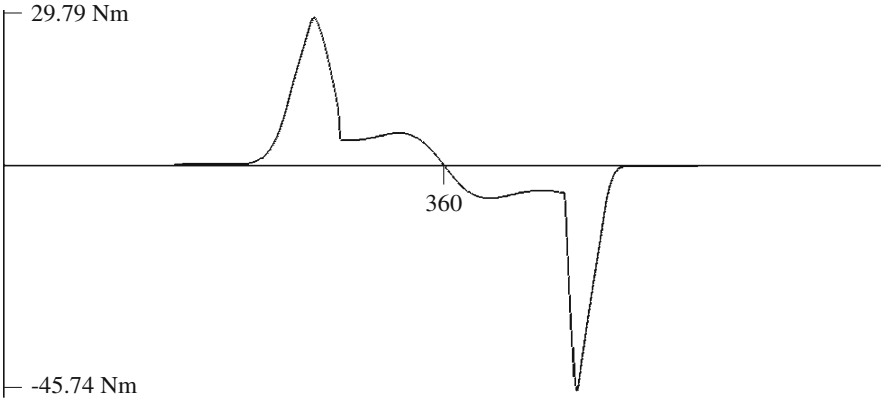


**Fig. 9.1** Inlet cam torque for one cam with valve fully open at TDC

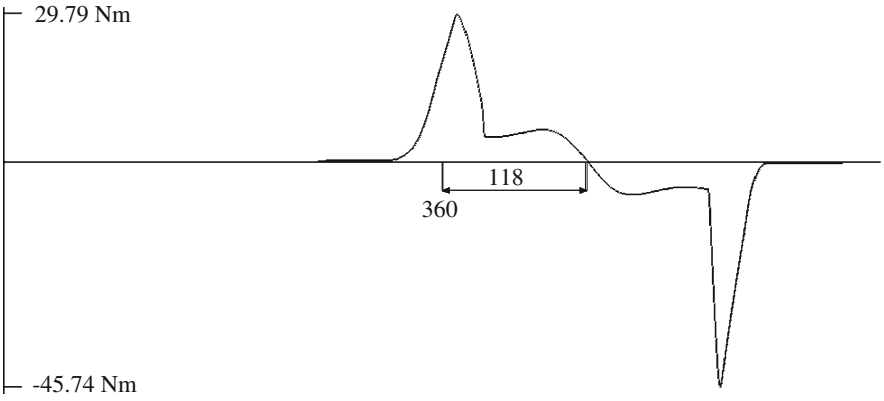


**Fig. 9.2** Inlet cam torque with valve fully open at 118° ATDC

### *9.2.2 Exhaust Cam Torque*

Figures 9.3 and 9.4.

### *9.2.3 Inlet Camshaft Torque*

If there are two inlet valves per cylinder then the torque due to the inlet cam torque is doubled to obtain the total inlet cam torque for one cylinder. When the inlet cam torques for all four cylinders on one bank are algebraically added together the

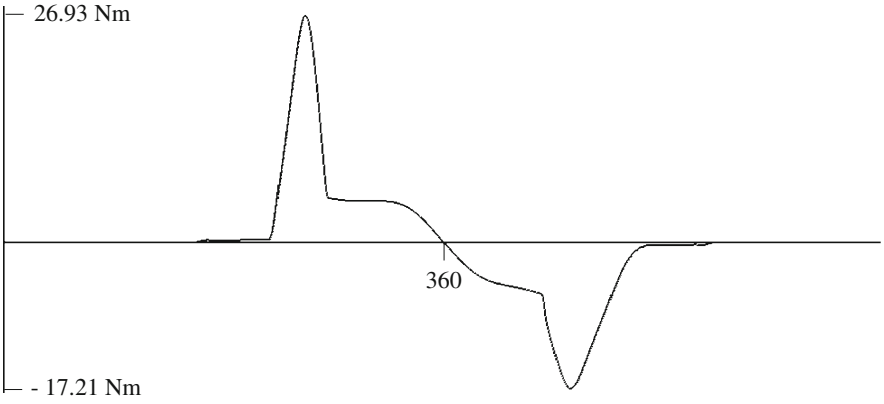


**Fig. 9.3** Exhaust cam torque for one cam with valve fully open at TDC

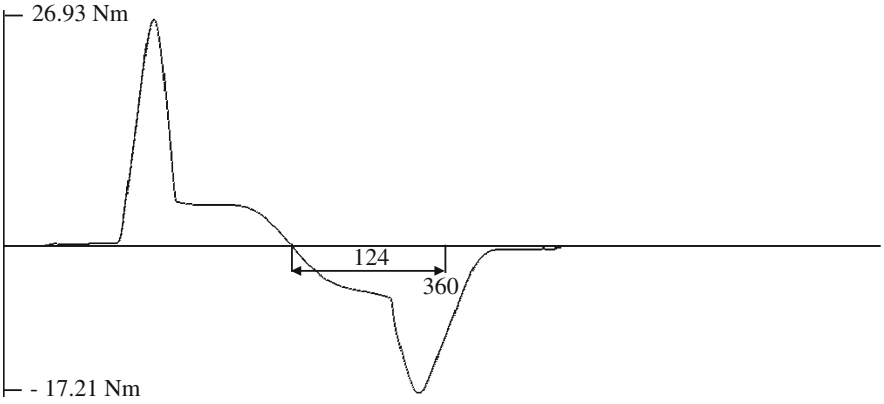


**Fig. 9.4** Exhaust cam torque with valve fully open at 124° BTDC

torque generated by the inlet camshaft over one revolution of the camshaft is obtained. Figure 9.5 shows the un-damped inlet camshaft torque.

This torque can be represented by an infinite Fourier series, which can be adequately represented by a finite series as the higher terms rapidly diminish. The significant individual Fourier components are multiples of 4, the number of cylinders involved. These are known as the engine orders. The frequencies of each component are given by the product of the order and the speed of rotation of the shaft. The invention of the Fast Fourier Transform [1, 2] together with the current speed of computation permitted by modern personal computers ensures that the magnitude of the Fourier components can be easily and rapidly evaluated.

Table 9.1 The other terms, 1, 2 3, 5, 6 etc. are all less than 0.5. The most important terms are the first three, of which the eighth order is the largest. This would be the most important one to damp.

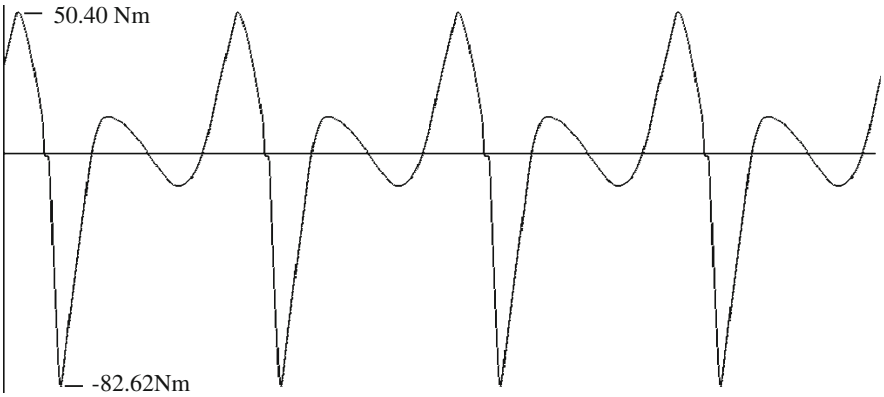


**Fig. 9.5** Inlet camshaft torque for four cylinders and two valves per cylinder

**Table 9.1** First four orders of the significant components of the inlet camshaft torque

| Order | Fourier component |
|---|---|
| 4 | 15.79 |
| 8 | 31.51 |
| 12 | 16.22 |
| 16 | 7.40 |

### *9.2.4 Exhaust Camshaft Torque*

If there are two exhaust valves per cylinder then the torque due to the exhaust cam torque is similarly doubled to obtain the total exhaust cam torque for one cylinder.

When the exhaust cam torques, for all four cylinders on one bank, are algebraically added together the torque generated by the exhaust camshaft over one revolution of the camshaft is obtained. Figure 9.6 shows the un-damped exhaust camshaft torque.

The largest component is the eighth order, this is the most important one to damp (Table 9.2).

**Table 9.2** First four significant orders of the exhaust camshaft torque

| Order | Fourier component |
|---|---|
| 4 | 11.58 |
| 8 | 18.52 |
| 12 | 9.26 |
| 16 | 4.89 |

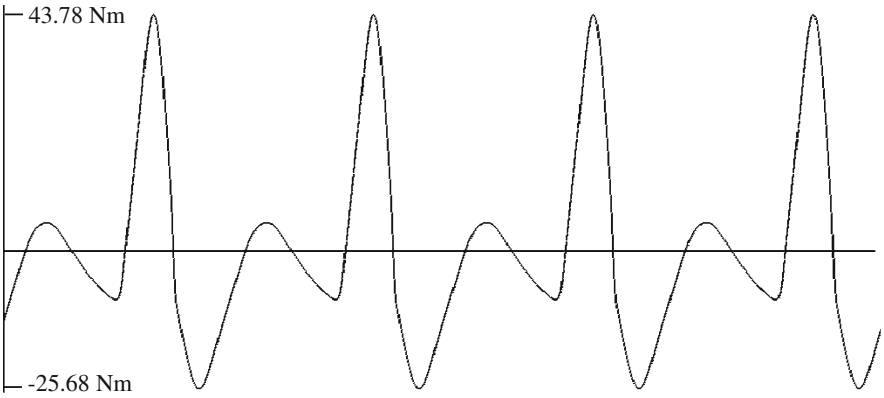


**Fig. 9.6** Exhaust camshaft torque for four cylinders and two valves per cylinder

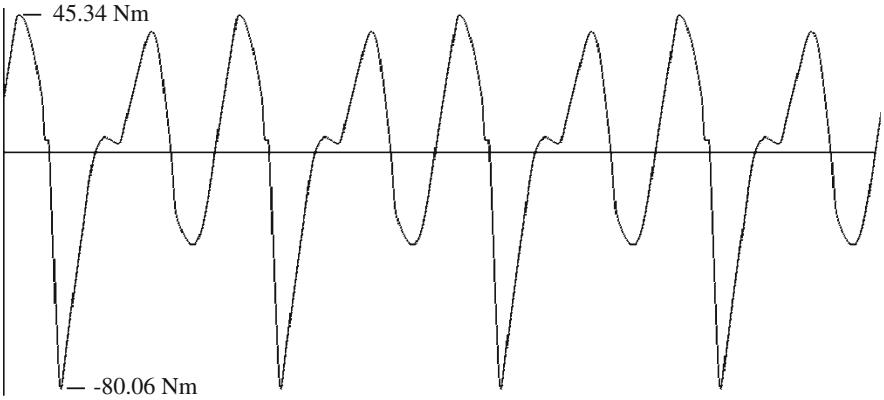


**Fig. 9.7** Camshaft torque for one bank, timed 118° and 124°

## 9.3 Combined Camshaft Torques for One Bank

The results shown above are for valve timing of 118° ATDC and 124° BTDC. If these two camshaft torques are added together to give the torque for one bank or a straight four engine, the resultant torque is shown below in Fig. 9.7, and the largest Fourier components are shown in Table 9.3.

**Table 9.3** First four orders of the significant components for one bank timed 118° and 124°

| Order | Fourier component |
|---|---|
| 4 | 12.57 |
| 8 | 35.53 |
| 12 | 18.74 |
| 16 | 11.04 |

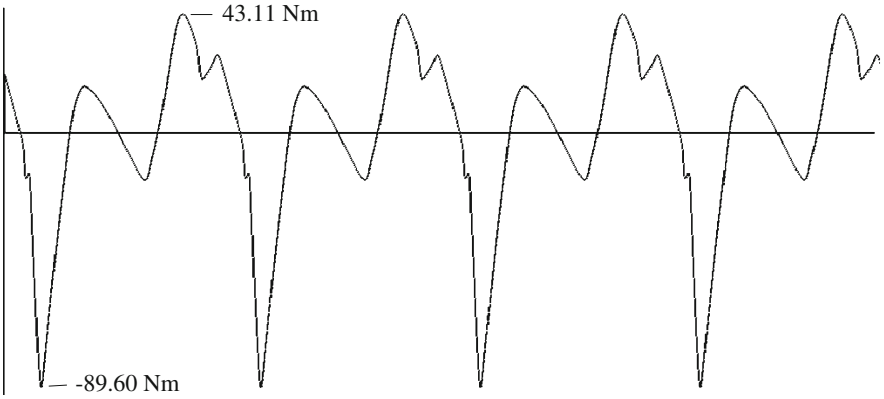


**Fig. 9.8** Camshaft torque for one bank, timed 102° and 103°

**Table 9.4** First four orders of the significant components for one bank timed 102° and 103°

| Order | Fourier component |
|---|---|
| 4 | 24.47 |
| 8 | 27.96 |
| 12 | 12.09 |
| 16 | 12.21 |

**Table 9.5** First four orders for both banks, V-angle 82°, timed 118° and 124°

| Order | Fourier component |
|---|---|
| 4 | 3.50 |
| 8 | 68.30 |
| 12 | 15.24 |
| 16 | 18.73 |

### *9.3.1 Effect of Valve Timing on Torques for One Bank*

If the valve timing is changed to102° ATDC and 103° BTDC the combined torques for one bank will be affected. The torques for this revised valve timing is shown in Fig. 9.8, and the major Fourier components are shown in Table 9.4. (Tables 9.6 and 9.7).

**Table 9.6** First four orders for both banks, V-angle 90°, timed 118° and 124°

| Order | Fourier component |
|---|---|
| 4 | <0.5 |
| 8 | 71.05 |
| 12 | <0.5 |
| 16 | 22.09 |

**Table 9.7** First four orders for both banks, V-angle 82°, timed 102° and 103°

| Order | Fourier component |
|---|---|
| 4 | 6.82 |
| 8 | 53.76 |
| 12 | 9.84 |
| 16 | 20.70 |

## 9.4 Torques for Both Banks

By adding the camshaft torques for each bank the total torque for both banks can be obtained.

Figure 9.9 shows the un-damped camshaft torques for both banks for valve timing of 118° ATDC and 124° BTDC, at a V-angle of 82.0°.

Recall that for both camshafts Tables 9.1 and 9.2 show that the largest Fourier component is for the eighth order. As would be expected the largest Fourier component for one bank is shown Table 9.5 to again be the eighth order.

### *9.4.1 Effect of Valve Timing and V-angle on Torques for Both Banks*

Figure 9.10 shows the un-damped camshaft torques for both banks for valve timing of 118° ATDC and 124° BTDC, and a V-angle of 90.0°. All torques shown above assume no friction torque and although the maxima and minima may have differing absolute magnitudes the respective areas under the curves are equal.

Figure 9.11 shows the un-damped camshaft torques for both banks for valve timing of 102° ATDC and 103° BTDC, and a V-angle of 82.0°.

Figure 9.12 shows the un-damped camshaft torques for both banks for valve timing of 102° ATDC and 103° BTDC, and a V-angle of 90.0°. In Table 9.8 the fourth and twelfth orders both have components less than 0.5. The addition of the inlet and exhaust torques for both banks due to the valve timing and the V-angle results in a very dominant eighth order. The other significant components are all integer multiples of 8.

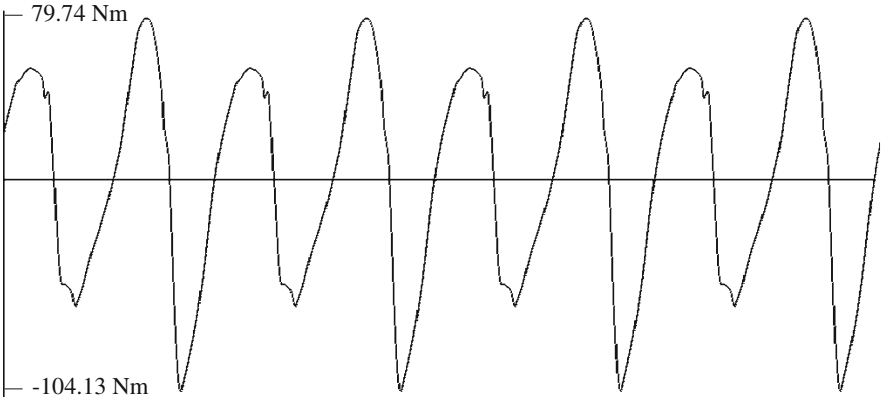


**Fig. 9.9** Torque for both banks, V-angle 82°, timed at 118° and 124°

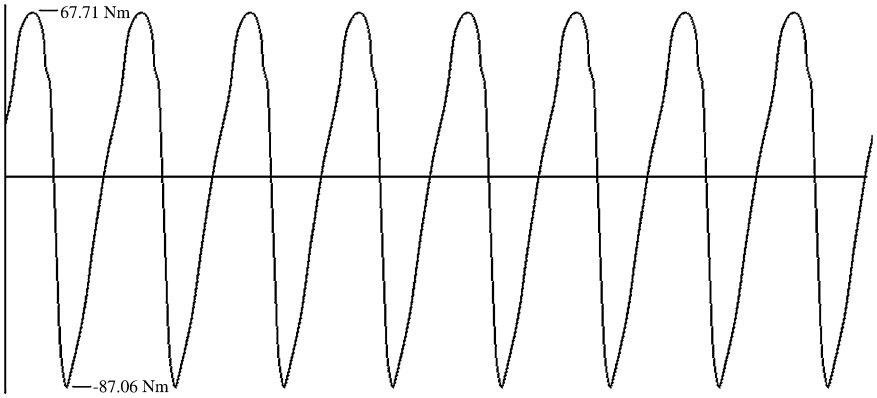


**Fig. 9.10** Torque for both banks, V-angle 90°, timed at 118° and 124°

## 9.5 Choice of Orders for Pendulum Damper

### *9.5.1 One Bank*

Figure 9.13 shows the optimum effect of damping with a reactive damper which is designed to damp the fourth and eighth orders. The maxima and minima of the torques are given in Table 9.9. This method of damping could be employed for a straight four, or both banks of a V8 engine. An alternative method for a V8 is given below.

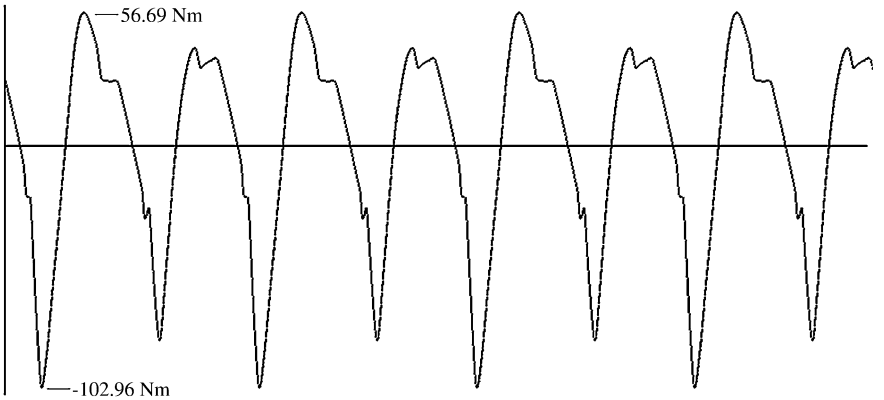


**Fig. 9.11** Torque for both banks, V-angle 82°, timed at 102° and 103°

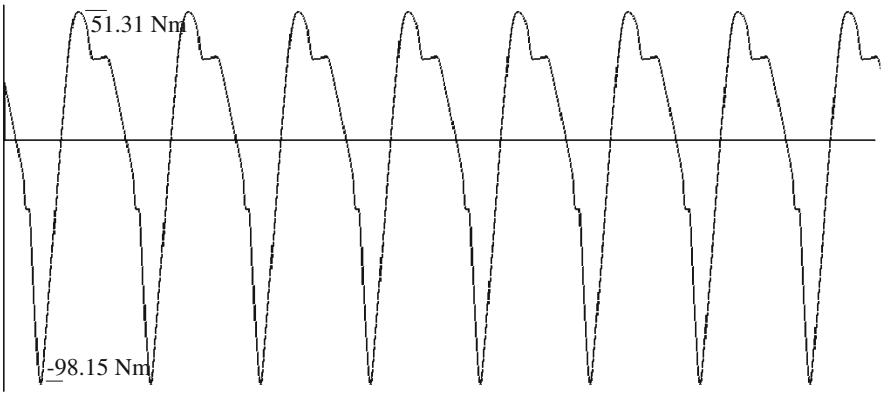


**Fig. 9.12** Torque for both banks, V-angle 90°, timed at 102° and 103°

**Table 9.8** First four orders for both banks, V-angle 90°, timed 102° and 103°

| Order | Fourier component |
|---|---|
| 4 | <0.5 |
| 8 | 55.93 |
| 12 | <0.5 |
| 16 | 24.42 |

## *9.5.2 Both Banks*

In order to damp the torques which may otherwise excite a significant resonant response in an engine component or several components it is often convenient to mount the damper on an idler gear, which transmits the drive from the crankshaft

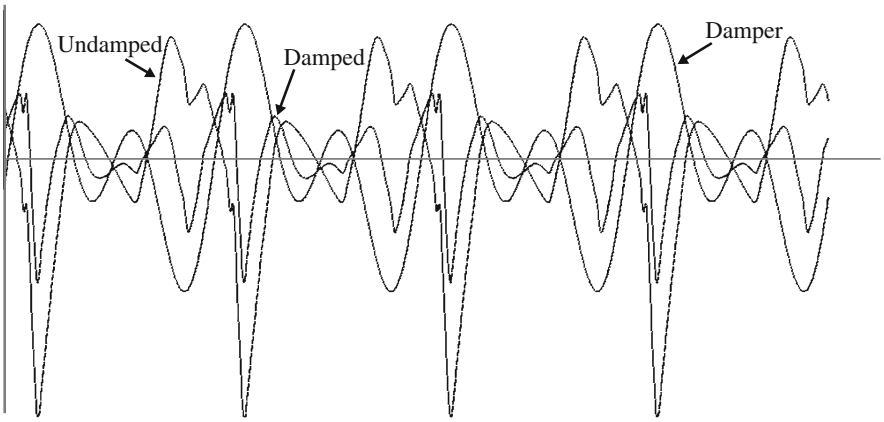


**Fig. 9.13** Effect of damping for one bank

**Table 9.9** Effect of damping for one bank

| Torque damped by fourth and eighth orders | |
|---|---|
| Maximum undamped torque | 43.11 Nm |
| Minimum undamped torque | −89.60 Nm |
| Maximum damper torque | 45.16 Nm |
| Minimum damper torque | −47.58 Nm |
| Maximum damped torque | 23.65 Nm |
| Minimum damped toque | −42.05 Nm |

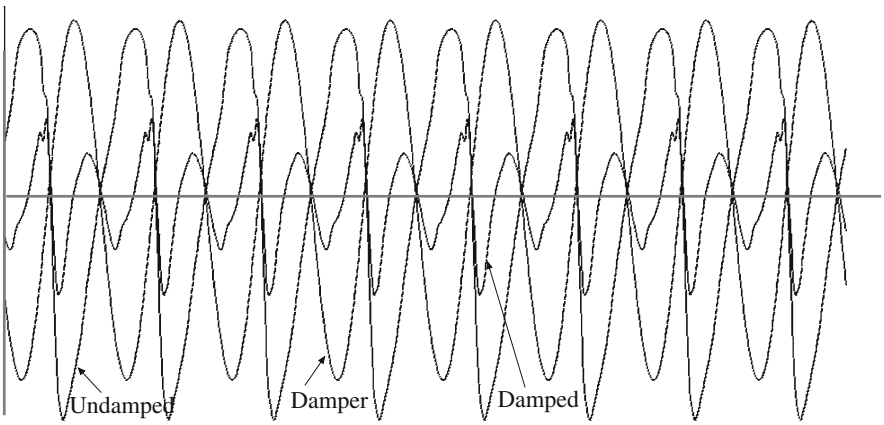


**Fig. 9.14** Effect of damping for both banks

to each bank. From examination of Tables 9.5 to 9.8 it can be seen that the worst two cases are for a valve timing of 118° ATDC and 124° BTDC. (Fig. 9.14 and Table 9.10).

**Table 9.10** Effect of damping for both banks

| Torque damped by eighth order damper | |
|---|---|
| **Maximum undamped torque | 67.71 Nm |
| Minimum undamped torque | −87.06 Nm |
| Maximum damper torque | 71.05 Nm |
| Minimum damper torque | −71.05 Nm |
| Maximum damped torque | 32.08 Nm |
| Minimum damped toque | −37.45 Nm |

The largest component is for a V-angle of 90°, and in all cases the largest order is the eighth.

Figure 9.13 and Table 9.9 shows the maximum effect which an eighth order pendulum damper would have on the torque of both banks timed at 118° ATDC and 124° BTDC with a V-angle of 90°.

The theory and design of pendulum dampers is described in detail in Chap. 10.

## References

1. Press WH et al (1996) Numerical recipes in Pascal, chapter 12. Cambridge University Press, Cambridge ISBN: 0-521-37516-9
2. Cooley J, Tukey JW (1965) An algorithm for the machine calculation of complex Fourier series. Math Comp 19:297–301

# Chapter 10
# Theory and Design of Pendulum Dampers

**Abstract** There is sometimes a need to damp the camshaft torques described in Chap. 9. The reactive pendulum damper described below has been described in the literature. In the past it was used to damp the torsional vibrations of crankshafts used in both automotive and aero engines, which had long crankshafts that lacked torsional stiffness. The theory on which it is based is also widely available in the literature. However, both the basic vibration theory and a description of the damper are given as it is relevant to the subject considered in this book. The advantage of this damper is that it is almost purely reactive and therefore dissipates very little energy. An incorrectly designed or significantly worn damper can exacerbate the problem rather than alleviating it. The maximum damping torques generated by the damper while retaining linear motion must be equal to the torques causing the vibration. It is therefore necessary to ensure the damper has sufficient capacity. An oversize damper will add additional inertia to the engine which will cause slower transient response and will reduce the effective power available when engine speed is increasing.

## 10.1 Introduction

High speed internal combustion engines develop high inertia loads and these include the camshaft torques developed while opening and closing the valves.

In Chap. 9 it was shown that for certain combinations of engine configuration and valve timing these torques can combine to result in significant camshaft torques, which can induce torsional vibration. V8 and V10 engines can be particularly prone to this problem, whose magnitude is dependent on the way the torques generated by individual camshafts interact with one another. This effect is very dependent upon the V-angle and the valve timing, which affect the way the torques from differing camshafts add together. The constituent frequencies of the exciting torques are at certain integer multiples, n, or orders, of the camshaft speed.

J. J. Williams, *Introduction to Analytical Methods for Internal Combustion Engine Cam Mechanisms*, DOI: 10.1007/978-1-4471-4564-6_10, © Springer-Verlag London 2013

For a four stroke V8 these integer values, n, will be 4, 8, 12, 16, etc. The eighth order is usually the largest component. The magnitude of the higher orders rapidly decreases, and either the fourth order or the twelfth order is usually the next largest component.

One way to reduce the effects of these torques is to use rotating pendulum dampers. These act as rotating dynamic absorbers, which are almost purely reactive, and therefore dissipate very little power. They do however, have significant polar moments of inertia, which should be minimised for a racing engine. As both the inertia forces and the restoring forces increase with the square of engine speed, the dampers remain tuned at all engine speeds.

In this chapter derivatives will be denoted using Newton's notation.

## 10.2 Notation

$C$ Phase angle
$D_1$ Distance defined in text
$D_2$ Diameter of damper mounting pin
$F$ Force
$\hat{F}$ Maximum force
$I$ Inertia
$I_E$ Equivalent or effective inertia
$k$ Stiffness
$m$ Mass
$m_E$ Equivalent or effective mass
$M$ Mass
$n$ Order of exciting torque
$\tilde{n}$ Order of idler gear damper
$N$ Number of dampers required
$N_1$ Number of idler gear teeth
$N_2$ Number of cam gear teeth
$r$ Radius of pendulum damper
$R$ Radius of damper mounting
$t$ Time
$T$ Torque
$x$ Displacement
$\hat{x}$ Maximum displacement
$\bar{x}$ Static displacement
$X$ Displacement of large mass
$\hat{X}$ Maximum displacement of large mass
$\alpha$ Angular displacement of camshaft
$\hat{\alpha}$ Amplitude of camshaft vibration
$\beta$ Angular displacement of pendulum damper

$\hat{\beta}$ Amplitude of pendulum damper vibration
$\hat{\Gamma}$ Amplitude of idler gear vibration
$\Delta$ Moment arm for pendulum damper
$\theta$ Angular displacement of simple pendulum
$\hat{\theta}$ Amplitude of simple pendulum vibration
$\Lambda$ Angular displacement of camshaft gear
$\hat{\Lambda}$ Amplitude of camshaft gear vibration
$\varpi$ Angular velocity of idler
$\omega$ Angular frequency of system vibration, angular velocity of camshaft vibration
$\omega_0$ Natural angular frequency of system
$\Omega$ Angular velocity of camshaft
$\Omega_0$ Mean angular velocity of camshaft

## 10.3 An Introduction to Elementary Mechanical Vibration

These simple concepts are well documented in the literature and can be found described in greater detail in introductory texts on Mechanical Vibration, such as that by Den Hartog [1]. Many readers may be familiar with them already.

### *10.3.1 Single Degree of Freedom System*

If the single degree of freedom system shown in Fig. 10.1 is perturbed from the equilibrium position by a distance $x$ then the equation of motion is:

$$m\ddot{x} + kx = 0 \tag{10.1}$$

From Eq. (10.1):

$$\ddot{x} = -\frac{k}{m}x \tag{10.2}$$

A solution of this equation is:

$$x = \hat{x}\cos\left[\left(\frac{k}{m}\right)^{\frac{1}{2}} + C\right] \tag{10.3}$$

Differentiating with respect to time $t$:

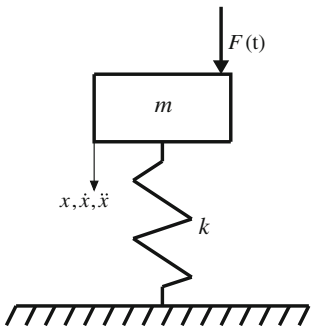


**Fig. 10.1** Single degree of freedom system

$$\dot{x} = -\left(\frac{k}{m}\right)^{\frac{1}{2}} \hat{x} \sin\left[\left(\frac{k}{m}\right)^{\frac{1}{2}} + C\right] \tag{10.4}$$

$$\ddot{x} = -\left(\frac{k}{m}\right) \hat{x} \cos\left[\left(\frac{k}{m}\right)^{\frac{1}{2}} + C\right] \tag{10.5}$$

Substitution of Eq. (10.3) into Eq. (10.5) we recover Eq. (10.2) and prove that Eq. (10.3) is a solution of Eq. (10.2). If $x = X_0$ at $t = 0$ then $C = 0$ and

$$x = \hat{x} \cos \omega_0 t \tag{10.6}$$

where $\omega = \left(\frac{k}{m}\right)^{\frac{1}{2}}$ and $\omega_0$ is known as the natural frequency of vibration of the system. For natural vibration the value of $C$ can be any value and we can also write:

$$x = \hat{x} \sin\ \omega_0 t \tag{10.7}$$

If the force exciting the system shown in Fig. 10.1 is given by

$$F(t) = \hat{F} \sin\ \omega t \tag{10.8}$$

For forced vibration of an un-damped single degree of freedom system we can write the equation of motion as:

$$m\ddot{x} + kx = \hat{F} \sin\ \omega t \tag{10.9}$$

If the solution of Eq. (10.9) is:

$$x = \hat{x} \sin\ \omega t \tag{10.10}$$

Then Eq. (10.9) can be written as:

$$-m\omega^2 \hat{x} \sin\ \omega t + \hat{k} \sin\ \omega t = F_0 \sin\ \omega t \tag{10.11}$$

$$\hat{x}\left(k - m\omega^2\right) = \hat{F} \tag{10.12}$$

Hence:

$$\hat{x} = \frac{\hat{F}}{(k - m\omega^2)} \tag{10.13}$$

Recall that the natural frequency of the system is:

$$\omega_0 = \left(\frac{k}{m}\right)^{\frac{1}{2}} \tag{10.14}$$

From Eqs. (10.13) and (10.14):

$$\hat{x} = \frac{\hat{F}}{k\left[1 - \left(\frac{\omega}{\omega_0}\right)^2\right]} \tag{10.15}$$

$$x = \frac{\hat{F}}{k\left[1 - \left(\frac{\omega}{\omega_0}\right)^2\right]} \sin \omega t \tag{10.16}$$

If $\omega = 0$ then a static load $\hat{F}$ the displacement of the mass will be $\bar{x}$ which is given by

$$\bar{x} = \frac{\hat{F}}{k} \tag{10.17}$$

$$\frac{x}{\bar{x}} = \frac{1}{\left[1 - \left(\frac{\omega}{\omega_0}\right)^2\right]} \sin \omega t \tag{10.18}$$

From consideration of Eq. (10.18) as $\omega \to 0$ then $\frac{x}{\bar{x}} \to 1$ and as $\omega \to \omega_0$ then $\frac{x}{\bar{x}} \to \infty$. At frequencies near to the natural frequency of the system the response becomes very large and at the natural frequency the response is infinite. In practice all systems have some damping but the response of lightly damped systems can be very large. If $\omega > \omega_0$, then:

$$1 - \left(\frac{\omega}{\omega_0}\right)^2 < 0 \tag{10.19}$$

This means there is a phase change of $\pi$ at $\omega = \omega_0$ and for progressively larger values of $\frac{\omega}{\omega_0}$ the response becomes progressively smaller as $\frac{x}{\bar{x}} \to 0$.

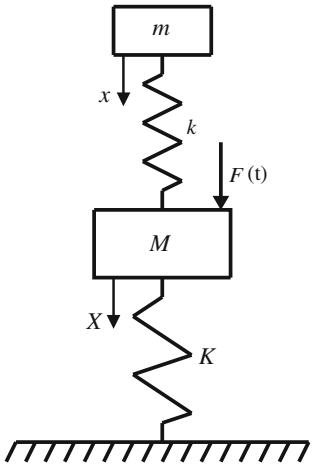


**Fig. 10.2** The dynamic absorber

### *10.3.2 The Dynamic Absorber*

With notation of Fig. 10.2; the mass, $M$, is supported by a spring of stiffness, $K$, and is excited by a periodic force, $F(t)$, where

$$F(t) = \hat{F} \sin\ \omega t \tag{10.20}$$

The dynamic absorber is of mass, $m$, and is connected to the larger mass, $M$, by a spring of stiffness, $k$. The equation of motion of the mass, $m$, is:

$$m\ddot{x} = +k(x - X) = 0 \tag{10.21}$$

and

$$X = \hat{X} \sin \omega t \tag{10.22}$$

$$x = \hat{x} \sin\ \omega t \tag{10.23}$$

Differentiating Eq. (10.23) we obtain:

$$\ddot{x} = -\omega^2 \hat{x} \sin\ \omega t \tag{10.24}$$

Equation (10.21) can be written as:

$$-k\hat{X} + \hat{x}\left(k - m\omega^2\right) = 0 \tag{10.25}$$

Recall that the natural frequency of a single degree of freedom system is:

$$\omega_0 = \left(\frac{k}{m}\right)^{\frac{1}{2}} \tag{10.14}$$

Equation (10.25) can now be written as:

$$\hat{X} = \hat{x}\left[1 - \left(\frac{\omega}{\omega_0}\right)^2\right] \tag{10.26}$$

Hence

$$\frac{\hat{x}}{\hat{X}} = \frac{1}{\left[1 - \left(\frac{\omega}{\omega_0}\right)^2\right]} = \frac{\ddot{x}}{\ddot{X}} \tag{10.27}$$

If an additional mass, $m$ were rigidly attached to the mass, $M$ then the inertia force exerted on the mass, $M$ would be $m\ddot{X}$.The force exerted by the mass, $m$ attached by the spring, $k$ is $m\ddot{x}$, let $m_E$ be the effective value of the mass, $m$ if it were rigidly attached to the mass, $M$ and exerting the same inertia force, $m\ddot{x}$.

Then

$$m\ddot{x} = m_E\ddot{X} \tag{10.28}$$

From Eqs. (10.27) and (10.28):

$$\frac{m_E}{m} = \frac{1}{\left[1 - \left(\frac{\omega}{\omega_0}\right)^2\right]} = \frac{\ddot{x}}{\ddot{X}} \tag{10.29}$$

Hence

$$\frac{m_E}{m} = \frac{1}{1 - \frac{\omega^2}{\omega_0^2}} \tag{10.30}$$

Note that $m_E$, the effective value of the mass, $m$, is dependent upon $\omega_0$ the natural frequency of the dynamic absorber, and as previously:

$$\omega_0 = \left(\frac{k}{m}\right)^{\frac{1}{2}} \tag{10.14}$$

Note that $\frac{\omega}{\omega_0}$ must be slightly less than or equal to 1. If $\frac{\omega}{\omega_0} > 1$ then the dynamic absorber will make the vibration of the mass, $M$, greater, rather than attenuating it, which would seriously exacerbate the problem.

Equation (10.30) is shown graphically in Fig. 10.3

## 10.4 The Simple Pendulum

With notation of Fig. 10.4, resolving forces tangentially:

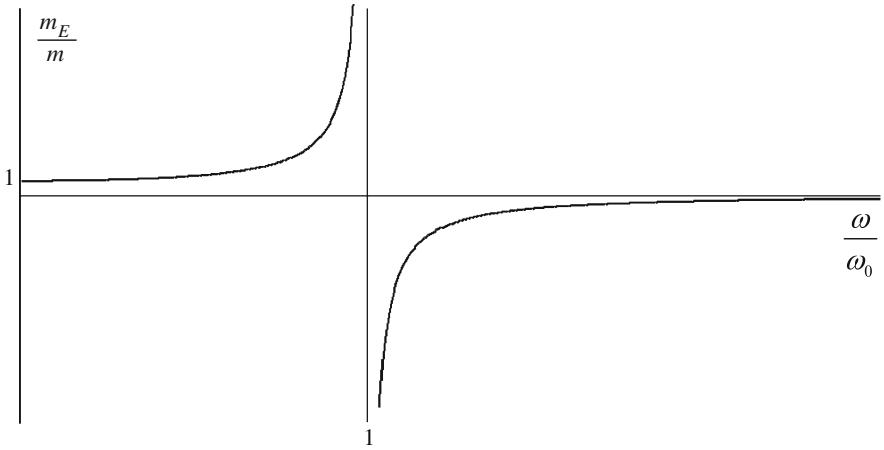


**Fig. 10.3** Frequency response of dynamic absorber

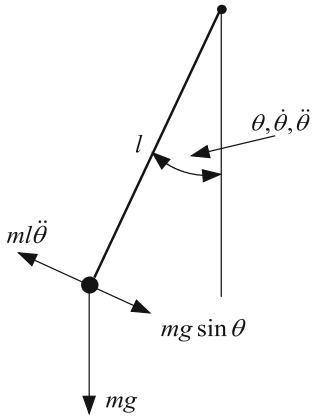


**Fig. 10.4** A simple pendulum

$$ml\ddot{\theta} + mg \sin \theta = 0 \tag{10.31}$$

For small values of $\theta$:

$$\sin \theta \simeq \theta \tag{10.32}$$

Equation (10.31) can therefore be written as:

$$l\ddot{\theta} + g\theta = 0 \tag{10.33}$$

Equation (10.33) is similar to Eq. (10.1) and therefore:

$$\theta = \hat{\theta} \sin \omega_0 t \tag{10.34}$$

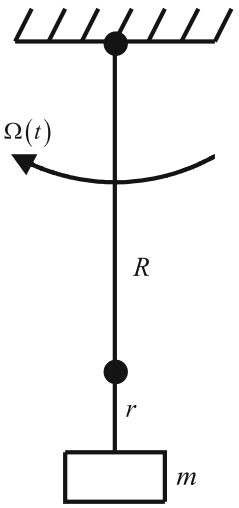


**Fig. 10.5** A pendulum damper

where

$$\omega_0 = \left(\frac{g}{l}\right)^{\frac{1}{2}} \tag{10.35}$$

## 10.5 The Pendulum Damper

A damper is shown schematically in Fig. 10.5. The shaft rotates with a varying angular velocity, $\Omega(t)$, given by

$$\Omega(t) = \Omega_0 + \hat{\Lambda} \sin n\Omega_0 t \tag{10.36}$$

In practice there will be an infinite number of values of $n$, but each one of concern can be considered separately, and only the lowest are of importance.

### *10.5.1 Pendulum Damper Dynamics*

With notation of Fig. 10.6, where $\alpha$ and $\beta$ are small angles, but are shown large for clarity:

$$\alpha(t) = \hat{\alpha} \sin n\Omega_0 t \tag{10.37}$$

and

$$\beta(t) = \hat{\beta} \sin n\Omega_0 t \tag{10.38}$$

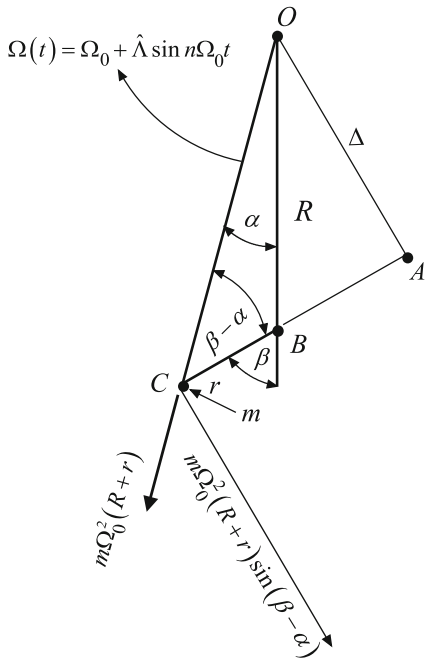


**Fig. 10.6** Kinematics of pendulum damper

If $\alpha$ and $\beta$ are small angles, which is consistent with linear vibration, we can write:

$$(R + r)\alpha = r\beta \tag{10.39}$$

For motion relative to a system rotating with angular velocity, $\Omega_0$, the centrifugal force, normal to BC, for a pendulum of mass, $m$, is given by

$$F = -m\Omega_0^2(R + r)\sin(\beta-\alpha) \tag{10.40}$$

For small values of $\beta-\alpha$, Eq. (10.40) can be written as:

$$F = -m\Omega_0^2(R + r)(\beta-\alpha) \tag{10.41}$$

From Eqs. (10.39) and (10.40):

$$(R + r)(\beta-\alpha) = R\beta + r\beta-R\alpha-r\alpha = R\beta + r\beta-r\beta = R\beta \tag{10.42}$$

In practice $R \gg r$ and when the damper is operating correctly $\beta \gg \alpha$, therefore $r\alpha$ can be safely neglected in comparison to $R\beta$

Hence

$$F = -m\Omega_0^2 R\beta \tag{10.43}$$

where the tangential acceleration of C is $-\Omega_0^2 R\beta$, and the tangential displacement of C with respect to the rotating coordinate system is: $(R + r)\Lambda + r\beta$. The

corresponding acceleration is: $(R+r)\ddot{\Lambda}+r\ddot{\beta}$. The equation of motion of the system is therefore:

$$(R+r)\ddot{\Lambda}+r\ddot{\beta}=-\Omega_0^2 R\beta \tag{10.44}$$

For simple harmonic motion:

$$\Lambda=\hat{\Lambda}\sin n\Omega_0 t \tag{10.45}$$

Differentiating twice w. r. t:

$$\ddot{\Lambda}=-n^2\Omega_0^2\hat{\Lambda}\sin n\Omega_0 t \tag{10.46}$$

Similarly:

$$\beta=\hat{\beta}\sin n\Omega_0 t \tag{10.47}$$

and

$$\ddot{\beta}=-n^2\Omega_0^2\hat{\beta}\sin n\Omega_0 t \tag{10.48}$$

We can therefore write the equation of motion as:

$$-(R+r)n^2\Omega_0^2\hat{\Lambda}\sin n\Omega_0 t-rn^2\Omega_0^2\hat{\beta}\sin \Omega_0 t=-\Omega_0^2 R\hat{\beta}\sin n\Omega_0 t \tag{10.49}$$

Hence:

$$(R+r)n^2\hat{\Lambda}+rn^2\hat{\beta}=R\hat{\beta} \tag{10.50}$$

and

$$(R+r)n^2\hat{\Lambda}=\left(R-rn^2\right)\hat{\beta} \tag{10.51}$$

Hence:

$$\frac{\hat{\beta}}{\hat{\Lambda}}=\frac{(R+r)n^2}{R-rn^2} \tag{10.52}$$

The centrifugal force in the direction BC is $m\Omega_0^2(R+r)\cos(\beta-\alpha)$ which for small angular displacements approximates to $m\Omega_0^2(R+r)$. The moment arm about O, is given by $R\sin(\beta-\alpha)=\Delta$, which approximates to $R\beta$. The resulting torque, $T$, is given by

$$T=m\Omega_0^2(R+r)\Delta=m\Omega_0^2(R+r)R\beta \tag{10.53}$$

Recall that:

$$\beta=\hat{\beta}\sin n\Omega_0 t \tag{10.54}$$

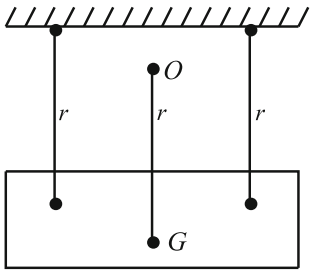


**Fig. 10.7** A bifilar suspension

Hence:

$$T = m\Omega_0^2(R+r)R\frac{(R+r)n^2}{R-rn^2}\hat{\Lambda}\sin\,\Omega_0 t = m\Omega_0^2\frac{(R+r)^2n^2}{1-\frac{r}{R}n^2}\hat{\Lambda}\sin\,\Omega_0 t \qquad (10.55)$$

and

$$T = -m\frac{(R+r)^2}{1-\frac{r}{R}n^2}\ddot{\Lambda} = -I_E\ddot{\Lambda} \qquad (10.56)$$

where $I_E$ is the equivalent or effective inertia, and is given by

$$I_E = \frac{m(R+r)^2}{1-\frac{r}{R}n^2} \qquad (10.57)$$

For a tuned damper:

$$1-\frac{r}{R}n^2 \to 0 \qquad (10.58)$$

Hence:

$$n^2 = \frac{R}{r} \qquad (10.59)$$

In order to ensure that the effective damper inertia, $I_E$, is large and positive we need to ensure that the inequality, $\frac{R}{r} > n^2$ is satisfied. In practice this means that $\frac{R}{r}$ must be slightly greater than $n^2$.

The damper needs to be compact, and the best solution to the practical design problem is due to Sarazin [2] and Chilton [3], who independently proposed the so-called bifilar suspension in the late 1930s. This mechanism is kinematically similar to a single point of support but permits comparatively large masses with a small value of $r$ compared to $R$.

Consider the four bar chain shown in Fig. 10.7. The centre of mass of the lower link is at G and this point has an instantaneous centre of rotation at O distance r from G, as all points on the lower link describe similar paths.

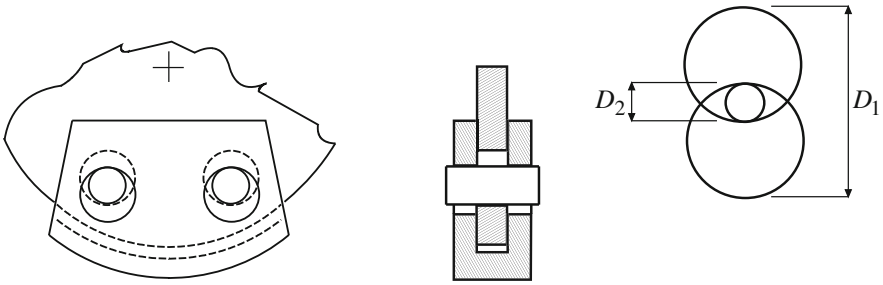


**Fig. 10.8** A practical pendulum damper design

## 10.6 Practical Design

With notation of Fig. 10.8 the damper weights are usually U-shaped and have two holes of diameter, $D_1$, symmetrically drilled through with respect to the centre of mass. Similar holes with the same diameter, $D_1$, and spacing are drilled in the carrier disc which fits with slight clearance in the centre of the U. Pins of diameter, $D_2$, are fitted in the holes to support the damper weight.

The effective length of the pendulum is given by

$$r = D_1 - D_2 \tag{10.60}$$

This design and others are described by Ker Wilson [4], and elsewhere.

### *10.6.1 Damper Size*

In Chap. 9 a method was presented for determining the magnitude of the orders of the damper torques. For example the eighth order torque, $T$ given in Table 9.10 has a maximum value of 71.05 Nm. In order to check the design of an effective set of dampers for this torque, it is necessary to ascertain whether the dampers will be of sufficient size to ensure that the dampers oscillate linearly. This will require small amplitudes of oscillation.

Recall that the effective damper inertia determined for a single damper in Sect. 10.5.1 is given by

$$I_E = \frac{m(R+r)^2}{1-\frac{r}{R}n^2} \tag{10.57}$$

If in place of a single damper there are N dampers for engine order, $n = 8$, then Eq. (10.56) can be re-written as:

$$\frac{T}{N} = -I_E \ddot{\Lambda}_{Max} \tag{10.61}$$

where $N$ is the number of eighth order dampers. From Eq. (10.46):

$$\left|\ddot{\Lambda}_{Max}\right| = n^2\Omega_0^2\hat{\Lambda} \tag{10.62}$$

Hence from Eqs. (10.61) and (10.62):

$$n^2\Omega_0^2\hat{\Lambda} = \frac{T}{NI_E} \tag{10.63}$$

Hence:

$$\hat{\Lambda} = \frac{T}{Nn^2\Omega_0^2 I_E} \tag{10.64}$$

From Eq. (10.52):

$$\hat{\beta} = \frac{\hat{\Lambda}(R+r)n^2}{R-rn^2} \tag{10.65}$$

If this value of $\hat{\beta}$ is not sufficiently small to ensure sensibly linear motion of the dampers there will be a need to either increase the number of dampers or the effective inertia of the dampers. During initial testing of the engine it is advisable to check the damper pins and the region around their holes for excessive wear or overheating of the material.

### *10.6.2 Need to Avoid Wear*

Since it is essential that $\frac{R}{r}$ is slightly greater than $n^2$ consider the effect of wear on the holes and pins. The diameter, $D_1$, of the holes will tend to get larger and the diameter, $D_2$, of the pins will tend to get smaller. Therefore the value of $r = D_1 - D_2$ will increase and if sufficient wear occurs the effective inertia, $I_E$, will become large and negative. These damper components therefore need to be made of high alloy steel which is hardened and has a smooth surface finish to ensure that wear is minimised.

The size of the dampers with respect to the exciting torques is important. If the dampers are too small then the amplitude of their oscillations will be too large, resulting in non-linear behaviour, and possible overheating and failure of the damper. If they are too large the engine mass and inertia will have been increased unnecessarily.

For a V8 engine a damper for $n = 4$ is frequently required. However, the largest component may be $n = 8$ or $n = 12$, this will depend on V-angle and valve timing. Which of these harmonics is the largest can change if the valve timing is altered during development.

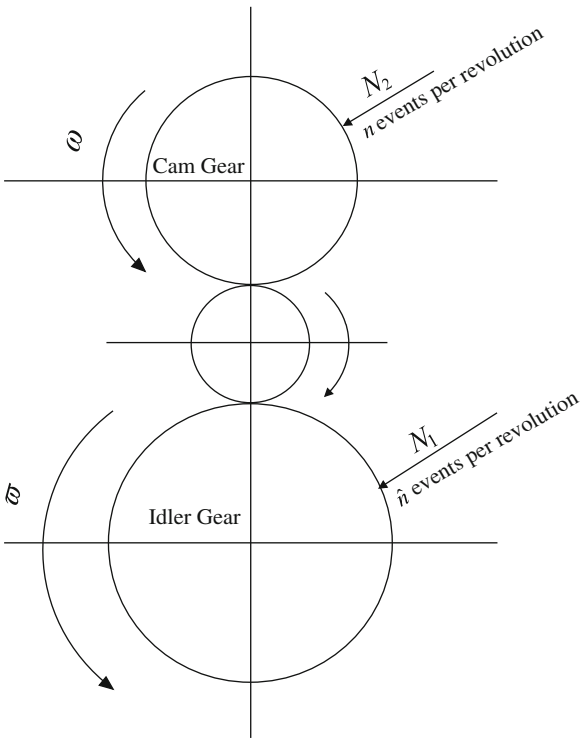


**Fig. 10.9** A simple gear train

Dampers for $n = 12$ are more difficult to design, and wear is more of a problem. Those for $n = 16$ are usually best avoided. If two orders are to be damped, then often the best solution is to have two opposing pairs of dampers, with differing values of n, mounted on the same disc.

## 10.7 Effect of Gearing on Damper Orders

It may be advantageous to mount the dampers on a comparatively large idler gear in the camshaft drive train if this is available. The polar moment of inertia of a pendulum damper can add significantly to the total polar moment of inertia of an engine, and the effective polar moment of the damper is proportional to the square of the angular velocity. Also a large wheel will have more space to attach comparatively large dampers, which will be more effective, and if necessary dampers of higher order may be possible.

If a pendulum damper is mounted on a shaft whose angular velocity is given by

$$\Omega(t) = \Omega_0 t + \hat{\Lambda} \sin n\Omega_0 t \tag{10.36}$$

If the unsteady motion is due to regularly spaced events, for example, stab torques caused by cams opening poppet valves with high accelerations, then n will be an integer, and will be equal to the number of events, n, or some multiple of n.

In a four stroke engine the camshaft rotates at half engine speed, i.e. half the crankshaft speed. It follows that the number of events which affect the crankshaft in one revolution is half the number generated in one revolution of the camshaft.

If the gear train includes an idler gear, which has $N_1$ teeth, which drives a gear wheel with $N_2$ teeth on the camshaft, as shown in Fig. 10.9, then the speed of the idler will be $\frac{N_2}{N_1}$ of the speed of the camshaft. If the camshaft speed is $\omega$, then the idler speed will be:

$$\varpi = \frac{N_2}{N_1}\omega \tag{10.66}$$

In one revolution of the idler the camshaft will do $\frac{N_1}{N_2}$ revolutions. If the camshaft experiences $n$ events per revolution, then the idler will experience $\frac{N_1}{N_2}n$ events per revolution. A damper mounted on the idler will therefore have an order number of:

$$\tilde{n} = \frac{N_1}{N_2}n \tag{10.67}$$

From Eq. (10.66) the angular velocity of the idler will be given by

$$\varpi(t) = \varpi_0 t + \hat{\Gamma}\sin\frac{N_2}{N_1}n\varpi_0 t = \varpi_0 t + \hat{\Gamma}\sin\tilde{n}\varpi_0 t \tag{10.68}$$

In general the value of $\tilde{n}$ will not be an integer, but the damper will remain tuned at all engine speeds.

## References

1. Den Hartog JP (1956) Mechanical vibrations. Chapters 2, 3 and 5, 4th edn. McGraw-Hill, New York
2. Sarazin GF (1937) U.S. Patent 2079226, May 1937
3. Chilton R (1939) U.S. Patent 2184734, December 1939
4. Ker Wilson W (1956) Practical solutions of vibration problems, devices for controlling vibrations, 3rd Edn, Vol. 4. Chapman Hall, London

# Chapter 11
# Push Rod Mechanisms

**Abstract** Some of the previous cam mechanisms considered are widely employed, but push rod mechanisms are no longer so widely used. However for engines with a V configuration they are still used for both commercial and domestic vehicles with V8 engines and for NASCAR, where the valve gear design is strictly specified. The advantage of this mechanism is that only one camshaft is required, located in the centre of the V. This reduces the cost of the engine, but at the expense of higher valve gear inertia, which tends to limit engine speeds. The usual mechanism has a translating follower which actuates the push rod. The use of a finger follower is not so widely employed but was widely used in the JAP engine which was used in some light sports cars and more recently in the Mercedes-Benz 500I engine which dominated the Indy 500 in 1994 in a Penske. This mechanism permits higher engine speeds, but is more costly to manufacture and the analysis of the mechanism is more complex.

## 11.1 Introduction

Most modern engines no longer employ push rods to actuate the valve gear. However there are still many push rod V8 engines used in various types of vehicle for commercial and domestic use as well as NASCAR racing.

The J.A.P. engine had a different push rod mechanism. This engine was used in motor cycles and small sports cars, such as the Three Wheeled Morgan of the 1930s, and later in 500 cc racing, which became Formula 3 in the 1950s. The same type of mechanism was also used in the Mercedes-Benz 500I V8 engine which won the Indy 500 in 1994 in a Penske. This mechanism is a four bar chain, this has the advantage of providing a more robust mechanism, which will permit higher engine speeds, but is analytically more complex, and more expensive to manufacture.

J. J. Williams, *Introduction to Analytical Methods for Internal Combustion Engine Cam Mechanisms*, DOI: 10.1007/978-1-4471-4564-6_11, © Springer-Verlag London 2013

## 11.2 Simple Push Rod Mechanism Kinematics

### 11.2.1 Notation

| | |
|---|---|
| $D_1$ | Length of rocker arm on push rod side |
| $D_2$ | Length of rocker arm on valve side |
| $D_{PR}$ | Length of push rod |
| $L_V$ | Maximum valve lift |
| $s_V$ | Valve lift |
| $\bar{x}$ | Coordinate |
| $y$ | Coordinate |
| $y_0$ | Coordinate |
| $\bar{y}$ | Coordinate |
| $\alpha_0$ | Angle between rocker arms |
| $\beta$ | Angle which defines position of pushrod side of rocker |
| $\beta_0$ | Angle which defines position of the pushrod side of rocker with valve closed |
| $\gamma$ | Angle between $Y$ direction and valve axis |
| $\varepsilon$ | Angle which defines position of pushrod side of rocker |
| $\theta$ | Angle of cam rotation |
| $\lambda$ | Fraction of valve lift when rocker arm centre line is perpendicular to valve axis |
| $\phi$ | Angle which defines position of valve side rocker |
| $\phi_0$ | Angle which defines position of valve side rocker with valve closed |
| $\psi$ | Angle which defines angular position of push rod |
| $\psi_0$ | Angle which defines angular position of push rod with valve closed |

### 11.2.2 Rocker Kinematics

This analysis is restricted to a plane push rod mechanism. The mechanism shown in Fig. 11.1 has a flat translating follower. Some push rod mechanisms employ a curved translating follower, but this can lead to problems if the follower radius is small, as consequently there can be appreciable transverse forces. $L$ is the maximum valve lift, $\lambda L$ is the valve lift when the follower centre line is perpendicular to the valve axis, and $D_2$ is the effective rocker length. This analysis is basically similar to that given in Sect. 7.7, where Leibnitz's notation was used.

$$D_2 \sin(\phi - \phi_0) = s_V - \lambda L_V \tag{11.1}$$

From Eq. (11.1):

$$s_V = D_2 \sin(\phi - \phi_0) + \lambda L_V \tag{11.2}$$

and

$$\phi = \phi_0 + \sin^{-1}\frac{s_V - \lambda L_V}{D_2} \tag{11.3}$$

Using Newton's notation and differentiating Eq. (11.2) w.r.t. $\theta$:

$$\dot{s}_V = D_2 \cos(\phi - \phi_0)\dot{\phi} \tag{11.4}$$

$$\dot{\phi} = \frac{\dot{s}_V}{D_2 \cos(\phi - \phi_0)} \tag{11.5}$$

Differentiating Eq. (11.5) w.r.t. $\theta$:

$$\ddot{\phi} = \frac{\ddot{s}_V D_2 \cos(\phi - \phi_0) + \dot{s}_V D_2 \sin(\phi - \phi_0)\dot{\phi}}{D_2^2 \cos^2(\phi - \phi_0)} \tag{11.6}$$

From Eqs. (11.5) and (11.6):

$$\ddot{\phi} = \frac{\ddot{s}_V}{D_2 \cos(\phi - \phi_0)} + \frac{\dot{s}_V \sin(\phi - \phi_0)\dot{\phi}}{D_2^2 \cos^3(\phi - \phi_0)} \tag{11.7}$$

### *11.2.3 Push Rod Kinematics*

Equations (11.3), (11.5) and (11.7) give the angular displacement, velocity and acceleration of the rocker. It will be useful to be able to relate other angles and their derivatives to these parameters.

$$\beta_0 = \frac{\pi}{2} - (\gamma + \alpha_0 + \phi_0) \tag{11.8}$$

$$\beta = \beta_0 + \phi \tag{11.9}$$

$$\varepsilon = \phi - \phi_0 - \alpha_0 - \gamma = \beta - \frac{\pi}{2} \tag{11.10}$$

Differentiating Eq. (11.10) w.r.t. $\theta$:

$$\dot{\varepsilon} = \dot{\phi} = \dot{\beta} \tag{11.11}$$

$$\ddot{\varepsilon} = \ddot{\phi} = \ddot{\beta} \tag{11.12}$$

With notation of Fig. 11.1:

$$\bar{x} = D_1 \sin\beta_0 + D_{PR} \sin\psi_0 \tag{11.13}$$

$$\bar{x} = D_{PR} \sin\psi + D_1 \cos\varepsilon \tag{11.14}$$

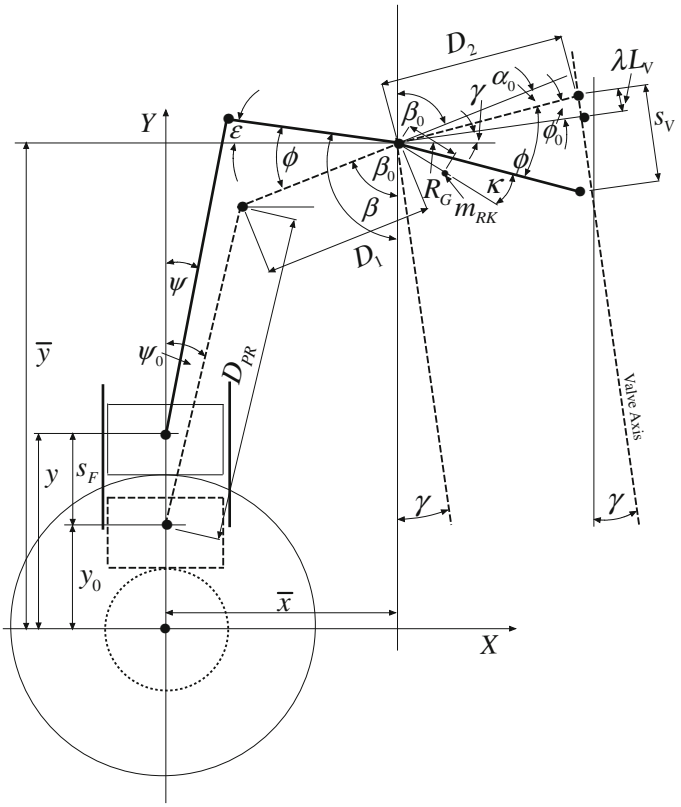


**Fig. 11.1** Flat translating follower push rod kinematics

From Eq. (11.13):

$$\sin\psi_0 = \frac{\bar{x} - D_1 \sin\beta_0}{D_{PR}} \tag{11.15}$$

$$\psi_0 = \sin^{-1}\left[\frac{\bar{x} - D_1 \sin\beta_0}{D_{PR}}\right] \tag{11.16}$$

Similarly from Eq. (11.14)

$$\psi = \sin^{-1}\left[\frac{\bar{x} - D_1 \cos\varepsilon}{D_{PR}}\right] \tag{11.17}$$

Differentiating Eq. (11.14) w.r.t. $\theta$:

$$D_{PR}\cos\psi\dot{\psi} - D_1 \sin\varepsilon\dot{\varepsilon} = 0 \tag{11.18}$$

Substituting Eq. (11.11) into Eq. (11.18):

$$\dot{\psi} = \frac{D_1 \sin \varepsilon \dot{\phi}}{D_{PR} \cos \psi} \tag{11.19}$$

Differentiating Eq. (11.18) w.r.t. $\theta$:

$$D_{PR} \cos \psi \ddot{\psi} - D_{PR} \sin \psi \dot{\psi}^2 = D_1 \sin \varepsilon \ddot{\varepsilon} + D_1 \cos \varepsilon \dot{\varepsilon}^2 \tag{11.20}$$

From Eqs. (11.11), (11.12) and (11.20):

$$\ddot{\psi} = \frac{D_{PR} \sin \psi \dot{\psi}^2 + D_1 \sin \varepsilon \ddot{\phi} + D_1 \cos \varepsilon \dot{\phi}^2}{D_{PR} \cos \psi} \tag{11.21}$$

With notation of Fig. 11.1:

$$y_0 = \bar{y} - (D_{PR} \cos \psi_0 + D_1 \cos \beta_0) \tag{11.22}$$

$$y = \bar{y} - (D_{PR} \cos \psi - D_1 \sin \varepsilon) \tag{11.23}$$

$$s_F = y - y_0 = D_{PR}(\cos \psi_0 - \cos \psi) + D_1(\cos \beta_0 + \sin \varepsilon) \tag{11.24}$$

Differentiating Eq. (11.24) w.r.t. $\theta$:

$$\dot{s}_F = D_{PR} \sin \psi \dot{\psi} + D_1 \cos \varepsilon \dot{\varepsilon} \tag{11.25}$$

From Eqs. (11.11), (11.19) and (11.25):

$$\dot{s}_F = \frac{-D_{PR} \sin \psi D_1 \sin \varepsilon \dot{\phi}}{D_{PR} \cos \psi} - D_1 \cos \varepsilon \dot{\phi} \tag{11.26}$$

Using Eqs. (11.11) and (11.19), Eq. (11.26) can be simplified to give:

$$\dot{s}_F = D_1[\tan \psi \sin \varepsilon + \cos \varepsilon]\dot{\phi} \tag{11.27}$$

Differentiating Eq. (11.27) and using Eqs. (11.11) and (11.12):

$$\ddot{s}_F = D_1\left[\tan \psi \sin \varepsilon \ddot{\phi} + \sec^2 \psi \dot{\psi} \sin \varepsilon \dot{\phi} + \tan \psi \cos \varepsilon \dot{\phi}^2 + \cos \varepsilon \ddot{\phi} - \sin \varepsilon \dot{\phi}^2\right] \tag{11.28}$$

Using Eqs. (11.11) and (11.19), Eq. (11.28) can be simplified to give:

$$\ddot{s}_F = D_1\left[\{\tan \psi \sin \varepsilon + \cos \varepsilon\}\ddot{\phi} + \left\{\tan \psi \cos \varepsilon + \frac{D_1 \sin^2 \varepsilon}{D_{PR} \cos^3 \psi} - \sin \varepsilon\right\}\dot{\phi}^2\right] \tag{11.29}$$

With notation of Fig. 11.2:

$$\ddot{x}_1 = D_1 \dot{\phi}^2 \cos \psi + D\ddot{\phi} \sin \psi \tag{11.30}$$

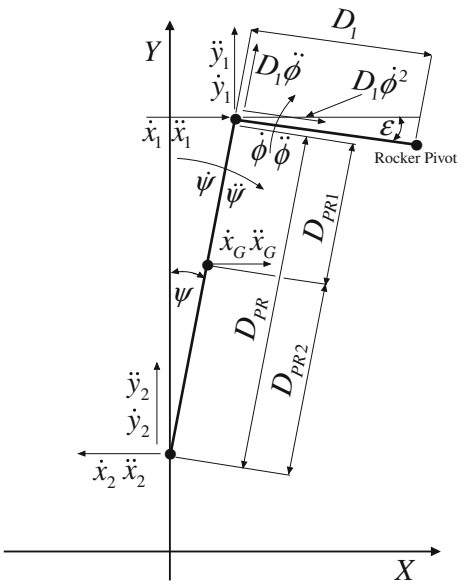


**Fig. 11.2** Push rod kinematics

$$\ddot{y}_1 = D_1\dot{\phi}^2 \sin\psi + D\ddot{\phi}\cos\psi \tag{11.31}$$

Note that:

$$\ddot{x}_2 = 0 \tag{11.32}$$

$$\ddot{y}_2 = \ddot{s}_F \tag{11.33}$$

The magnitude of the acceleration vectors of the centre of mass of the push rod are:

$$\ddot{x}_G = \frac{\ddot{x}_1 D_{PR2} + \ddot{x}_2 D_{PR1}}{D_{PR}} \tag{11.34}$$

and

$$\ddot{y}_G = \frac{\ddot{y}_1 D_{PR2} + \ddot{y}_2 D_{PR1}}{D_{PR}} \tag{11.35}$$

## 11.3 Kinetics

### *11.3.1 Notation*

| | |
|---|---|
| $A$ | Distance between rocker pivot and cam follower centre line in $x$- direction |
| $D_1$ | Length of rocker arm on push rod side |
| $D_2$ | Length of rocker arm on valve side |
| $D_{PR}$ | Length of push rod |
| $D_{PR1}$ | Distance from follower to CG of push rod |
| $D_{PR2}$ | Distance from rocker to CG of push rod |
| $F_C$ | Cam force |
| $F_{PR}$ | Push Rod force acting on rocker |
| $F_{P_X}$ | Push rod force acting on follower in x-direction |
| $F_{P_Y}$ | Pivot force acting on rocker in y-direction |
| $F_{RK}$ | Rocker force acting on valve |
| $F_S$ | Spring force |
| $F_V$ | Valve force acting on rocker |
| $I_{PR}$ | Polar Moment of Inertia of push rod |
| $I_{RK}$ | Polar Moment of Inertia of rocker |
| $L_V$ | Maximum valve lift |
| $M_E$ | Mass of follower, shim, cotters, top spring retainer, and effective spring mass |
| $M_F$ | Mass of follower |
| $M_{PR}$ | Mass of push rod |
| $M_{RK}$ | Mass of rocker |
| N | Rotational speed of engine in rpm |
| $R_G$ | Distance between rocker pivot and centre of mass |
| $s_F$ | Follower displacement |
| $\dot{s}_F$ | Follower velocity |
| $\ddot{s}_F$ | Follower acceleration |
| $s_V$ | Valve lift |
| $\dot{s}_V$ | Valve velocity |
| $\ddot{s}_V$ | Valve acceleration |
| $X$ | Coordinate |
| $X_F$ | Valve force |
| $X_P$ | Pivot force in x-direction |
| $X_{RK}$ | Rocker force acting on push rod in x-direction |
| $Y$ | Coordinate |
| $Y_F$ | Follower force in y-direction |
| $Y_{RK}$ | Pivot force in y-direction |
| $\alpha_0$ | Angle between rocker arms |
| $\beta$ | Angle which defines position of pushrod side of rocker |
| $\beta_0$ | Angle which defines position of the pushrod side of rocker with valve closed |

$\gamma$ Angle between $Y$ direction and valve axis
$\Gamma$ Function defined in text
$\varepsilon$ Angle defining rocker arm position
$\theta$ Angle of cam rotation
$\kappa$ Angle defining position of centre of mass of rocker
$\lambda$ Fraction of total valve lift, when rocker centre line is perpendicular to valve axis
$\Lambda$ Function defined in text
$\phi$ Angle which defines angular position of rocker
$\dot{\phi}$ Angular velocity of rocker
$\ddot{\phi}$ Angular acceleration of rocker
$\phi_0$ Angle which defines position of valve side rocker with valve closed
$\psi$ Angle which defines angular position of push rod
$\dot{\psi}$ Angular velocity of push rod
$\ddot{\psi}$ Angular acceleration of push rod
$\psi_0$ Angle which defines angular position of push rod with valve closed

### *11.3.2 Rocker Kinetics*

To analyse the forces acting on the various components of this mechanism it is helpful to draw a free body diagram for each major component. In this section Newton's notation is used for derivatives.

With notation of Fig. 11.3, let

$$\varepsilon = \phi - \phi_0 - \alpha_0 - \gamma \tag{11.36}$$

and

$$\delta = \phi - \phi_0 - \gamma + \kappa \tag{11.37}$$

The moments about the rocker pivot are

$$(Y_1 \sin\varepsilon + X_1 \cos\varepsilon)D_1 = F_V D_2 \cos(\phi - \phi_0) + I_{RK}\ddot{\phi} \tag{11.38}$$

Resolving forces acting on the rocker in the x-direction

$$X_P = F_V \sin\gamma - X_1 - M_{RK}R_G\left(\ddot{\phi}\sin\delta + \dot{\phi}^2\cos\delta\right) \tag{11.39}$$

Resolving forces acting on the rocker in the Y-direction

$$Y_P = Y_1 - F_V \cos\gamma + M_{RK}R_G\left(\ddot{\phi}\cos\delta - \dot{\phi}^2\sin\delta\right) \tag{11.40}$$

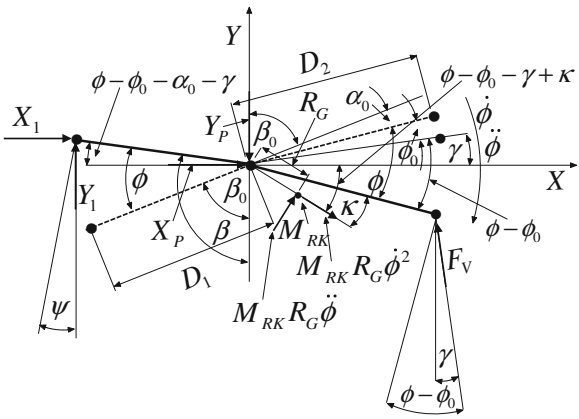


**Fig. 11.3** Rocker kinetics

### *11.3.3 Push Rod Kinetics*

With notation of Fig. 11.4.

The moments about the centre of mass of the push rod are

$$(Y_1\cos\psi - X_1\sin\psi)D_{PR1} + (Y_2\cos\psi - X_2\sin\psi)D_{PR2} = I_{PR}\ddot{\psi} \tag{11.41}$$

Resolving forces acting on the push rod in the y-direction

$$X_1 = X_2 - M_{PR}\ddot{x}_G \tag{11.42}$$

Resolving forces acting on the push rod in the Y-direction

$$Y_1 = Y_2 - M_{PR}\ddot{y}_G \tag{11.43}$$

Equations (11.38) to (11.43) are six equations in six unknowns. These can be solved to give the forces acting at on the push rod and the follower. After some manipulation, of Eqs. (11.38), (11.41), (11.42), and (11.43)

$$X_2 = \frac{1}{\cot\varepsilon - \tan\psi}\left[\begin{array}{r}\dfrac{I_{RK}\ddot{\phi} + F_V D_2\cos(\phi-\phi_0) + M_{PR}D_1(\ddot{x}_G\cos\varepsilon + \ddot{y}_G\sin\varepsilon)}{D_1\sin\varepsilon} \\ -\dfrac{I_{PR}\ddot{\psi} + M_{PR}(\ddot{y}_G\cos\psi - \ddot{x}_G\sin\psi)D_{PR1}}{D_{PR}\cos\psi}\end{array}\right] \tag{11.44}$$

$$Y_2 = \frac{1}{\cot\psi - \tan\varepsilon}\left[\begin{array}{r}\dfrac{I_{PR}\ddot{\psi} + M_{PR}(\ddot{y}_G\cos\psi - \ddot{x}_G\sin\psi)D_{PR1}}{D_{PR}\sin\psi} \\ -\dfrac{I_{RK}\ddot{\phi} + F_V D_2\cos(\phi-\phi_0) + M_{PR}D_1(\ddot{x}_G\cos\varepsilon + \ddot{y}_G\sin\varepsilon)}{D_1\cos\varepsilon}\end{array}\right] \tag{11.45}$$

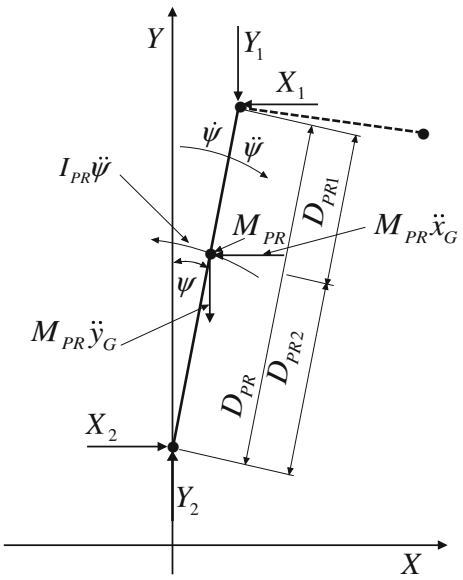


**Fig. 11.4** Push rod kinetics

By substituting Eq. (11.42) into Eq. (11.39) and Eq. (11.43) into Eq. (11.40), the forces acting on the rocker pivot can be determined.

$$X_P = F_V \sin\gamma - X_2 + M_{PR}\ddot{x}_G - M_{RK}R_G\left(\ddot{\phi}\sin\delta + \dot{\phi}^2\cos\delta\right) \tag{11.46}$$

$$Y_P = Y_2 - M_{PR}\ddot{y}_G - F_V\cos\gamma + M_{RK}R_G\left(\ddot{\phi}\cos\delta - \dot{\phi}^2\sin\delta\right) \tag{11.47}$$

### *11.3.4 Follower Kinetics*

Recall Eq. (11.31) and with notation of Fig. 11.5:

$$F_C = Y_2 + M_F\ddot{s}_F = Y_2 + M_F\ddot{s}_F \tag{11.48}$$

From Eq. (11.45) and Eq. (11.48):

$$F_C = \frac{1}{\cot\psi - \tan\varepsilon}\left[\begin{array}{r} \dfrac{I_{PR}\ddot{\psi} + M_{PR}(\ddot{y}_G\cos\psi - \ddot{x}_G\sin\psi)D_{PR1}}{D_{PR}\sin\psi} \\ -\dfrac{I_{RK}\ddot{\phi} + F_V D_2\cos(\phi-\phi_0) + M_{PR}(\ddot{x}_G\cos\varepsilon + \ddot{y}_G\sin\varepsilon)}{D_1\cos\varepsilon} \end{array}\right] + M_F\ddot{s}_F \tag{11.49}$$

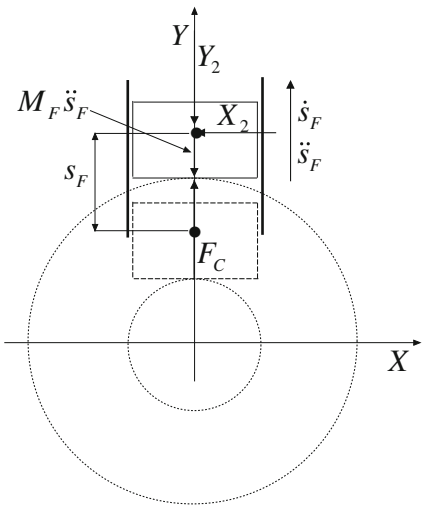


**Fig. 11.5** Flat translating follower kinetics

## 11.4 Cam Shape and Other Parameters

The equations required to compute the cam shape, cam torque, curvature, entrainment velocity and contact stress are given in Sects. 4.4–4.7. The follower lift, $s_F$is given by Eq. (11.24), the follower velocity, $\dot{s}_F$ by Eq. (11.25), the follower acceleration, $\ddot{s}_F$ by Eq. (11.29), and the cam force, $F_C$ is given by Eq. (11.49).

## 11.5 Maximum Speed to Maintain Contact

Let

$$\Lambda = \frac{I_{PR}\ddot{\psi} + M_{PR}(\ddot{y}_G \cos\psi - \ddot{x}_G \sin\psi)D_{PR1}}{D_{PR}\sin\psi} \tag{11.50}$$

and

$$\Gamma = \frac{I_{RK}\ddot{\phi} + M_{PR}(\ddot{x}_G \cos\varepsilon + \ddot{y}_G \sin\varepsilon)}{D_1 \cos\varepsilon} \tag{11.51}$$

Equation (11.47) can be rewritten:

$$F_C = \frac{1}{\tan\varepsilon - \cot\psi}\left[\Gamma - \Lambda + \frac{F_V D_2 \cos(\phi - \phi_0)}{D_1 \cos\varepsilon}\right] + M_F \ddot{s}_F \tag{11.52}$$

$$F_V = M_E \ddot{s}_V + F_S \tag{11.53}$$

Recall that in Eq. (11.53) the valve acceleration is in m/radian$^2$. With reference to Sect. 1.14, can now be rewritten:

$$F_V = M_E \ddot{s}_V \left(\frac{\pi N}{60}\right)^2 + F_S \tag{11.54}$$

The forces are now in N and the effective mass is in kg. The linear accelerations, $\ddot{s}_V$, $\ddot{x}_G$ and $\ddot{y}_G$, need to be multiplied by $\left(\frac{\pi N}{60}\right)^2$to convert them to m/s$^2$. Similarly, the angular accelerations $\ddot{\phi}$ and $\ddot{\psi}$ need to be multiplied by $\left(\frac{\pi N}{60}\right)^2$to convert radians$^{-2}$ to s$^2$.

If $F_C = 0$, Eq. (11. 52) can be written as

$$-F_s D_2 \cos(\phi - \phi_0) = \left[\frac{\pi N}{60}\right]^2 \left\{ \begin{array}{r} [\Gamma - \Lambda + M_F \ddot{s}_F(\tan\varepsilon - \cot\psi)] D_1 \cos\varepsilon \\ + M_E \ddot{s}_V D_2 \cos(\phi - \phi_0) \end{array} \right\} \tag{11.55}$$

hence

$$N = \frac{60}{\pi}\left[\frac{-F_S D_2 \cos(\phi - \phi_0)}{[\Gamma - \Lambda + M_F \ddot{s}_F(\tan\varepsilon - \cot\psi)] D_1 \cos\varepsilon + M_E \ddot{s}_V D_2 \cos(\phi - \phi_0)}\right]^{\frac{1}{2}} \tag{11.56}$$

Sections (11.3), (11.4) and (11.5) can easily be extended to a radial translating follower by reference to Chap. 5 or an offset translating follower by reference to Chap. 6.

## 11.6 Introduction to Four Bar Chain Push Rod Mechanism

This mechanism which is shown in Fig. 11.6 is less widely used than that considered above. However it is more robust and can withstand higher loads and therefore higher engine speeds. The 500I Indy 500 Engine had the cam and follower, and the rocker rotating in differing planes, as described by Ludvigsen [1]. To analyse such a mechanism accurately requires a three-dimensional mathematical model. However, for simplicity the analysis given below is in two dimensions.

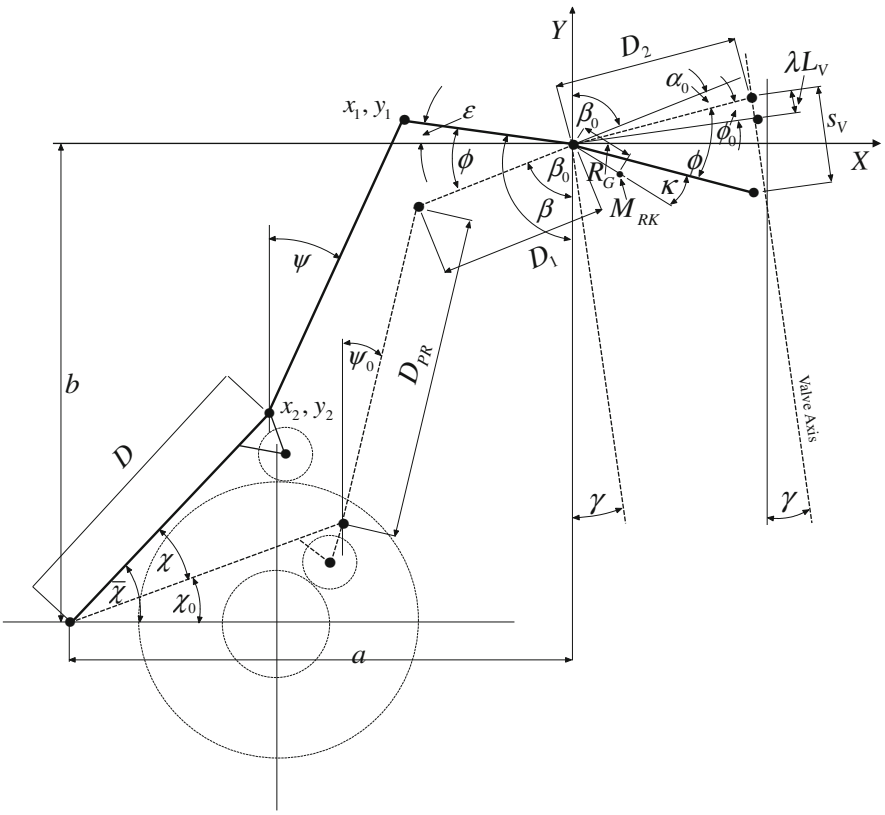


**Fig. 11.6** Finger follower push rod kinematics

## 11.7 Kinematics of Four Bar Chain

### *11.7.1 Notation*

| | |
|---|---|
| $a$ | Distance between follower pivot and rocker pivot in $x$-direction |
| $b$ | Distance between follower pivot and rocker pivot in $y$-direction |
| $c$ | Length of rocker arm |
| $d$ | Length of push rod |
| $D$ | Distance from follower pivot to push rod and follower joint |
| $D_1$ | Length of rocker arm on push rod side |
| $D_2$ | Length of rocker arm on valve side |
| $D_F$ | Distance from follower pivot to centre of curvature of follower |
| $D_{PR}$ | Length of push rod |
| $D_{PR1}$ | Distance from follower to CG of push rod |
| $D_{PR2}$ | Distance from rocker to CG of push rod |

| | |
|---|---|
| $e$ | Length of follower |
| $F$ | Parameter defined in text |
| $x_1$ | Coordinate of push rod and rocker joint |
| $x_2$ | Coordinate of push rod and follower joint |
| $y_1$ | Coordinate of push rod and rocker joint |
| $y_2$ | Coordinate of push rod and follower joint |
| $\varepsilon$ | Rocker angle |
| $\theta$ | Angle of cam rotation |
| $\chi$ | Increase in angle of follower rotation due to valve lift |
| $\chi_0$ | Follower angle valve closed |
| $\bar{\chi}$ | Follower angle |
| $\dot{\chi}$ | Angular velocity of follower |
| $\ddot{\chi}$ | Angular acceleration of follower |
| $\psi$ | Push rod angle |
| $\psi_0$ | Push rod angle valve closed |
| $\dot{\psi}$ | Angular velocity of push rod |
| $\ddot{\psi}$ | Angular acceleration of push rod |

The four bar chain shown in Fig. 11.7a, b has the two possible configurations called closures shown. The part of the cam mechanism which comprises the four bar chain is shown in Fig. 11.6, and corresponds to the closure shown in Fig. 11.7b. Analysis of the kinematics of this mechanism is described by Molian [2].

The mechanism shown in Fig. 11.6 consists in part of a four bar chain made up of the cam follower, the push rod and part of the rocker. As this mechanism has two possible closures, it is not surprising that the analysis of the kinematics involves a quadratic equation. The closure that is of present interest is shown in Figs. 11.7b and 11.8.

### *11.7.2 Displacements*

With notation of Figs. 11.6 and 11.8, differing symbols denote the three lengths $D_1$, $D_{PR}$ and $D$ in Fig. 11.6 and the corresponding lengths $c$, $d$ and $e$ in Fig. 11.8. This simplifies the notation in Sects. 11.7.2–11.7.4. With notation of Fig. 11.8 the ends of the rocker have coordinates:

$$x_1 = -c\cos\varepsilon \tag{11.57}$$

$$y_1 = c\sin\varepsilon \tag{11.58}$$

The locus of the end of the rocker, $x_1$, $y_1$ is a circle given by:

$$x_1^2 + y_1^2 = c^2 \tag{11.59}$$

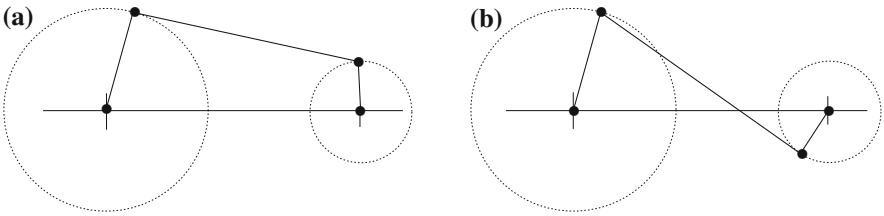


**Fig. 11.7** **a**, **b** Closures of four bar chain

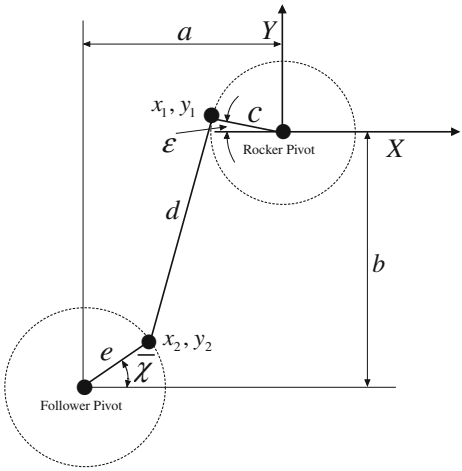


**Fig. 11.8** Four bar chain kinematics

Similarly the ends of the follower have coordinates:

$$x_2 = e\cos\bar{\chi} - a \tag{11.60}$$

$$y_2 = e\sin\bar{\chi} - b \tag{11.61}$$

The locus of the end of the follower, $x_2$, $y_2$ is a circle given by:

$$(x_2 + a)^2 + (y_2 + b)^2 = e^2 \tag{11.62}$$

The ends of the push rod form diametrically opposed points on a circle diameter, $d$, given by:

$$(x_1 - x_2)^2 + (y_1 - y_2)^2 = d^2 \tag{11.63}$$

The values of $x_1$, $y_1$ are known for any angle, $\xi$, and Eqs. (11.62) and (11.63) are two simultaneous quadratic equations in $x_2$, and $y_2$. These two equations expand to give:

$$x_2^2 + a^2 + 2ax_2 + y_2^2 + b^2 + 2by_2 = e^2 \tag{11.64}$$

and

$$x_1^2 + x_2^2 - 2x_1x_2 + y_1^2 + y_2^2 - 2y_1y_2 = d^2 \tag{11.65}$$

Subtracting Eq. (11.64) from Eq. (11.65):

$$x_1^2 - 2x_1x_2 - 2ax_2 + y_1^2 - 2y_1y_2 - 2by_2 = a^2 + b^2 + d^2 - e^2 \tag{11.66}$$

Substituting Eq. (11.59) into Eq. (11.66):

$$-2x_1x_2 - 2ax_2 - 2y_1y_2 - 2by_2 = a^2 + b^2 - c^2 + d^2 - e^2 \tag{11.67}$$

Let

$$a^2 + b^2 - c^2 + d^2 - e^2 = F \tag{11.68}$$

From Eqs. (11.67) and (11.68):

$$-2x_2(x_1 + a) = F + 2y_2(y_1 + b) \tag{11.69}$$

$$x_2 = -\left\{\frac{F + 2y_2(y_1 + b)}{2(x_1 + a)}\right\} \tag{11.70}$$

Substituting Eq. (11.70) into Eq. (11.62):

$$\left\{\frac{F + 2y_2(y_1 + b)}{2(x_1 + a)} - a\right\}^2 + (y_2 + b)^2 = e^2 \tag{11.71}$$

Equation (11.71) is a quadratic equation in $y_2$, where the two roots correspond to the two closures shown in Fig. 7a, b. Expanding and re-arranging Eq. (11.71)

$$\begin{aligned} &y_2^2\left[4\left\{(y_1 + b)^2 + (x_1 + a)^2\right\}\right] \\ &\quad + y_2\left[4F(y_1 + b) + 4a(x_1 + a)(y_1 + b) + 8b(x_1 + a)^2\right] \\ &\quad + 4\left[(x_1 + a)\left\{a^2(x_1 + a) + aF + \left(b^2 - e^2\right)(x_1 + a)\right\}\right] = 0 \end{aligned} \tag{11.72}$$

Equation (11.72) can be written as

$$Ay_2^2 + By_2 + C = 0 \tag{11.73}$$

where

$$A = \left[4\left\{(y_1 + b)^2 + (x_1 + a)^2\right\}\right] \tag{11.74}$$

$$B = \left[4F(y_1 + b) + 4a(x_1 + a)(y_1 + b) + 8b(x_1 + a)^2\right] \tag{11.75}$$

$$C = 4\left[(x_1 + a)\left\{a^2(x_1 + a) + aF + \left(b^2 - e^2\right)(x_1 + a)\right\}\right] = 0 \tag{11.76}$$

The two roots of the quadratic equation are:

$$y_2 = \frac{-B \pm \sqrt{B^2 - 4AC}}{2A} \tag{11.77}$$

We require the solution show in Figs. 11.7b, 11.8, where $y_2$ is negative

$$y_2 = \frac{-B - \sqrt{B^2 - 4AC}}{2A} \tag{11.78}$$

Substituting $y_2$ into Eq. (11.70) gives $x_2$

### 11.7.3 Velocities

Differentiating Eqs. (11.57) and (11.58) w.r.t. $\theta$:

$$\dot{x}_1 = c \sin \varepsilon \dot{\varepsilon} \tag{11.79}$$

Substituting Eq. (11.11) into Eq. (11.79):

$$\dot{x}_1 = c \sin \varepsilon \dot{\phi} \tag{11.80}$$

$$\dot{y}_1 = c \sin \varepsilon \dot{\varepsilon} \tag{11.81}$$

Substituting Eq. (11.11) into Eq. (11.81):

$$\dot{y}_1 = c \sin \varepsilon \dot{\phi} \tag{11.82}$$

Differentiating Eq. (11.62) w.r.t. $\theta$:

$$(x_2 + a)\dot{x}_2 + (y_2 + b)\dot{y}_2 = 0 \tag{11.83}$$

Differentiating Eq. (11.63) w.r.t. $\theta$:

$$(x_1 - x_2)(\dot{x}_1 - \dot{x}_2) + (y_1 - y_2)(\dot{y}_1 - \dot{y}_2) = 0 \tag{11.84}$$

Equation (11.84) can be written as

$$(x_1 - x_2)\dot{x}_1 + (y_1 - y_2)\dot{y}_1 = (x_1 - x_2)\dot{x}_2 + (y_1 - y_2)\dot{y}_2 \tag{11.85}$$

Since $\dot{x}_1$ and $\dot{y}_1$ are known from Eqs. (11.80) and (11.82), the two simultaneous Eqs. (11.83) and (11. 85) can be solved to obtain $\dot{x}_2$ and $\dot{y}_2$

### 11.7.4 Accelerations

Differentiating Eq. (11.83) w.r.t. $\theta$:

$$(x_2 + a)\ddot{x}_2 + \dot{x}_2^2 + (y_2 + b)\ddot{y}_2 + \dot{y}_2^2 = 0 \tag{11.86}$$

hence

$$(x_2 + a)\ddot{x}_2 + (y_2 + b)\ddot{y}_2 = -\dot{x}_2^2 - \dot{y}_2^2 \tag{11.87}$$

Differentiating Eq. (11.85) w.r.t. $\theta$:

$$\begin{aligned}(x_1 - x_2)\ddot{x}_1 + (\dot{x}_1 - \dot{x}_2)\dot{x}_1 + (y_1 - y_2)\ddot{y}_1 + (\dot{y}_1 - \dot{y}_2)\dot{y}_1 = \\ (x_1 - x_2)\ddot{x}_2 + (\dot{x}_1 - \dot{x}_2)\dot{x}_2 + (y_1 - y_2)\ddot{y}_2 + (\dot{y}_1 - \dot{y}_2)\dot{y}_2\end{aligned} \tag{11.88}$$

Equation (11.88) can be written as

$$(x_1 - x_2)\ddot{x}_2 + (y_1 - y_2)\ddot{y}_2 = (x_1 - x_2)\ddot{x}_1 + (y_1 - y_2)\ddot{y}_1 + (\dot{x}_1 - \dot{x}_2)^2 + (\dot{y}_1 - \dot{y}_2)^2 \tag{11.89}$$

The simultaneous Eqs. (11.88) and (11.89) can be solved to obtain $\ddot{x}_2$ and $\ddot{y}_2$. Differentiating Eq. (11.80) w.r.t. $\theta$ and recalling Eqs. (11.11) and (11.12):

$$\ddot{x}_1 = -c\cos\varepsilon\ddot{\phi} + c\sin\varepsilon\dot{\phi}^2 \tag{11.90}$$

Differentiating Eq. (11.82) w.r.t. $\theta$ and recalling Eqs. (11.11) and (11.12):

$$\ddot{y}_1 = -c\cos\varepsilon\ddot{\phi} + c\sin\varepsilon\dot{\phi}^2 \tag{11.91}$$

Equations (11.87) and (11.89) can now be solved to obtain $\ddot{x}_2$ and $\ddot{y}_2$

### *11.7.5 Push Rod Angular Displacement*

With notation of Fig. 11.9:

$$\cos\psi = \frac{y_1 - y_2}{D_{PR}} \tag{11.92}$$

$$\sin\psi = \frac{x_1 - x_2}{D_{PR}} \tag{11.93}$$

### *11.7.6 Push Rod Angular Velocity*

Differentiating Eq. (11.92) w.r.t. $\theta$:

$$-\sin\psi\dot{\psi} = \frac{\dot{y}_1 - \dot{y}_2}{D_{PR}} \tag{11.94}$$

From Eqs. (11.93) and (11.94):

$$-(x_1 - x_2)\dot{\psi} = \dot{y}_1 - \dot{y}_2 \tag{11.95}$$

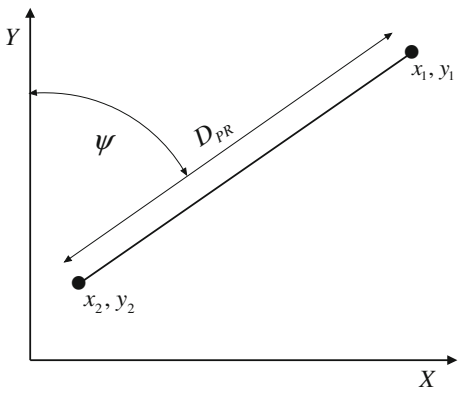


**Fig. 11.9** Push rod kinematics

hence

$$\dot{\psi} = -\frac{\dot{y}_1 - \dot{y}_2}{x_1 - x_2} \tag{11.96}$$

Differentiating Eq. (11.93) w.r.t $\theta$:

$$\cos\psi\dot{\psi} = \frac{\dot{x}_1 - \dot{x}_2}{D_{PR}} \tag{11.97}$$

From Eqs. (11.92) and (11.97):

$$(y_1 - y_2)\dot{\psi} = \dot{x}_1 - \dot{x}_2 \tag{11.98}$$

$$\dot{\psi} = \frac{\dot{x}_1 - \dot{x}_2}{y_1 - y_2} \tag{11.99}$$

### *11.7.7 Push Rod Angular Acceleration*

Differentiating Eq. (11.96) w.r.t $\theta$:

$$\ddot{\psi} = \frac{(x_1 - x_2)(\ddot{y}_1 - \ddot{y}_2) - (\dot{y}_1 - \dot{y}_2)(\dot{x}_1 - \dot{x}_2)}{(x_1 - x_2)^2} \tag{11.100}$$

Differentiating Eq. (11.99) w.r.t $\theta$:

$$\ddot{\psi} = \frac{(y_1 - y_2)(\ddot{x}_1 - \ddot{x}_2) - (\dot{x}_1 - \dot{x}_2)(\dot{y}_1 - \dot{y}_2)}{(y_1 - y_2)^2} \tag{11.101}$$

If $\psi = 0$ or $\psi = \pi$ then $x_1 = x_2$ and Eqs. (11.99) and (11.101) should be used.

If $\psi = \pi/2$ or $\psi = 3\pi/2$ then $y_1 = y_2$ and Eqs. (11.96) and (11.100) should be used.

### 11.7.8 Cam Follower Angular Displacement

From Sect. 11.7.2 the coordinates of the end of the follower $x_2$ and $y_2$ are known.

Equations (11.60) and (11.61) can be re-written as

$$\bar{\chi} = \cos^{-1}\left(\frac{x_2 + a}{e}\right) \tag{11.102}$$

$$\bar{\chi} = \sin^{-1}\left(\frac{y_2 + b}{e}\right) \tag{11.103}$$

### 11.7.9 Cam Follower Angular Velocity

From Sect. 11.7.3, $\dot{x}_2$ and $\dot{y}_2$ are known. Differentiating Eq. (11.60) w.r.t. $\theta$:

$$\dot{x}_2 = -e\dot{\chi}\sin\bar{\chi} \tag{11.104}$$

$$\dot{\chi} = -\frac{\dot{x}_2}{e\sin\bar{\chi}} \tag{11.105}$$

Differentiating Eq. (11.61) w.r.t. $\theta$:

$$\dot{y}_2 = e\dot{\chi}\cos\bar{\chi} \tag{11.106}$$

$$\dot{\chi} = \frac{\dot{y}_2}{e\cos\bar{\chi}} \tag{11.107}$$

Differentiating Eq. (11.104) w.r.t $\theta$:

$$\ddot{x}_2 = -e\ddot{\chi}\sin\bar{\chi} - e\dot{\chi}^2\cos\bar{\chi} \tag{11.108}$$

$$\ddot{\chi} = -\left[\frac{\ddot{x}_2 + e\dot{\chi}^2\cos\bar{\chi}}{e\sin\bar{\chi}}\right] \tag{11.109}$$

Differentiating Eq. (11.106) w.r.t $\theta$:

$$\ddot{y}_2 = e\ddot{\chi}\cos\bar{\chi} - e\dot{\chi}^2\sin\bar{\chi} \tag{11.110}$$

$$\ddot{\chi} = \frac{\ddot{y}_2 + e\dot{\chi}^2\sin\bar{\chi}}{e\cos\bar{\chi}} \tag{11.111}$$

Note: If $\bar{\chi} = 0$ or $\bar{\chi} = \pi$, then use Eqs. (11.107), and (11.111). If $\bar{\chi} = \frac{\pi}{2}$ or $\bar{\chi} = \frac{3\pi}{2}$ then use Eqs. (11.105) and (11.109).

## 11.8 Kinetics of Four Bar Chain Mechanism

### *11.8.1 Notation*

| | |
|---|---|
| $a$ | Distance between follower pivot and rocker pivot in $x$-direction |
| $b$ | Distance between follower pivot and rocker pivot in $y$-direction |
| $c$ | Length of rocker arm |
| $d$ | Length of push rod |
| $D$ | Distance from follower pivot to push rod and follower joint |
| $D_1$ | Length of rocker arm on push rod side |
| $D_2$ | Length of rocker arm on valve side |
| $D_F$ | Distance from follower pivot to centre of curvature of follower |
| $D_{PR}$ | Length of push rod |
| $D_{PR1}$ | Distance from follower to CG of push rod |
| $D_{PR2}$ | Distance from rocker to CG of push rod |
| $e$ | Length of follower |
| $F$ | Parameter defined in text |
| $F_C$ | Cam force |
| $F_S$ | Spring force |
| $F_V$ | Valve force acting on rocker |
| $I_{PR}$ | Polar moment of inertia of push rod |
| $I_{RK}$ | Polar moment of inertia of rocker |
| $M_E$ | Mass of follower, shim, cotters, top spring retainer, and effective spring mass |
| $M_F$ | Mass of follower |
| $M_{PR}$ | Mass of push rod |
| $R_{CG}$ | Distance from follower pivot to CG of follower |
| $\ddot{s}_V$ | Valve acceleration |
| $x_1$ | Coordinate of push rod and rocker joint |
| $x_2$ | Coordinate of push rod and follower joint |
| $\ddot{x}_G$ | Acceleration of CG of push rod in $x$ - direction |
| $X_2$ | Force on push rod and follower joint in $x$- direction |
| $X_{FP}$ | Force on follower pivot in $x$- direction |
| $y_1$ | Coordinate of push rod and rocker joint |
| $y_2$ | Coordinate of push rod and follower joint |
| $\ddot{y}_G$ | Acceleration of CG of push rod in $y$- direction |
| $Y_2$ | Force on push rod and follower joint in $y$- direction |
| $Y_{FP}$ | Force on follower pivot in $y$- direction |
| $\beta_F$ | Pressure angle |

$\Delta$ Function defined in text
$\zeta$ Angle defined in Fig. 11.10
$\eta$ Angle defined in Fig. 11.10
$\theta$ Angle of cam rotation
$\xi$ Rocker angle
$\Sigma$ Function defined in text
$\chi$ Increase in angle of follower rotation due to valve lift
$\chi_0$ Follower angle valve closed
$\bar{\chi}$ Follower angle
$\dot{\chi}$ Angular velocity of follower
$\ddot{\chi}$ Angular acceleration of follower
$\psi$ Push rod angle
$\psi_0$ Push rod angle valve closed
$\dot{\psi}$ Angular velocity of push rod
$\ddot{\psi}$ Angular acceleration of push rod

### *11.8.2 Kinetics of Rocker and Push Rod*

The motion of the rocker will be as for the previous mechanism but owing to the difference in motion of the push rod and follower the forces will also differ. The equations derived in Sect. (11.4.2) still apply but with new values for the accelerations, $\ddot{x}_G$ and $\ddot{y}_G$.

Equations (11.34) and (11.35) are as given in Sect. 11.3.3, but $\ddot{x}_2$is now given by Eq. (11.110) and $\ddot{y}_2$ is now given by Eq. (11.112). Substitution of these new values in Eqs. (11.34) and (11.35), will give the required new values of $\ddot{x}_G$ and $\ddot{y}_G$

### *11.8.3 Kinetics of Cam and Follower*

A towards clockwise cam was analysed in Chap. 7. The mechanism shown in Fig. 11.10 is a clockwise away cam, shown with the valve opening. Towards and away cams are discussed in Sect. 8.5.1. With notation of Fig. 11.10 let

$$\bar{\chi} - \zeta + \frac{\pi}{2} - \beta_F = \eta \tag{11.112}$$

Moments about the follower pivot:

$$F_C D_F \cos\beta_F = D(Y_2 \cos\bar{\chi} - X_2 \sin\bar{\chi}) + I_{FP}\ddot{\chi} \tag{11.113}$$

The cam force is given by

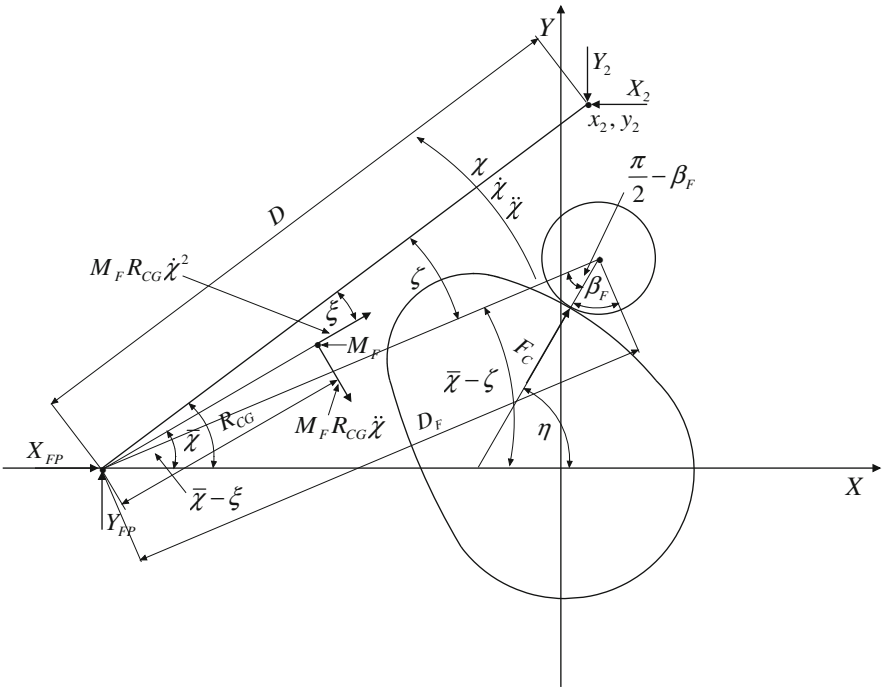


**Fig. 11.10** Cam and follower kinetics

$$F_C = \frac{D(Y_2 \cos\bar{\chi} - X_2 \sin\bar{\chi}) + I_{FP}\ddot{\chi}}{D_F \cos\beta_F} \tag{11.114}$$

The pivot forces are:

$$X_{FP} = X_2 - F_C \cos\eta - M_F R_{CG}\left[\ddot{\chi}\sin(\bar{\chi} - \xi) + \dot{\chi}^2\cos(\bar{\chi} - \xi)\right] \tag{11.115}$$

$$Y_{FP} = Y_2 - F_C \sin\eta + M_F R_{CG}\left[\ddot{\chi}\cos(\bar{\chi} - \xi) - \dot{\chi}^2\sin(\bar{\chi} - \xi)\right] \tag{11.116}$$

## 11.9 Maximum Speed to Maintain Contact

Recall Eqs. (11.44) and (11.44) from Sect. 11.4.3

$$X_2 = \frac{1}{\cot\varepsilon - \tan\psi}\left[\begin{array}{c}\dfrac{I_{RK}\ddot{\phi} + F_V D_2\cos(\phi-\phi_0) + M_{PR}D_1(\ddot{x}_G\cos\varepsilon + \ddot{y}_G\sin\varepsilon)}{D_1\sin\varepsilon} \\ -\dfrac{I_{PR}\ddot{\psi} + M_{PR}(\ddot{y}_G\cos\psi - \ddot{x}_G\sin\psi)D_{PR1}}{D_{PR}\cos\psi}\end{array}\right] \tag{11.44}$$

$$Y_2 = \frac{1}{\cot\psi - \tan\varepsilon}\left[\begin{array}{c}\dfrac{I_{PR}\ddot{\psi} + M_{PR}(\ddot{y}_G\cos\psi - \ddot{x}_G\sin\psi)D_{PR1}}{D_{PR}\sin\psi} \\ -\dfrac{I_{RK}\ddot{\phi} + F_V D_2\cos(\phi-\phi_0) + M_{PR}D_1(\ddot{x}_G\cos\varepsilon + \ddot{y}_G\sin\varepsilon)}{D_1\cos\varepsilon}\end{array}\right] \tag{11.45}$$

In the two equations above the various parameters are those for the four bar chain mechanism considered in Sect. 11.7, not those evaluated in Sect. 11.2.

The force due to valve inertia and spring force is:

$$F_V = M_E\ddot{s}_V + F_S \tag{11.53}$$

Equation (11.44) can be re-written as:

$$X_2 = \frac{1}{\cot\varepsilon - \tan\psi}\left\{\left[\begin{array}{c}\dfrac{I_{RK}\ddot{\phi} + M_{PR}D_1(\ddot{x}_G\cos\varepsilon + \ddot{y}_G\sin\varepsilon)}{D_1\sin\varepsilon} - \\ \dfrac{I_{PR}\ddot{\psi} + M_{PR}D_{PR1}(\ddot{y}_G\cos\psi - \ddot{x}_G\sin\psi)}{D_{PR}\cos\psi}\end{array}\right] + \frac{F_V D_2\cos(\phi-\phi_0)}{D_1\sin\varepsilon}\right\} \tag{11.117}$$

In order to separate the inertia forces and the spring forces in Eq. (117) let

$$\Delta = \left[\begin{array}{c}\dfrac{I_{RK}\ddot{\phi} + M_{PR}D_1(\ddot{x}_G\cos\varepsilon + \ddot{y}_G\sin\varepsilon)}{D_1\sin\varepsilon} \\ -\dfrac{I_{PR}\ddot{\psi} + M_{PR}(\ddot{y}_G\cos\psi - \ddot{x}_G\sin\psi)D_{PR1}}{D_{PR}\cos\psi}\end{array}\right] + \frac{M_E\ddot{s}_V D_2\cos(\phi-\phi_0)}{D_1\sin\varepsilon} \tag{11.118}$$

And Eq. (11.45) can be re-written as:

$$Y_2 = \frac{1}{\cot\psi - \tan\varepsilon}\left\{\left[\begin{array}{c}\dfrac{I_{PR}\ddot{\psi} + M_{PR}(\ddot{y}_G\cos\psi - \ddot{x}_G\sin\psi)D_{PR1}}{D_{PR}\sin\psi} \\ -\dfrac{I_{RK}\ddot{\phi} + M_{PR}D_1(\ddot{x}_G\cos\varepsilon + \ddot{y}_G\sin\varepsilon)}{D_1\cos\varepsilon}\end{array}\right] - \frac{F_V D_2\cos(\phi-\phi_0)}{D_1\cos\varepsilon}\right\} \tag{11.119}$$

In order to separate the inertia forces and the spring forces in Eq. (119) let

$$\Sigma = \begin{bmatrix} \dfrac{I_{PR}\ddot{\psi} + M_{PR}(\ddot{y}_G \cos\psi - \ddot{x}_G \sin\psi) D_{PR1}}{D_{PR} \sin\psi} \\ -\dfrac{I_{RK}\ddot{\phi} + M_{PR} D_1 (\ddot{x}_G \cos\varepsilon + \ddot{y}_G \sin\varepsilon)}{D_1 \cos\varepsilon} \end{bmatrix} - \frac{M_E \ddot{s}_V D_2 \cos(\phi - \phi_0)}{D_1 \cos\varepsilon} \tag{11.120}$$

Equations (11.117) and (11.119) can now be written as:

$$X_2 = \frac{1}{\cot\varepsilon - \tan\psi}\left[\Delta + \frac{F_S D_2 \cos(\phi - \phi_0)}{D_1 \sin\varepsilon}\right] \tag{11.121}$$

and

$$Y_2 = \frac{1}{\cot\psi - \tan\varepsilon}\left[\Sigma - \frac{F_V D_2 \cos(\phi - \phi_0)}{D_1 \cos\varepsilon}\right] \tag{11.122}$$

Substituting Eqs. (11.121) and (11.122) into Eq. (11.113):

$$F_C = \frac{D\cos\bar{\chi}}{D_F \cos\beta_F(\cot\psi - \tan\varepsilon)}\left[\Sigma - \frac{F_S D_2 \cos(\phi - \phi_0)}{D_1 \cos\varepsilon}\right] - \frac{D\sin\bar{\chi}}{D_F \cos\beta_F(\cot\varepsilon - \tan\psi)}\left[\Delta + \frac{F_S D_2 \cos(\phi - \phi_0)}{D_1 \sin\varepsilon}\right] + \frac{I_{FP}\ddot{\chi}}{D_F \cos\beta_F} \tag{11.123}$$

Recall that in Eq. (11.53) the valve acceleration is in m/radian$^2$. With reference to Sect. 1.14 this can now be written:

$$F_V = M_E \ddot{s}_V \left(\frac{\pi N}{60}\right)^2 + F_S \tag{11.54}$$

The forces are now in N and the effective mass is in kg. The linear accelerations, $\ddot{s}_V$, $\ddot{x}_G$ and $\ddot{y}_G$, need to be multiplied by $\left(\frac{\pi N}{60}\right)^2$ to convert them to m/s$^2$. Similarly, the angular accelerations $\ddot{\phi}$, $\ddot{\psi}$ and $\ddot{\chi}$ need to be multiplied by $\left(\frac{\pi N}{60}\right)^2$ to convert radians$^{-2}$ to s$^{-2}$. If $F_C = 0$, then from Eqs. (11.125) and (11.54):

$$\left(\frac{\pi N}{60}\right)^2 \left\{\frac{D}{D_F}\left[\frac{\Sigma\cos\bar{\chi}}{\cos\beta_F(\cot\psi - \tan\varepsilon)} - \frac{\Delta\sin\bar{\chi}}{\cos\beta_F(\cot\varepsilon - \tan\psi)}\right] + \frac{I_{FP}\ddot{\chi}}{D_F\cos\beta_F}\right\} = -\frac{F_S D_2 \cos(\phi - \phi_0)}{D_1 \cos\varepsilon}\left[\frac{1}{\cos\varepsilon(\cot\psi - \tan\varepsilon)} - \frac{1}{\sin\varepsilon(\cot\varepsilon - \tan\psi)}\right] \tag{11.124}$$

and

$$N = \frac{60}{\pi}\left\{\frac{-\frac{F_S D_2 \cos(\phi-\phi_0)}{D_1 \cos\varepsilon}\left[\frac{1}{\cos\varepsilon(\cot\psi-\tan\varepsilon)} - \frac{1}{\sin\varepsilon(\cot\varepsilon-\tan\psi)}\right]}{\frac{D}{D_F\cos\beta_F}\left[\frac{\Sigma\cos\bar{\chi}}{(\cot\psi-\tan\varepsilon)} - \frac{\Delta\sin\bar{\chi}}{(\cot\varepsilon-\tan\psi)}\right] + I_{FP}\ddot{\chi}}\right\}^{\frac{1}{2}} \tag{11.125}$$

## 11.10 Pressure Angle, Cam Shape and Other Parameters

In Fig. 11.6 the cam is rotating clockwise as the valve opens. If the cam were rotating anticlockwise the valve would be closing. This is a clockwise away cam. Part of the same diagram is shown in Fig. 11.11a. If the mechanism were mirrored, the cam would be rotating clockwise as the valve opens, and anticlockwise as the valve closes. A mirrored version of Fig. 11.11a is shown in Fig. 11.11b. This is a clockwise towards cam.

Recall Sect. 8.5. In a V8 engine with one central camshaft one bank will have towards cams and the other bank will have away cams. If the engine is viewed from the end for which the camshaft is rotating clockwise, then the mechanism shown in part in Fig. 11.11b is applicable and can be related to the analysis given in Chap. 7. The equations required to compute the pressure angle, cam shape, cam torque, curvature, entrainment velocity and contact stress are given in Sects. 7.3–7.6. The follower angular displacement is, $\chi$, the follower angular velocity is $\dot{\chi}$ the follower acceleration is, $\ddot{\chi}$. These data are similar to those denoted by $\phi$, $\dot{\phi}$ and $\ddot{\phi}$ in Chap. 7.

To compute the pressure angle, the cam shape, curvature and entrainment velocity recall Sects. 7.3–Sects. 7.6. The follower centre line is defined by the angle $\bar{\chi} - \zeta$. The cam force,$F_C$ is given by Eq. (11.114), and the contact stress is obtained as described in Sects. 7.8.2.

## 11.11 The Effects of Elastic Deformation

There is a tendency for these push rod mechanisms to have high inertia and to require much stiffer valve springs than a lighter mechanism. The elastic flexibility is also higher. If the valve lift is checked on assembly, it is best to temporarily replace the valve spring with a much weaker spring. Otherwise the elastic deformation of the mechanism and the associated engine components will result in a lower reading of maximum valve lift. However at high engine speeds the inertia loads will largely offset the spring force and the design valve lift will be obtained.

In order to minimise unstable behaviour at higher engine speeds due to elastic response of the mechanism, the valve acceleration diagram needs to be much milder than that which would be acceptable for the cam mechanisms considered in

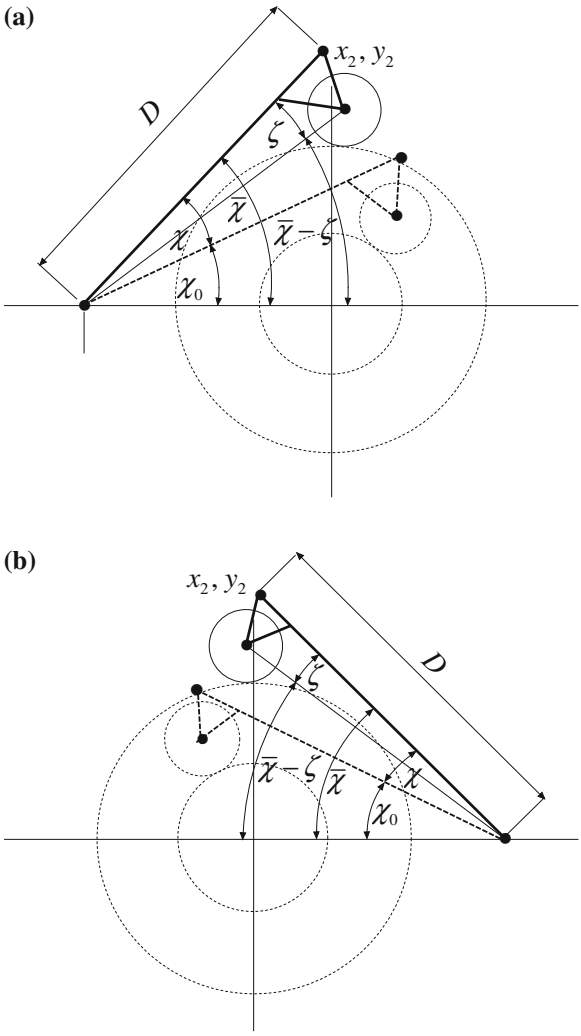


**Fig. 11.11** **a** Clockwise away cam, **b** Clockwise towards cam

previous chapters. Any tendency to dynamic instability should be checked by rig testing and by a simulation program, which accurately models the stiffness of all the cam mechanism components.

## References

1. Ludvigsen K (1995) Mercedes Benz Quicksilver Century, Transport Bookman Publications, London, Photographs, pp 566–567, ISBN 0 85184 051 5
2. Molian S (1982) Mechanism design, Ch 11, 1st edn. Cambridge University Press, Cambridge, ISBN 0 521 29863 6

# Appendix 1

To use the cam lift curve analysis described in Chap. 3 it may be helpful to have an initial example. The angular data which specify the acceleration diagram are given in one-eighth of one degree steps.

| | |
|---|---|
| Length of initial ramp, $T_0$ | 12.000 |
| Length of constant acceleration ramp, $T_1$ | 16.000 |
| Length of first fillet, $T_2$ | 3.250 |
| Length of linearly increasing acceleration, $T_3$ | 1.000 |
| Length of second fillet, $T_4$ | 4.250 |
| Length of linear acceleration, $T_5$ | 0.125 |
| Length of third fillet, $T_6$ | 4.000 |
| Length of linearly decreasing acceleration, $T_7$ | 6.500 |
| Length of fourth fillet, $T_8$ | 3.000 |
| Length of linearly decreasing acceleration, $T_9$ | 2.000 |
| Length of fifth fillet, $T_{10}$ | 2.500 |
| Length of Polynomial, $T_{11}$ | 50.000 |
| Length of sixth fillet, $T_{12}$ | 3.500 |
| Fraction of $A_0$ from $T_0$ to $T_1$ | 0.001 |
| Fraction of acceleration, A, at $T_4$ at $T_2$ | 0.400 |
| Fraction of acceleration, A, at $T_4$ at $T_3$ | 0.600 |
| Fraction of acceleration, A, at $T_4$ at $T_5$ | 1.000 |
| Fraction of acceleration, A, at $T_4$ at $T_6$ | 0.800 |
| Fraction of acceleration, A, at $T_4$ at $T_7$ | 0.250 |
| Fraction of acceleration, A, at $T_4$ at $T_8$ | 0.075 |
| Fraction of acceleration, A, at $T_4$ at $T_{10}$ | 0.230 |
| Deceleration, $F_0$ at $T_{12}$ | 0.004450 mm/degree$^2$ |
| Lower index of polynomial, p | 1.35 |
| Higher index of polynomial, q | 70.0 |
| Lift at $T_1$ in mm | 0.24 mm |
| Lift at $T_{12}$ in mm | 9.25 mm |
| Engine speed in rpm | 8000.0 rpm |

J. J. Williams, *Introduction to Analytical Methods for Internal Combustion Engine Cam Mechanisms*, DOI: 10.1007/978-1-4471-4564-6, © Springer-Verlag London 2013

# Appendix 2

There may be a need to try to reproduce a cam shape from an old engine for which no data is available. Providing the cam mechanism is available, the valve lift can be measured by rotating the camshaft in steps of, say, one degree and measuring the valve lift with a dial gauge. It should be possible to obtain an acceptable curve but this will lack both the accuracy and precision which can be computed if the original data is known. There may also be other situations where the valve lift curve is known but not the valve velocity, and acceleration.

Approximate curves of velocity and acceleration can be obtained by the method of central differences. If the valve lift data lacks precision, 6 or 7 significant figures is preferable, there will be some lack of accuracy for the velocity curve and the acceleration curve can be far worse, as the method involves the differences of two nearly equal numbers which can lead to significant rounding errors. Despite this the acceleration curve may still be of some help in obtaining a copy of the valve lift curve.

Consider a series of equally spaced values of $x$ and associated values of $y = f(x)$ as shown in Fig. A2.1. The derivative of the curve at $x_i$, $y_i$ can be approximated by the slope of the line joining two adjacent points.

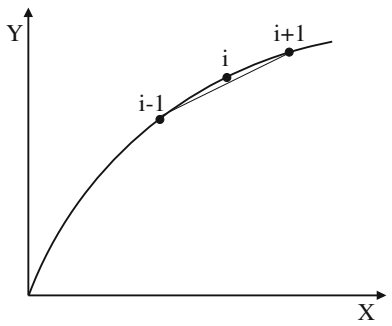


**Fig. A2.1** Numerical differentiation using central differences

J. J. Williams, *Introduction to Analytical Methods for Internal Combustion Engine Cam Mechanisms*, DOI: 10.1007/978-1-4471-4564-6, © Springer-Verlag London 2013

$$\left(\frac{\Delta y}{\Delta x}\right)_i = \frac{y_{i+1} - y_{i-1}}{x_{i+1} - x_{i-1}} \simeq \left(\frac{dy}{dx}\right)_i$$

If the data $x_i$, $y_i$, are available from $i = 0$ to $i = n$, then an approximation to $\left(\frac{dy}{dx}\right)_i$ can be determined from $i = 1$ to $i = n - 1$. An approximation to the second derivative is given by

$$\left(\frac{\Delta\left(\frac{dy}{dx}\right)}{\Delta x}\right)_i = \frac{\left(\frac{dy}{dx}\right)_{i+1} - \left(\frac{dy}{dx}\right)_{i-1}}{x_{i+1} - x_{i-1}} \simeq \left(\frac{d^2y}{dx^2}\right)_i$$

The approximations to the second derivative can be determined from $i = 2$ to $i = n - 2$.

# Appendix 3

The following equations are given for reference:

$$\sin(A+B) = \sin A \cos B + \cos A \sin B$$

$$\sin(A-B) = \sin A \cos B - \cos A \sin B$$

$$\cos(A+B) = \cos A \cos B - \sin A \sin B$$

$$\cos(A-B) = \cos A \cos B + \sin A \sin B$$

$$\sin \pi = 0$$

$$\cos \pi = -1$$

$$\sin \frac{\pi}{2} = 1$$

$$\cos \frac{\pi}{2} = 0$$

$$\sin(\theta+\pi) = \sin \theta \cos \pi + \cos \theta \sin \pi = -\sin \theta$$

$$\sin(\theta-\pi) = \sin \theta \cos \pi - \cos \theta \sin \pi = -\sin \theta$$

$$\cos(\theta+\pi) = \cos \theta \cos \pi - \sin \theta \sin \pi = -\cos \theta$$

$$\cos(\theta-\pi) = \cos \theta \cos \pi + \sin \theta \sin \pi = -\cos \theta$$

J. J. Williams, *Introduction to Analytical Methods for Internal Combustion Engine Cam Mechanisms*, DOI: 10.1007/978-1-4471-4564-6, © Springer-Verlag London 2013

$$\sin\left(\theta+\frac{\pi}{2}\right)=\sin\theta\cos\frac{\pi}{2}+\cos\theta\sin\frac{\pi}{2}=\cos\theta$$

$$\sin\left(\theta-\frac{\pi}{2}\right)=\sin\theta\cos\frac{\pi}{2}-\cos\theta\sin\frac{\pi}{2}=-\cos\theta$$

$$\cos\left(\theta+\frac{\pi}{2}\right)=\cos\theta\cos\frac{\pi}{2}-\sin\theta\sin\frac{\pi}{2}=-\sin\theta$$

$$\cos\left(\theta-\frac{\pi}{2}\right)=\cos\theta\cos\frac{\pi}{2}+\sin\theta\sin\frac{\pi}{2}=\sin\theta$$

# Appendix 4

## A4.1 Trifilar Suspension

The use of a so-called trifilar suspension to experimentally measure the polar moment of inertia of components has been largely superseded by CAD, which computes these data. However if a CAD workstation is not available this method is still useful. A circular metal plate is suspended on three long light wires, and the period of torsional vibration is timed with and without the component whose polar moment of inertia is to be measured.

### *A4.1.1 Notation*

| | |
|---|---|
| $f$ | Frequency of oscillation |
| $g$ | Acceleration due to gravity |
| $I_p$ | Polar moment of Inertia |
| $L$ | Length of suspension wires |
| $m$ | Mass of assembly |
| $n$ | Number of suspension wires, usually 3 |
| $P$ | Tensile force in suspension wire |
| $r$ | Radius of support plate |
| $T_I$ | Inertia torque |
| $T_R$ | Restoring torque |
| $\theta$ | Angular deflection of suspension wire |
| $\tau$ | Period if oscillation |
| $\phi$ | Angular displacement of support plate |
| $\omega$ | Circular frequency |

J. J. Williams, *Introduction to Analytical Methods for Internal Combustion Engine Cam Mechanisms*, DOI: 10.1007/978-1-4471-4564-6, © Springer-Verlag London 2013

**Fig. A4.1** Trifilar suspension

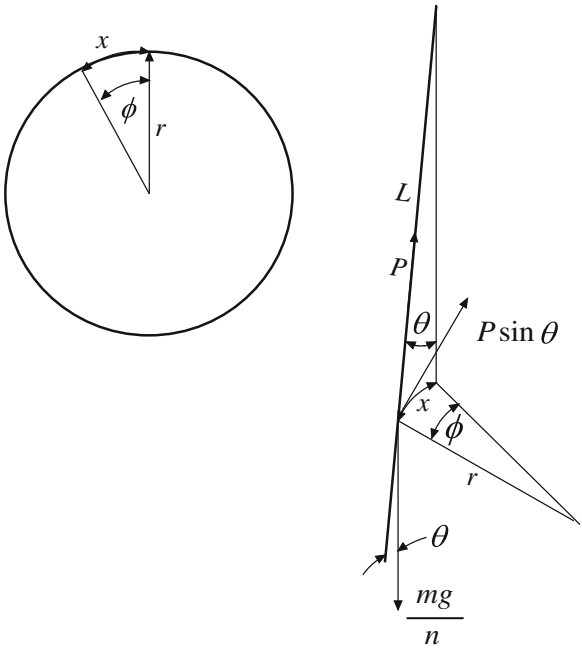


With notation of Fig. A4.1 and using Newton's notation for derivatives w.r.t. time:

$$P\cos\theta = \frac{mg}{n} \tag{A4.1}$$

The restoring torque is:

$$T_R = nPr\sin\theta \tag{A4.2}$$

Substituting for $P$ from Eq. (A4.1) into Eq. (A4.2):

$$T_R = \frac{mgr\sin\theta}{\cos\theta} \tag{A4.3}$$

The inertia torque is given by

$$T_I = I_P\ddot{\phi} \tag{A4.4}$$

For small displacements and angles:

$$x = r\phi = L\theta \tag{A4.5}$$

Differentiating Eq. (A4.5) twice:

$$\ddot{\phi} = \frac{L\ddot{\theta}}{r} \tag{A4.6}$$

Equating torques and substituting for $\ddot{\phi}$:

$$I_P \frac{L\ddot{\theta}}{r} + mgr\frac{\sin\theta}{\cos\theta} = 0 \tag{A4.7}$$

For small amplitude oscillations the system can be assumed to behave linearly. Hence:

$$\sin\theta \simeq \theta \tag{A4.8}$$

and

$$\cos\theta \simeq 1 \tag{A4.9}$$

Equation (A4.7) can therefore be written as:

$$-I_P L\ddot{\theta} + mgr^2\theta = 0 \tag{A4.10}$$

For simple harmonic motion Eq. (A4.10) becomes:

$$-I_P L\omega^2 + mgr^2 = 0 \tag{A4.11}$$

Equation (A4.8) can be written as:

$$I_P = \frac{mgr^2}{L\omega^2} \tag{A4.12}$$

Recall that:

$$\omega = 2\pi f \tag{A4.13}$$

and

$$\tau = \frac{1}{f} \tag{A4.14}$$

Substituting Eq. (A4.13) and (A4.14) into (A4.12) gives:

$$I_p = \frac{mgr^2\tau^2}{4\pi^2 L} \tag{A4.15}$$

The time for several oscillations should be measured to obtain an accurate value of the period of oscillation.

# Appendix 5

## A5.1 Slider Crank Chain Kinematics

When computing the piston and connecting rod kinematics, the expression for the piston motion is frequently considered to involve an infinite series in $\sin\theta$ which is truncated to the first two terms. If the ratio of connecting rod length to crank throw is less than, say, 3 then the truncation error can result in the computed value of the maximum inertia loads being too small. This error can be avoided if the procedure outlined below is employed. This method can also be used for computing the nearest approach of valve and piston. This distance can be very dependent upon the valve timing, and allowance should be made for changes in valve timing during engine development if damage to the engine is to be avoided.

### *A5.1.1 Notation*

$l$ Length of connecting rod
$r$ Radius of crank
$t$ Time
$\phi$ Crank angle
$\theta$ Connecting rod angle

With notation of Fig. A5.1:

$$x = r\cos\theta + l\cos\phi \tag{A5.1}$$

and

$$r\sin\theta = l\sin\phi \tag{A5.2}$$

J. J. Williams, *Introduction to Analytical Methods for Internal Combustion Engine Cam Mechanisms*, DOI: 10.1007/978-1-4471-4564-6, © Springer-Verlag London 2013

**Fig. A5.1** Slider crank chain

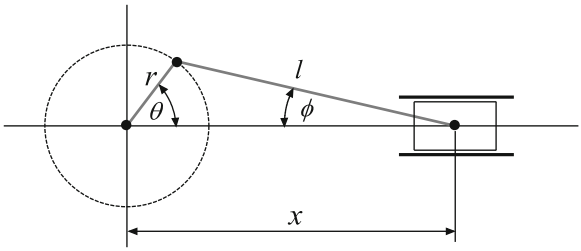


Differentiating Eq. (A5.1) w.r.t.t. and using Newton's notation, the piston velocity is given by

$$\dot{x} = -r\sin\theta\dot{\theta} - l\sin\phi\dot{\phi} \tag{A5.3}$$

Differentiating Eq. (A5.3) w.r.t.t. the piston acceleration is given by

$$\ddot{x} = -r\sin\theta\ddot{\theta} - r\cos\theta\dot{\theta}^2 - l\sin\phi\ddot{\phi} - l\cos\phi\dot{\phi}^2 \tag{A5.4}$$

Differentiating Eq. (A5.2) w.r.t.t.:

$$r\cos\theta\dot{\theta} = l\cos\phi\dot{\phi} \tag{A5.5}$$

Differentiating Eq. (A5.5) w.r.t.t.:

$$r\cos\theta\ddot{\theta} - r\sin\theta\dot{\theta}^2 = l\cos\phi\ddot{\phi} - l\sin\phi\dot{\phi}^2 \tag{A5.6}$$

From Eq. (A5.2):

$$\phi = \sin^{-1}\left(\frac{r\sin\theta}{l}\right) \tag{A.5.7}$$

From Eq. (A5.5)

$$\dot{\phi} = \frac{r\cos\theta\dot{\theta}}{l\cos\phi} \tag{A5.8}$$

From Eq. (A5.6)

$$\ddot{\phi} = \frac{r\cos\theta\ddot{\theta} - r\sin\theta\dot{\theta}^2 + l\sin\phi\dot{\phi}^2}{l\cos\phi} \tag{A5.9}$$

For constant engine speed $\ddot{\theta} = 0$ hence:

$$\ddot{\phi} = \frac{-r\sin\theta\dot{\theta}^2 + l\sin\phi\dot{\phi}^2}{l\cos\phi} \tag{A5.10}$$

The angle and the angular velocity of the connecting rod are given by Eqs. (A5.7) and (A5.8), the angular acceleration of the connecting rod can be obtained from Eq. (A5.10). In high speed engines the piston inertia force at TDC can cause significant elastic deformation of the connecting rod and this should be considered when computing the valve-piston clearance.

# Appendix 6

## A6.1 Camshaft Speed Oscillations

### *A6.1.1 Notation*

| | |
|---|---|
| $t$ | Time |
| $x$ | Valve lift |
| $\theta$ | Camshaft angle |
| $\omega$ | Unsteady component of camshaft speed |
| $\varpi$ | Steady component of camshaft speed |
| $\Omega$ | Angular frequency of cam oscillation |

The valve lift can be expressed as a function of cam angle, $\theta$

$$x = f(\theta) \tag{A6.1}$$

Where $\theta$ is the camshaft angle and $\theta$ is a function of time, $t$

$$\theta = g(t) \tag{A6.2}$$

Differentiating w.r.t.t and using Newton's notation for derivatives

$$\dot{x} = \dot{f}(\theta)\dot{\theta} \tag{A6.3}$$

and

$$\ddot{x} = \ddot{f}(\theta)\dot{\theta}^2 + \dot{f}(\theta)\ddot{\theta} \tag{A6.4}$$

For constant camshaft speed $\ddot{\theta} = \omega = 0$, and Eq. (A6.4) reduces to:

$\ddot{x} = \ddot{f}(\theta)\dot{\theta}^2$, which is the usual expression used for the valve acceleration

If the camshaft speed varies sinusoidally with amplitude, $\omega$ and circular frequency, $\Omega$ about a mean value, $\varpi$.

J. J. Williams, *Introduction to Analytical Methods for Internal Combustion Engine Cam Mechanisms*, DOI: 10.1007/978-1-4471-4564-6, © Springer-Verlag London 2013

The angular velocity is given by

$$\dot{\theta} = \varpi + \omega \sin \Omega t \tag{A6.5}$$

$$\ddot{\theta} = \omega \Omega \cos \Omega t \tag{A6.6}$$

Substituting Eqs. (A6.5) and (A6.6) into Eq. (A6.4):

$$\ddot{x} = \ddot{f}(\theta)\{\varpi + \omega \sin \Omega t\}^2 + \dot{f}(\theta)\varpi \Omega \cos \Omega t \tag{A6.7}$$

# Appendix 7

## A7.1 Computing Torque Timing

It may be helpful to show how to compute torque curves described in Chap. 9. The torque curves with the valve fully open at TDC are denoted by a three-dimensional array, Tq(total, nCyls, q). Where total is the number of steps the torque is evaluated over one revolution of the camshaft, and nCyls is the number of cylinders in one bank. The inlet torque is denoted by q = 1 and the exhaust torque by q = 2. Recall that for one revolution of the camshaft there will be two revolutions of the crankshaft. The valve timing can usually be to an accuracy of one half degree, therefore the value of total should be at least 360 × 4 camshaft degrees or 360 × 2 crankshaft degrees. The valve timing is usually measured in crankshaft degrees from TDC. The initial torque curves with the valve fully open at TDC, can be denoted by Tq(total,0,q).

These fragments of code, given here in a form of BASIC, will need to be in separate subroutines or procedures, and variables will need to be declared and dimensioned.

### *A7.1.1 Timing the Valve Torques*

Let total = 360 × fraction, where fraction is an integer multiple of 2, and is the number of steps in camshaft degrees.

```
(n = angle in crankshaft degrees/2, ATDC that inlet valve is fully open)
j(1) = total−n
k(1) = n
(n = angle in crankshaft degrees/2, ATDC that exhaust valve is fully open)
j(2) = n
k(2) = total−n
```

J. J. Williams, *Introduction to Analytical Methods for Internal Combustion Engine Cam Mechanisms*, DOI: 10.1007/978-1-4471-4564-6, © Springer-Verlag London 2013

```
p = 0
For q = 1 to 2
   For i = 1 to k(q)
      m = i + j(q)
      Tq(m, p + 1, q) = Tq(i, p, q)
   Next
   For i = 1 to j(q)
      m = i + k(q)
      Tq(m, p + 1, q) = Tq(i, p, q))
 Next
Next
```

### *A7.1.2 Timing the Cam Torques for the Other 3 Cylinders*

This code should be in a separate subroutine or procedure.

```
ns = total/nCyls
nb = ns x (nCyls−1)
For q = 1 to 2
   For p = 2 to 4
      For i = 1 to nb
         m = i + ns
         Tq(i, p, q) = Tq(m, p−1, q)
      Next
      For i = 1 to ns
         j = 1 to nb
         T q(j, p, q) = Tq(i, p−1, q)
      Next
   Next
 Next
```

### *A7.1.3 Adding the Cam Torques for one Bank*

These calculations involve once again, one revolution of the camshaft, and are for two inlet and two exhaust valves per cylinder. The inlet camshaft torques are denoted by TqIn(total) and the exhaust camshaft torques by TqEx(total). The torque for one bank is denoted by TqBank1(total).

```
For i = 1 to total
   TqIn(i) = 0.0
   TqEx(i) = 0.0
 Next
```

The above loop may not be necessary but is good practice which ensures that the two arrays are initialised to zero.

```
For i = 1 to total
   For p = 1 to nCyls
      TqIn(i) = TqIn(i) + Tq(i, p, 1) × 2.0
      TqEx(i) = TqEx(i) + Tq(i, p, 2) × 2.0
   Next
Next
For i = 1 to total
      TqBank1(i) = TqIn(i) + TqEx(i)
Next
```

### *A7.1.4 Torques for Both Banks*

For a V engine the V angle is Vangle in degrees. The second bank torque is denoted by TqBank2(total), and for both banks by TqBothBank(total).

```
va = Vangle x fraction/2
m = total−va
For i = 1 to m
   j = i + va
   TqBank2(i) = TqBank1(j)
Next
For i = 1 to va
   j = i + m
TqBank2(j) = TqBank1(i)
Next
For i = 1 to total
   TqBothBanks(i) = TqBank1(i) + TqBank2(i)
Next
```

# Subject Index



J. J. Williams, *Introduction to Analytical Methods for Internal Combustion Engine Cam Mechanisms*, DOI: 10.1007/978-1-4471-4564-6, © Springer-Verlag London 2013

# Author Index



J. J. Williams, *Introduction to Analytical Methods for Internal Combustion Engine Cam Mechanisms*, DOI: 10.1007/978-1-4471-4564-6, © Springer-Verlag London 2013